Lecture Notes in Physics

Springer
Berlin
Heidelberg
New York
Barcelona
Hong Kong
London
Milan
Paris
Tokyo

Physics and Astronomy ONLINE LIBRARY
http://www.springer.de/phys/

The Editorial Policy for Monographs

The series Lecture Notes in Physics reports new developments in physical research and teaching - quickly, informally, and at a high level. The type of material considered for publication in the monograph Series includes monographs presenting original research or new angles in a classical field. The timeliness of a manuscript is more important than its form, which may be preliminary or tentative. Manuscripts should be reasonably self-contained. They will often present not only results of the author(s) but also related work by other people and will provide sufficient motivation, examples, and applications.
The manuscripts or a detailed description thereof should be submitted either to one of the series editors or to the managing editor. The proposal is then carefully refereed. A final decision concerning publication can often only be made on the basis of the complete manuscript, but otherwise the editors will try to make a preliminary decision as definite as they can on the basis of the available information.
Manuscripts should be no less than 100 and preferably no more than 400 pages in length. Final manuscripts should be in English. They should include a table of contents and an informative introduction accessible also to readers not particularly familiar with the topic treated. Authors are free to use the material in other publications. However, if extensive use is made elsewhere, the publisher should be informed. Authors receive jointly 30 complimentary copies of their book. They are entitled to purchase further copies of their book at a reduced rate. No reprints of individual contributions can be supplied. No royalty is paid on Lecture Notes in Physics volumes. Commitment to publish is made by letter of interest rather than by signing a formal contract. Springer-Verlag secures the copyright for each volume.

The Production Process

The books are hardbound, and quality paper appropriate to the needs of the author(s) is used. Publication time is about ten weeks. More than twenty years of experience guarantee authors the best possible service. To reach the goal of rapid publication at a low price the technique of photographic reproduction from a camera-ready manuscript was chosen. This process shifts the main responsibility for the technical quality considerably from the publisher to the author. We therefore urge all authors to observe very carefully our guidelines for the preparation of camera-ready manuscripts, which we will supply on request. This applies especially to the quality of figures and halftones submitted for publication. Figures should be submitted as originals or glossy prints, as very often Xerox copies are not suitable for reproduction. For the same reason, any writing within figures should not be smaller than 2.5 mm. It might be useful to look at some of the volumes already published or, especially if some atypical text is planned, to write to the Physics Editorial Department of Springer-Verlag direct. This avoids mistakes and time-consuming correspondence during the production period.
As a special service, we offer free of charge LaTeX and TeX macro packages to format the text according to Springer-Verlag's quality requirements. We strongly recommend authors to make use of this offer, as the result will be a book of considerably improved technical quality.
For further information please contact Springer-Verlag, Physics Editorial Department II, Tiergartenstrasse 17, D-69121 Heidelberg, Germany.

Series homepage -- http://www.springer.de/phys/books/lnpm

Stefan Odenbach

Magnetoviscous Effects in Ferrofluids

Springer

Authors

Stefan Odenbach
Universität Bremen
ZARM
Am Fallturm
28359 Bremen, Germany

Cover picture: by S. Odenbach.

Library of Congress Cataloging-in-Publication Data applied for.
Die Deutsche Bibliothek - CIP-Einheitsaufnahme

Odenbach, Stefan:
Magnetoviscous effects in ferrofluids / Stefan Odenbach. - Berlin ;
Heidelberg ; New York ; Barcelona ; Hong Kong ; London ; Milan ; Paris ;
Tokyo : Springer, 2002
(Lecture notes in physics : N.s. M, Monographs ; 71)
(Physics and astronomy online library)
ISBN 3-540-43068-7

ISSN 0940-7677 (Lecture Notes in Physics. Monographs)
ISBN 3-540-43068-7 Springer-Verlag Berlin Heidelberg New York

Springer-Verlag Berlin Heidelberg New York
a member of BertelsmannSpringer Science+Business Media GmbH

http://www.springer.de

Printed in Germany

Typesetting: Camera-ready by the author
Camera-data conversion by Steingraeber Satztechnik GmbH Heidelberg
Cover design: *design & production*, Heidelberg

Printed on acid-free paper
SPIN: 10862307 55/3141/du - 5 4 3 2 1 0

Preface

Within the scope of this work we've investigated the magnetoviscous effects – i.e. the changes of viscous properties due to the action of magnetic fields – in so-called ferrofluids. These fluids, suspensions of magnetic nanoparticles in appropriate carrier liquids, show a pronounced increase of viscosity in the presence of moderate magnetic fields with strengths of the order of several tens of mT. Classically this effect is explained by the hindrance of the free rotation of magnetic particles – with a magnetic moment spatially fixed in the particle – in a shear flow due to magnetic torques trying to align the particles' magnetic moments with the magnetic field direction.

Starting from the classical theory by Mark Shliomis (Shliomis, 1972) we've performed a couple of experiments to validate the predictions of the theory. The use of relatively concentrated commercial magnetic fluids lead to the conclusion that the mentioned theory – developed for highly diluted fluids – is not able to give a quantitative description of the behavior of commercial fluids. The discrepancies have been attributed to the appearance of interparticle interactions between the magnetic particles.

Since the microscopic make-up of commercial ferrofluids is relatively complicated, and in particular parameters like the size distribution of the magnetic particles are not known precisely, a theoretical description of the microscopic reasons for the fluids' macroscopic behavior is impossible without further information. Therefore we've started a series of investigations shedding light on the viscous behavior of magnetic fluids in the presence of magnetic fields, stepwise reducing the number of relevant microscopic parameters to prepare a basis for sufficient modeling of concentrated ferrofluids.

As a first step in this development a specialized rheometer for the investigation of magnetic fluids has been designed. With this rheometer, allowing well-defined application of a magnetic field to a rheometric flow of ferrofluids, we've investigated the shear dependence of the magnetoviscous effect in commercial ferrofluids. These investigations showed that the field-dependent increase of viscosity reduces with increasing shear rate. On the basis of this result we developed a model, assuming that the formation of chains of magnetic particles dominates the magnetoviscous properties of magnetic fluids. The chains themselves represent large magnetic structures which lead to pronounced changes of viscosity if a field is applied. Furthermore, the rupture of the chains in a shear flow and the resulting reduction of the size of the magnetic structures is a starting point for the explanation of the observed shear thinning.

Since chains of magnetic particles can only be formed by particles exhibiting a sufficient interparticle interaction, and since this interaction depends furthermore

on the size of the particles, the next step had to be a clarification, whether the relatively small fraction of large particles in the suspension used is of major importance for magnetoviscosity in ferrofluids. These large particles exhibit – in contrast to the majority of particles with diameters of about 10 nm – sufficiently strong interaction to explain at least the appearance of chain formation.

To get an insight into these questions, we've performed experiments using ferrofluids with variable contents of large particles. In these experiments it was clearly shown that the magnetoviscous effect rises with an increasing amount of large particles. This leads to further input for the theoretical modeling. In an extended approach the ferrofluid is assumed to be a bidisperse system containing a large fraction of small particles, which do not directly contribute to magnetoviscosity, and a small fraction of large particles which form chains determining the field-dependent changes of viscosity. On the basis of these assumptions the magnetoviscous properties could be fitted quantitatively to the experimental data using methods of statistical physics. Thus, a first quantitative description of the microscopic reasons for the rheological behavior of ferrofluids was found, taking into account the effects to the formation of magnetic particle chains. The conclusion that chains exist in the fluids gives rise to the assumption that these fluids should exhibit viscoelastic effects too. To prove this, we finally carried out experiments on the Weissenberg effect, i.e. the climb of a free surface of magnetic fluids at a rotating axis, showing the field-dependent existence of normal stress differences in ferrofluids. Again, the experimentally found behavior could be explained by the formation and rupture of chains of magnetic particles in the fluid.

Thus – within the scope of this work – we've been able to develop a microscopic model of ferrofluids allowing a quantitative description of their rheological behavior, and to prove this model with numerous experimental results on field-dependent effects in ferrofluids rheology. On the basis of these results, information for the optimization of ferrofluids with respect to their magnetoviscous behavior can be obtained, leading to the synthesis of new ferrofluids. Such fluids with enhanced magnetoviscous properties may be used in the future development of devices using the magnetically induced control of viscous properties as an active part in technical applications like dampers or clutches.

Investigations like those described in this work require not only a certain time span to be performed but also the help and cooperation of numerous colleagues and the financial support enabling the research activities.

Thus I'd like to take the opportunity to express my gratitude to those helping me to do this research during recent years.

First of all I've to thank Prof. Dr.-Ing. H. J. Rath and Prof. Dr. K. Stierstadt for providing me with a working environment in Bremen as well as in former times in Munich that gave me the possibility of developing ideas and building up a research team able to explore this new and interesting field. Without these boundary conditions this wouldn't have been possible.

Furthermore my gratitude goes to my co-workers who were prepared to work even in difficult ways towards new scientific and technical goals: Dipl. Phys. H. Gilly for lively discussions during the time in Munich, Dipl. Phys. H. Störk who

built the first version of the ferrofluid rheometer in Wuppertal, and last but not least the members of the ZARM-ferrofluid team who participated in various experiments which led to the results presented, Dipl.-Ing. J. Fleischer, Dipl.-Ing. M. Heyen, Dipl.-Ing. K. Melzner, Dipl.-Ing. T. Rylewicz, Dipl.-Ing. S. Thurm and Dipl.-Ing. T. Völker.

Besides this I'm grateful to numerous colleagues and friends for fruitful and enlightening discussions. In this case it's nearly impossible to name all those who have been with me during the years, but I'd like to mention particularly: Prof. E. Blums, Prof. A. Zubarev and Prof. L. Vekas who were our guests in Bremen numerous times in the course of fruitful cooperations; Dr. K. Raj who provided us with the fluid series for the experiments concerning the influence of large particles; Prof. K. Stierstadt, Dr. H. W. Müller and Dipl.-Ing. Ch. Eigenbrod who helped me with deep and inspiring discussions; and numerous members of the German ferrofluid community who are helping to form a powerful research community on magnetic fluids.

As mentioned, financial support is also essential for the performance of research in general. In this respect I'd like to mention particularly the Deutsche Forschungsgemeinschaft (DFG) for granting most of the experimental work performed during the years in Bremen. In this context I'd like to express my gratitude to Dr. W. Lachenmeier from DFG for the excellent cooperation during the establishment of the DFG priority program on magnetic fluids focusing partly on the topics discussed here. Furthermore I've to thank the Deutsches Zentrum für Luft- und Raumfahrt (DLR), in particular Dr. H. Binnenbruck, for financial support over many years. In addition, the flight opportunities provided by DLR and ESA were of essential importance for the Weissenberg-effect experiments.

Since most of the work presented has an experimental character, the technical support provided by the workshop at ZARM and the Fallturm Betriebsgesellschaft was often of great importance to the success of our research. I'm especially grateful for this, since we often had to set extremely tight deadlines which were always observed.

Besides all the research work, these pages had finally to be written, and in this context I'd like to express my thanks to E. Renschen and C. Wieske for a lot of typing.

In general, the development of scientific activities is a part of life that can not be successful if it is not supported by an appropriate private environment. Many of the colleagues mentioned above have become real friends during the years, supporting me even in difficult times.

But particular gratitude in this respect goes to my parents and my wife Marlene, supporting me over all the years and understanding the difficulties and setbacks of this kind of life.

Bremen, 2001 *Stefan Odenbach*

Contents

1. Introduction

1.1 Magnetic fluids

Fluids which can be effectively controlled by magnetic fields of moderate strength are a challenging subject for scientists interested in the basics of fluid mechanics as well as for application engineers. For the basic research the introduction of a controllable force into the fundamental hydrodynamic equations opens a fascinating field of new phenomena.

Forces which can be varied over wide ranges in strength and direction relative to a flow are usually only applicable in theoretical treatments. For forces exhibited by magnetic field gradients the situation changes since magnetic fields can be varied quite well in strength and direction using different types of coils, pole shoes and permanent magnets. If the magnetic influence exerted by a magnetic field becomes strong enough to compete with gravitational forces, a new class of hydrodynamic phenomena becomes experimentally accessible.

Also the design of applications using fluids as relevant active or passive components gains new possibilities if the fluids can be positioned or moved by a force which can be produced by an electric current through a coil being controlled and switched electronically. Again – if the necessary forces can be produced by moderate fields which are generated with a relatively small technical effort – new design ideas using an additional control parameter can be realized.

Due to the fact that no natural liquids offer these features, the starting point of the field of magnetic fluid research can be found in theoretical treatments of magnetically controlled heat transfer machines (Resler and Rosensweig, 1964). Since these early ideas already showed that a liquid material with controllable magnetic properties would provide numerous development possibilities, strong efforts have been undertaken to synthesize a system enabling the mentioned magnetic control. As will be shown later on, suspensions of magnetic nanoparticles in appropriate carrier liquids are a sufficient realization of such a new class of smart materials. After their first stable synthesis in the early 1960s the development of these suspensions – called ferrofluids – proved the high potential of the new research field. Several hundred scientific publications per year and thousands of approved patents document the vitality of ferrofluid research as well as the close connection to applied engineering.

But not only engineers, experimental and theoretical physicists contribute to the development of the field called ferrohydrodynamics (Neuringer and Rosen-

S. Odenbach (Ed.): LNP m71, pp. 1–6, 2002.

sweig, 1964). The complexity of the system and its difficult chemical make-up require distinct knowledge in chemistry and colloidal physics to synthesize new and improved liquids and to modify the basic properties of the suspensions. Moreover the utilization of the system is not only restricted to technical applications – a use is also possible for various medical treatment purposes. Thus, the overall field of ferrofluid research has a highly interdisciplinary character, bringing chemists, experimental physicists, engineers, theoretical physicists, applied mathematicians and physicians together.

The interdisciplinarity of the field leads to the necessity for strong cooperation between scientists from different research directions. In principle, basic research has to provide information about the relation between the microstructural make-up and the macroscopic field-dependent properties of the liquids. This knowledge has to be used to tailor special suspensions for new application ideas defining certain requests concerning the fluids behavior in the presence of magnetic fields. Obviously such an interconnected research forces a mutual fertilization of the involved research areas, making the whole field highly challenging from a scientific point of view.

The future development perspective and this interdisciplinary aspect has been the driving force in the establishment of various national research programs, e.g. in Japan and France. The most recent of these programs, a DFG priority program started in Germany in 2000, accounts especially for the interdisciplinarity of the field by combining the efforts of chemists and basic researchers with application engineers and scientists from medical research fields.

These programs are actually leading to a new concentration of efforts in the field, where the investigation of magnetoviscous effects is one of the core points of interest.

1.2 Magnetoviscous effects

Shortly after the publication of the first patent on the synthesis of stable suspensions of nanosized magnetic particles intense research efforts were started in the field, leading to the development of a theoretical background – the theory of ferrohydrodynamics based on early papers by M. Shliomis (Zaitsev and Shliomis, 1969; Shliomis, 1972) – as well as to patents for numerous applications which partly gained commercial importance forcing further development of the whole research area. While basic research covered nearly all areas of flow control and property changes in the fluids induced by the action of magnetic fields, commercially successful applications just used the possibility of the magnetic positioning of the liquids.

The principally predicted employment of the magnetic control of flow in the fluid, or the change of its properties under the influence of a field did not reach the stage of experimental realization since they require relatively high concentration of the suspended magnetic material to achieve a reasonable strength of the effects. The high concentration leads to an interaction of particles, which can not be neglected. The need to account for the interparticle interaction increases the com-

plexity of the system essentially. Thus a well-founded understanding of phenomena observed in such suspensions is relatively hard to obtain. Nonetheless the knowledge about the microstructural properties and their importance for the fluids' macroscopic behavior is the background needed to synthesize application tailored suspensions and to design new devices based on magnetic liquids. Furthermore the influence of magnetic fields on changes in the microstructure of fluids of different make-up has to be taken into account in the prediction of their macroscopic properties.

These problems are of principal importance for the magnetically induced changes in the viscosity of magnetic fluids. The basic theories – formulated nearly three decades ago – model the microstructural make-up of the suspensions in an idealized way, neglecting any kind of interparticle interaction. Therefore these theories can only be used for quantitative predictions of the behavior of highly diluted fluids. In contrast "the promise of controllable fluids", as J.D. Carlson (Carlson, 1994) named the development of new applications of magnetorheological fluids, always requires highly interacting systems to obtain an order of magnitude of the relevant effects – e.g. the magnetoviscous effect – required for commercial needs.

Experimentally it has been found that relatively strong field influence on viscosity can be induced not only in magnetorheological fluids, but also in ferrofluids with sufficient particle-particle interaction. But only recently a deeper understanding of these interactions led to microscopic models quantitatively explaining the experimentally found phenomena. This knowledge is actually used to find ways to optimize the magnetorheological effects in long-term sedimentation stable ferrofluids.

In this context new research concepts have been set up to accelerate the development process. Synthesis of the fluids, basic understanding of their properties, and the development of applications using magnetoviscous properties of the fluids are no longer addressed as isolated research fields. Moreover, programs have been established combining the expertise of the different fields of knowledge in ferrofluid research. The mentioned priority program of DFG is an example of such an integrated research activity. Fluids produced by several synthesizing groups are characterized and rheologically tested and from the understanding of the fluids' behavior steps towards optimization are undertaken. Parallel to this development new applications are designed, using in the beginning existing magnetorheological fluids to define the necessary properties of the fluids to be developed, and thus provide a guideline for the further synthesis steps.

1.3 Publications on ferrofluids

As already mentioned, the field of ferrofluid research is actually more than 30 years old. Thus it is clear that not only original publications in journals or conferences have been released, but also textbooks have been published giving overviews on certain areas of the investigation of fluids containing magnetic nanoparticles. In 1985 the famous book "Ferrohydrodynamics" by Ronald Rosensweig

(Rosensweig, 1985) was issued, and it is still the standard textbook for people entering the field of magnetic fluid research. Rosensweig's book leads the reader through all areas of the research field – from the synthesis and properties of magnetic fluids and the foundation of the theory of ferrohydrodynamics towards problems of experimental hydrodynamics in ferrofluids as well as the description of various applications. It features examples for flow control and magnetically driven surface and transport instabilities as well as some remarks concerning field-induced changes of the properties of the fluids.

Looking to magnetoviscous effects only the first results of McTague (McTague, 1969) and Rosensweig (Rosensweig et al., 1969) are briefly mentioned, and a glance at the related theory by Shliomis (Shliomis, 1972) is given.

A slightly more detailed treatment of the rheology of ferrofluids in a magnetic field was given in the second general textbook on "Magnetic Fluids" by Blums, Cebers and Maiorov (Blums et al., 1997). They include an extended theoretical discussion of rotational viscosity and deal also with questions like the dependence of the magnetoviscous effects on particle shape and the effect of variation of shear rate for weak shear. In addition this book also gives a good overview on ferrofluid research enlightening the related question from a more theoretical point of view.

Besides these two books no general treatment of the whole area of ferrofluid research is currently available. All other books have been published with a focus on certain sub-areas and refer to Rosensweig and Blums for the general questions. The field of heat and mass transfer was well treated by Blums, Mikhailov and Ozols in "Heat and Mass Transfer in MHD Flows" (Blums et al., 1986) which contains a special section on heat and mass transfer effects in ferrofluids – while the main part of the book is devoted to conducting fluids and thus to the action of Lorentz forces rather than of magnetic body forces.

Furthermore two books on applications of magnetic fluids are available. "Magnetic Fluids and Applications Handbook" by Berkovsky and Bashtovoy (Berkovsky and Bashtovoy, 1996) and "Engineering Applications of Magnetic Fluids" (Berkovsky et al., 1993) give an overview on numerous kinds of usage of ferrofluids in different fields, for example mechanical positioning, separation or even medicine. Besides the mentioned books, further monographs are available in Russian, Berkovsky and Polevikov's work on "Numerical Experiments in Ferrofluids" (Berkovsky and Polevikov, 1988). But since these have not been translated into English, the availability of the information contained is unavailable for an English-speaking reader, reducing their importance and rating.

1.4 The scope of this work

With the present work the field of magnetoviscous properties of ferrofluids will be addressed. As mentioned above, the standard textbooks give only a short treatment of the early findings concerning field effects on the rheological behavior of ferrofluids. Moreover no special treatment of this subject has existed till now. On the other hand the investigation of field-induced changes of the viscosity of suspensions of magnetic nanoparticles is one of the most vital areas in magnetic fluid

research nowadays. The current research questions, focusing on the tailored design of fluids for new applications using the magnetoviscous effects, require a detailed understanding of the effect itself as well as of the influence of the microscopic make-up of the fluid on its macroscopic behavior. Since especially the latter mentioned question of the dependence of macroscopic effects on microscopic properties is based on experimental and theoretical results we obtained recently, no comprehensive description of the field exists yet.

So the idea of this work is to combine a description of the basics of magnetoviscous effects with a compilation of the most recent findings on the influence of structure formation on the viscosity of ferrofluids. To achieve this goal, the present work is organized in the following way.

Chapter 2 will introduce the material which is the focus of the discussion. Ferrofluids and their basic properties will be discussed to an extent that allows us to read the upcoming treatment of magnetoviscosity without further basic knowledge on suspensions of magnetic nanoparticles. Besides the discussion of basic properties, Chap. 2 will also contain a short glance on applications of ferrofluids. This part is thought to motivate the engineering aspect of the whole research field in general as well as to highlight the investigation of magnetoviscous effects for applications. This section does not claim to replace the standard textbooks mentioned in Sect. 1.3. Its scope is only to introduce those topics needed for the discussion of the main focus of this work. Thus a couple of references to the standard books are given to enable the reader to find more detailed information on topics from the field of ferrofluid research outside the focus of this work.

In Chap. 3 the basic phenomenon of rotational viscosity, i.e. the influence of a magnetic field on the viscosity of a suspension of noninteracting nanoparticles is discussed. Starting from an explanation of the basic physical background of the phenomena of field-induced viscosity changes in ferrofluids, the theoretical approach of Shliomis is reviewed. Particular interest is paid here to all aspects related to experimental proofs of the theory rather than to a deep theoretical discussion of the approach itself. Nonetheless, the derivation of the basic equation for rotational viscosity is briefly compiled to give the reader a general glance at one of the most fundamental theoretical developments of ferrohydrodynamics. Starting from the various theoretical predictions, experimental proofs of the theory are presented, leading to a discussion of the range of validity of the theory and in particular of the problems that appear if concentrated fluids are considered. Finally, for reasons of completeness, the phenomenon of viscosity reduction in alternating magnetic fields is briefly discussed to illustrate the wide range of phenomena based on the interaction of the magnetic field with the magnetic moment of the particles.

The magnetoviscous effects in concentrated suspensions, and thus in systems of interacting particles, are then discussed in Chap. 4. The starting points for this discussion are the discrepancies found in Chap. 3 in the comparison of Shliomis' theory with the experimental results for concentrated suspensions. Again the experimental investigation of magnetoviscous effects is the center of the discussion. The necessary experimental techniques, and the connected experimental problems are described in detail to form the basis for the discussion of the measured phe-

nomena. The major part of this section is occupied with rheological investigations showing field and shear dependence of the magnetoviscous effect and providing the information necessary to construct a microscopic model explaining the phenomena observed. The related model is then briefly introduced and its results are compared with the experimental findings. Finally – as one of the consequences of the model – the question on magnetically induced viscoelasticity is discussed on the basis of a series of experiments on the Weissenberg-effect in a ferrofluid under the influence of a magnetic field. Again various results leading to a microscopic understanding of the appearance of the phenomena are presented, and the existence of normal stress differences and their dependence on magnetic field strength is experimentally verified. As in Chap. 2, this section is not thought to replace or rewrite the content of the standard textbooks, this time those dealing with rheology. The general rheological background is only mentioned to an extent that makes the description of the effects in ferrofluids understandable. For a deeper insight into rheology the interested reader will be referred to rheology and rheometry textbooks.

Finally Chap. 5 focuses on magnetorheological fluids, i.e. on suspensions of micron-sized magnetic particles. The scope of this section is mainly those effects which can in principle be achieved in a magnetoviscous system. Thus it is a glance at the future of the research on magnetic fluids and it shows how strong magnetoviscous effects can become if interparticle interaction becomes dominant in the behavior of a magnetic suspension. The principal differences between ferrofluids and magnetorheological fluids are highlighted, to motivate again the need for an improvement of the magnetoviscous effects in stable suspensions of nanosized magnetic particles.

2. Magnetic fluids

The material in the focus of this work are liquids which can be controlled by moderate magnetic fields. Presently no molecular liquids exhibit this property in a way that it has importance for technical applications in everyday life. Looking to ferromagnetic materials, it is well known, that their Curie temperature is always well below the melting point, and thus the materials loose their spontaneous magnetic ordering before they become liquid (Kittel, 1996).

Focusing on liquid metals, a well-established technique of magnetic control is given in the field of magnetohydrodynamics. An electric current is applied to the liquid metal and the Lorentz forces in strong magnetic fields can be used to control the flow of such systems (Davidson and Thess, 2000). Nevertheless, reasonable forces, providing significant changes of the liquid metal flow, require extremely high magnetic field strength in the order of several Tesla. In addition a liquid metal requires usually a high temperature environment and thus does not fit the requirements for a broad technical application. Even stronger problems for technical applications appear if undercooled metallic melts are considered. Such melts of certain Co-Pd alloys, undercooled to a high degree, have been found to show magnetic ordering even in the liquid state (Wilde et al., 1996a, Wilde et al., 1996b). But obviously these magnetic properties can not be used in the design of a technical device, since the undercooled state does not allow any handling of the liquid. Comparably a technical use of liquid ^{3}He showing magnetic ordering at temperatures below 3 mK (Mermin and Lee, 1976) seems to be not realistic at all.

As already mentioned, flow control using the Lorentz force requires extremely high magnetic field strength. Thus the only hope to obtain a real magnetic control of a liquid must concentrate on the question of magnetic body forces, commonly written as the Kelvin force (Landau and Lifschitz, 1985)

$$F_K = \mu_0 \int M \nabla H dV \tag{2.1}$$

for a magnetizable material with susceptibility proportional to density. Here M denotes the magnetization of the fluid, ∇H the magnetic field gradient, μ_o the vacuum permeability (μ_o=1.2566·10^{-6} Vs/Am) and the integration is carried out over the volume of the sample V. In paramagnetic salt solutions this force is negligible compared e.g. with the gravitational force even for strong magnetic fields, since their magnetization is too small. To make real use of the magnetic body force, a liquid material is required, having high magnetization even for small magnetic field strength. The way out of this situation was shown in 1964 by S. Papell (Papell, 1964) by producing stable suspensions of magnetic nanoparticles in appropriate carrier liquids. As will be discussed later on, these suspensions,

S. Odenbach (Ed.): LNP m71, pp. 7–32, 2002.

commonly called ferrofluids, exhibit an extraordinary high initial susceptibility and thus show high magnetization for magnetic field strength in the order of about 50 mT. Thus their flow and properties can be controlled by such moderate magnetic fields. Before we will discuss the magnetic properties of these liquids and the resulting magnetic forces applicable to them, we will first have a glance on their basic make-up and the stability requirements they have to fulfill.

2.1 Basic structure and stability

As mentioned, the fluids we will have in focus from now on, are suspensions of magnetic particles in a liquid carrier medium. Obviously, the requirement of stability – being of outstanding importance if a technical use of the suspensions is considered – includes first of all the stability against sedimentation of the particles. Such sedimentation, and the connected demixing of the suspensions, can be driven by gravitational or magnetic forces. To ensure, that the particles do not sediment and that the suspension thus remains well dispersed, one has to observe, that the thermal energy of the particles $E_T=k_BT$ (k_B: Boltzmann's constant, T: absolute temperature) is high enough to provide sufficient mixing of the suspensions. Therefore it needs to be higher than the energy of the particles in the gravitational field or in a magnetic field respectively. As an example we will here shortly discuss this stability argument for the sedimentation in a magnetic field gradient. This sedimentation can be avoided, as long as the thermal energy is strong enough to enable the particles to move freely between a region with strong magnetic field and a field free region. Such a step in magnetic field strength can stand for an idealized magnetic field gradient. The energy of the particles in the field is given by (Landau and Lifschitz, 1985)

$$\left|E_H\right| = \mu_0 \, m \, H \quad , \tag{2.2}$$

where m is the magnetic moment of the particle. Using the spontaneous magnetization of the magnetic material of the particles M_0 one can rewrite their magnetic moment by

$$m = M_o \frac{\pi}{6} d^3 \tag{2.3}$$

with d being the particles' diameter.

Therefore the energy argument for sedimentation stability in a magnetic field gradient $E_H<E_T$ becomes

$$k_B T > \mu_0 M_0 \frac{\pi}{6} d^3 \, H \quad , \tag{2.4}$$

and thus we end up with a condition for the maximum size of the particles allowed if magnetic demixing in the fluid should be negligible

$$d < \left(\frac{6 k_B T}{\mu_0 M_0 \pi H} \right)^{\frac{1}{3}} \quad . \tag{2.5}$$

Using a typical field strength of $5 \cdot 10^4$A/m and the spontaneous magnetization of magnetite (Fe_3O_4) which is often used as magnetic material in the synthesis of ferrofluids $M_o = 4.5 \cdot 10^5$ A/m, the maximum diameter calculated from (2.5) becomes $d_{max} = 6$ nm. Similar, one can calculate a maximum diameter again in the order of 10 nm for gravitational stability of magnetite particles using their energy in the gravitational field $E_g = \Delta\rho g h \pi d^3/6$ with the density difference $\Delta\rho$ between the particles and the carrier liquid, g denoting gravitational acceleration and h the height of the sample.

Since sedimentation stability of the suspension can obviously be ensured by keeping a maximum diameter of the particles, one has additionally to avoid any agglomeration of these particles, since this would increase their active diameter and thus would cause a destabilization of the suspension by sedimentation. First of all the magnetic dipole-dipole interaction could in principle be able to force particle agglomeration. Again, the counteracting influence is the thermal motion of the interacting particles and thus the stability argument can be expressed as before by a comparison of the magnetic dipole interaction energy (Landau and Lifschitz, 1985) with the thermal energy of the two interacting particles

$$2 k_B T > \frac{\mu_0}{2\pi} \frac{m^2}{r^3} \quad . \tag{2.6}$$

Here we have assumed that the magnetic moments of the particles are parallel and aligned with the connecting vector $\vec{r}$ as shown in Fig. 2.1. Replacing the distance r by the sum of the diameters of the particles d and their surface distance δ and using $\ell = 2\delta/d$ one obtains with (2.3) in (2.6).

$$2 k_B T > \frac{\mu_0 \pi M_0^2}{9} \frac{d^3}{(\ell + 2)^3} \quad . \tag{2.7}$$

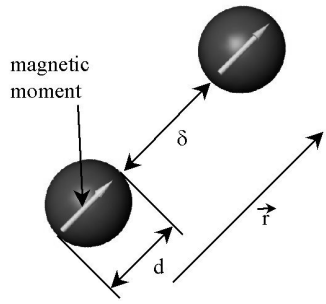

Fig. 2.1. Schematic sketch for the calculation of the magnetic dipole-dipole interaction between two magnetic particles in a ferrofluid.

The interaction energy reaches its maximum when the particles come into contact and thus we obtain again an expression for the maximum size of the particles

$$d < \left(144\, k_B T / \pi \mu_0 M_0^2\right)^{1/3} \quad . \tag{2.8}$$

Using once more the data for magnetite particles, (2.8) shows clearly, that agglomeration due to magnetic dipole-dipole interaction does not cause stability problems for 10 nm sized magnetite particles.

Nevertheless a suspension of bare magnetic particles in a carrier liquid will not be stable against agglomeration, since a second attractive interaction, the v.d.-Waals interaction will cause irreversible coagulation of the particles. The respective interaction energy for spherical particles of diameter d with distance δ can be written in the form (Rosensweig, 1985)

$$\left|E_{v.d.W.}\right| = \frac{A}{6}\left[\frac{2}{l^2+4l} + \frac{2}{(l+2)^2} + \ln\left(\frac{l^2+4l}{(l+2)^2}\right)\right] \tag{2.9}$$

with the normalized distance $l = 2\delta/d$ and the Hamaker constant A. For magnetite in water this constant takes the value $A \approx 10^{-19}$ Nm. In contrast to the magnetic dipole-dipole interaction energy, the expression in (2.9) diverges for vanishing interparticle distance ($l \to 0$). Therefore thermal energy can not protect the particles from coagulation as long as the Hamaker constant has a finite value. Thus the contact between the particles has to be avoided to guarantee the colloidal stability

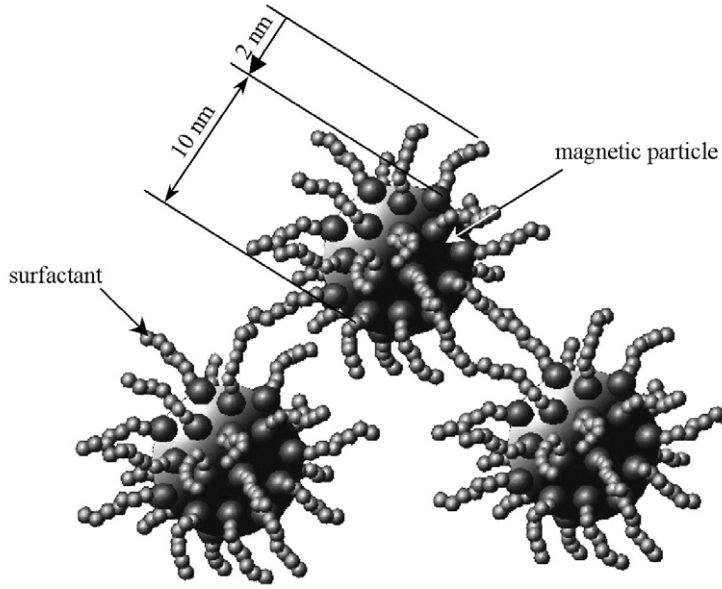

Fig. 2.2. Schematic sketch of the magnetic particles in a ferrofluid. Particles and surfactant are not shown in scale for reasons of clearness of the drawing.

of the system. The stabilization of the suspension, as it was first realized by Papell (Papell, 1964), is based on steric repulsion provided by a surfactant of long chained molecules (Rosensweig, 1985) (see Fig. 2.2). Such a surfactant provides a repulsive energy which can be written for spherical particles in the form

$$E_{Steric} = \frac{k_B T \pi d^2 \zeta}{2} \left[2 - \frac{l+2}{t} \ln\left(\frac{1+t}{1+l/2} \right) - \frac{l}{t} \right] , \quad (2.10)$$

where ζ denotes the surface density of the surfactant molecules, and one defines the normalized surfactant thickness $t = 2s/d$ with s the thickness of the surfactant layer.

The origin of this repulsive interaction is the reduction of the configuration possibilities of the surfactant molecules appearing when the particles distance is smaller than two times the thickness of the surfactant layer. As shown in Fig. 2.3, an exclusion region for the orientation of the molecules occurs as soon as the distance of particle surfaces becomes smaller than 2s. For sufficient surface density of the surfactant and appropriate thickness of the surfactant layer the repulsion can grow large enough to avoid the contact between the magnetic particles.

In Fig. 2.4 the different interaction energies and the resulting interparticle potential are plotted as a function of the interparticle distance for the usual surfactant

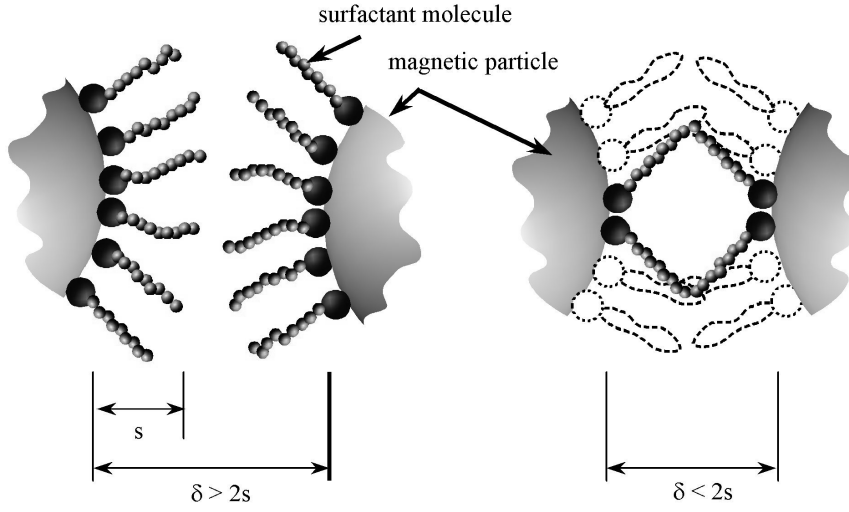

Fig. 2.3. The steric repulsion caused by the surfactant origins in the reduction of the configuration regime of the surfactant molecules. As long as the particles have a surface distance larger than twice the thickness of the surfactant layer no repulsive interaction exists. For smaller distance the surfactant molecules are hindered in their respective spatial arrangement leading to an exclusion region for their orientation. The interaction between neighboring molecules results in the steric repulsion.

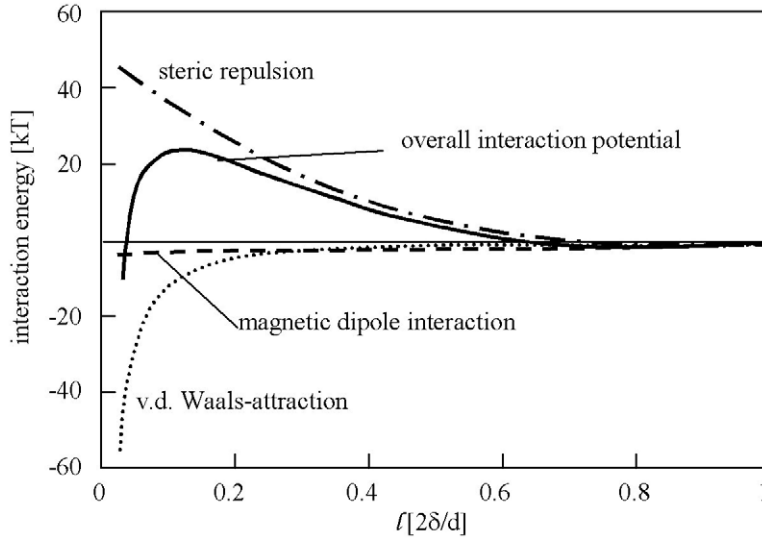

Fig. 2.4. Attractive and repulsive energy potentials between two magnetic particles. For the calculation a particle diameter of 10 nm, magnetite as magnetic material, 2 nm surfactant layer thickness and a surfactant density of 1 nm^{-2} have been assumed. In this situation the contact of the particles is prevented by an energy barrier of about 20 k_BT.

layer thickness of 2 nm. Magnetite particles with d = 10 nm and a surface density $\zeta = 1$ nm^{-2} of the surfactant have been considered for the calculation of the potential. Obviously a surfactant thickness of 2 nm provides an energy barrier of about 20 k_BT between the particles, being sufficient to avoid their contact and therefore their coagulation due to v.d.-Waals interaction. If the surfactant material is chosen in a way, that its dielectric properties match those of the carrier liquid (A = 0), no v.d.-Waals interaction between the surfactant molecules occurs and thus a stable colloidal suspension of the magnetic particles can be obtained.

For our further discussion of the properties and the behavior of ferrofluids we will have to keep in mind, that the surfactant layer causes a difference between the magnetic diameter of the particles and their hydrodynamic diameter. The first one is relevant for all questions concerning the particles' interaction with other particles or with external fields while the second one determines the particles' magnetic influence on the hydrodynamic properties of the suspension.

After the synthesis by Papel numerous further techniques have been developed to optimize the stability and properties of ferrofluids. Besides Papel's technique, using mechanical size reduction of the particles in ball mills, especially chemical precipitation became important for the commercial production of magnetic fluids. Various chemical processes for magnetite particles (see e.g. (Khallafalla and Reimers, 1973; Neal, 1977; Feltin and Pileni, 1997) as well as for mixed ferrites (Lefebure et al., 1998; Auzans et al., 1999) have been reported. Massart (Massart, 1981) developed a method to charge stabilize the particles avoiding the sur-

factant layer. Various authors reported efforts to synthesize ferrofluids containing Co-particles (Thomas, 1966; Hess and Parker, 1966; Chantrell et al., 1978). Such fluids are in principle of great technical interest due to the strong magnetic properties of Co, but the oxidation of Co to the diamagnetic CoO leads to serious problems concerning the chemical long term stability of the suspensions. Usual commercial ferrofluids contain nowadays magnetite particles with a mean diameter of about 10 nm. The volume concentration of the magnetic material reaches values up to 15 vol.% and the particles are stabilized by surfactants of about 2 nm thickness. As carrier liquids water, oils and various organic solvents are available. One of the backdraws of these fluids is their relatively broad size distribution as it is shown in Fig. 2.5. A couple of approaches have been undertaken to reduce the width of this size distribution (Nakatani et al., 1993; Pileni, 1993; Lefebure et al., 1998) but till now no technical process for monodisperse ferrofluids has been established.

We will not discuss the various preparation techniques here in detail, since this has no further importance for the questions addressed here. The interested reader is here referred to the textbooks by Rosensweig (Rosensweig, 1985) or Blums (Blums et al., 1997) for further information.

For all further discussions it will be generally assumed that ferrofluids containing magnetite particles are considered. In special cases, where other magnetic material is employed for the particles, this will be explicitly mentioned.

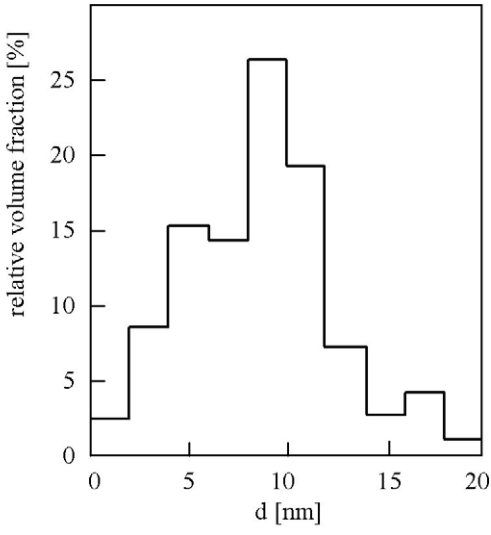

Fig. 2.5. Size distribution of magnetic particles in a commercial ferrofluid as obtained from electron microscopy.

2.2 Magnetic properties of ferrofluids

The basis for the specific properties of magnetic fluids is the possibility to control their flow and physical characteristics by means of moderate magnetic fields with a strength in the order of a few tens of mT. Thus, for all further discussion concerning the magnetic field-dependent phenomena in magnetic fluids, the knowledge about their magnetic properties will be of fundamental importance.

2.2.1 Equilibrium magnetization

To understand the magnetic properties, one has to have a glance on the magnetic structure of the suspended particles first.

These particles are assumed to have a mean diameter of about 10 nm. Thus – for magnetite – they can be assumed to be single domain particles (Kneller, 1962). Magnetite (Fe_3O_4) is a ferrimagnetic substance having inverse spinell structure. From text books on solid state physics (see e.g. (Kittel, 1996; Kneller, 1962) one can find that the unit cell of the crystal structure of magnetite has a volume of about 730 $Å^3$ and contains 8 molecules Fe_3O_4. Therefore each of the magnetic particles in a ferrofluid contains approximately $6 \cdot 10^3$ molecules Fe_3O_4, each of them having a magnetic moment of 4 μ_B ($\mu_B = 9.27 \cdot 10^{-24}$ Am^2; Bohr magneton). Since the particles are single domain particles we end up with a total magnetic moment of about $m = 2 \cdot 10^{-19}$ Am^2 for each of them. These particles can thus be treated as small magnetic dipoles in the carrier liquid.

For the following we will assume, that a ferrofluid is a system of non-interacting spherical particles of the type discussed above. Questions related to interaction of the particles are to be considered in a second step. Obviously the magnetic behavior of such a system can be described like the behavior of non interacting, thermally agitated magnetic dipoles or with other words we can reduce the description to the concepts used for paramagnetic systems.

Therefore the well-known relation deduced by Langevin (Langevin, 1905) can be used to describe the dependence of the magnetization of the fluid M on the strength of a magnetic field H

$$M = M_S \left(\operatorname{ctgh} \alpha - \frac{1}{\alpha} \right) \tag{2.11}$$

$$\text{with } \alpha = \frac{\mu_o m H}{k_B T} \quad ,$$

where $M_s = \phi M_o$ is the saturation magnetization of the liquid, being determined by the volume concentration of the magnetic component ϕ and its spontaneous magnetization M_o. Thus the magnetization curve of a ferrofluid shows the typical paramagnetic structure as it is shown in Fig. 2.6.

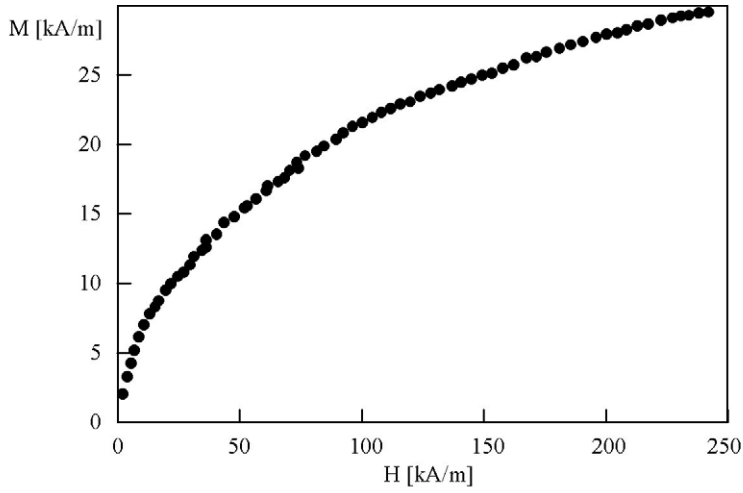

Fig. 2.6. Magnetization behavior of the ferrofluid APG513A containing 7.2 vol.% of magnetite particles with a mean diameter of 10 nm.

The difference in magnetic behavior between a paramagnetic salt solution and a ferrofluid results from the fact, that the units interacting with the magnetic field show a difference concerning the magnitude of their magnetic moment of about four orders of magnitude. This has significant influence on the magnetization behavior for small magnetic fields. To get a deeper insight in this we can approximate the function $L_{(\alpha)} = (\mathrm{ctgh}\ \alpha - 1/\alpha)$ for small values of the energy ratio α by $L_{(\alpha)} \approx 1/3\ \alpha$. Thus we obtain for the magnetization of a ferrofluid in small fields

$$M \approx \frac{M_s}{3} \frac{\mu_0 mH}{k_B T} = \chi_{in} H \tag{2.12}$$

with the initial susceptibility

$$\chi_{in} = \frac{M_s}{3} \frac{\mu_0 m}{k_B T} \quad . \tag{2.13}$$

One should observe, that the magnetic field mentioned here is not the external magnetic field but the inner one which can differ from the external field due to demagnetization effects. We will not introduce an extra symbol for the inner field since it is always the field inside the fluid which influences its behavior. In special cases where the outer field is used, this will be explicitly mentioned. Equation (2.13) shows clearly that the initial susceptibility of a ferrofluid is about four orders of magnitude larger than that of a paramagnetic salt solution due to the difference in the relevant values of the magnetic moment m of the units interacting with the field. As an example we can calculate from (2.13) the initial susceptibility

using the particles magnetic moment calculated before, for a standard ferrofluid containing 7 vol.% of magnetite to be approximately $\chi_{in} = 1$.

Writing the force, exerted by a magnetic field to a magnetic fluid, in the common form using the Kelvin force (2.1) (Rosensweig, 1985; Blums et al., 1997) we obtain for a homogenously magnetized sample at low field strength the force density to be

$$f_{mag} = \mu_0 \chi_{in} H \nabla H \quad . \tag{2.14}$$

Thus for our standard fluid and for a typical magnetic field at the pole of a small electromagnet with $H \approx 20$ kA/m and $\nabla H \approx 7 \cdot 10^5$ A/m^2 the magnetic force density is about 14 kN/m^3. For a fluid with a density of about $\rho = 1.28 \cdot 10^3$ kg/m^3 this is in the same order of magnitude as the gravitational force density acting on the fluid being f_{grav}=13 kN/m^3. Therefore even small magnetic fields like the one mentioned above are able to exert forces on the fluid which can significantly influence the behavior of the fluid. This is illustrated in Fig. 2.7 with a magnetic fluid being attracted to the pole of an electromagnet.

The magnetic force enters the basic hydrodynamic equations for magnetic fluids. For example the Navier-Stokes equation for a ferrofluid can be written in the form (Rosensweig, 1985)

$$\frac{d\vec{v}}{dt} = -\nabla p + \nu \nabla^2 \vec{v} + \mu_0 M \nabla H \quad , \tag{2.15}$$

where p denotes the hydrostatic pressure and ν the kinematic viscosity of the fluid; gravitational effects are neglected.

The fact, that magnetic fields can easily be varied concerning their strength and direction opens thus a wide variety of possibilities for basic research in hydrodynamics as well as for the design of applications using magnetic fluids. Using these control possibilities for the magnetic forces, numerous exciting hydrodynamic phenomena like normal field instability (Cowley and Rosensweig, 1967; Mahr and Rehberg, 1998) thermomagnetic convection (Finlayson, 1970; Schwab, 1989; Odenbach, 1995a), forced diffusion (Chukrov, 1986; Odenbach, 1994a, 1994b) or Soret effect (Blums, 1995; Blums et al., 1999) can be investigated under magnetic field action. These effects are not in the scope of this work, thus the reader has to be referred to the respective literature. A short outlook on applications based on the magnetic field influence on magnetic fluids is given at the end of Chap. 2 to enable an impression of the difference between these classical applications and those that may result from the efforts concerning the magnetoviscous effects mainly addressed in this work.

Stepping back to the magnetization curve, equations (2.11) and (2.13) show that important information on the microstructure of a magnetic fluid can be obtained by measuring $M_{(H)}$. From the high field limit one can obtain the saturation magnetization of the fluid, and thus, if the spontaneous magnetization of the magnetic material is known, the volume concentration of the magnetic component.

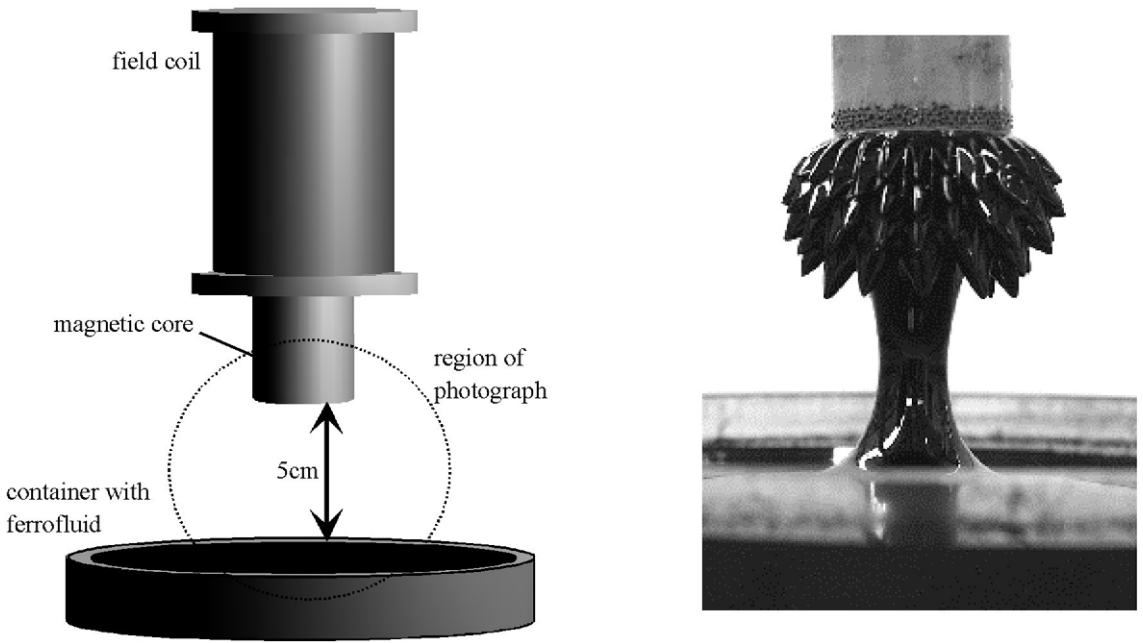

Fig. 2.7. Demonstration of the magnetic force acting on a ferrofluid. The fluid is attracted against gravity by the pole of a simple electromagnet. The spike structure results from an interaction of magnetic field, gravitational acceleration and the fluid's surface tension.

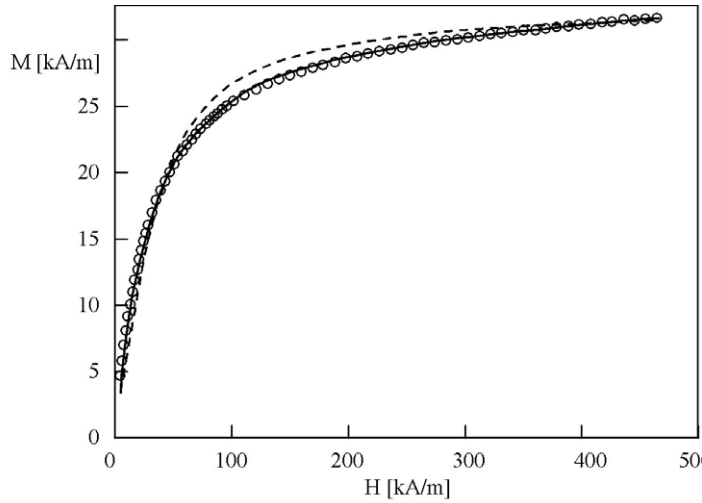

Fig. 2.8. Measured magnetization curve (circles) of a commercial ferrofluid with a Langevin fit assuming a mean diameter of the particles of 10 nm (dashed line) and a polydisperse fit resulting from a magnetogranulometric analysis (full line).

For large values of H and thus for large α the expression ctgh (α) tends to 1 and thus the magnetization becomes

$$M_{(H\to\infty)} = M_S - \frac{M_S}{\alpha} \quad . \tag{2.16}$$

Plotting M against 1/H and extrapolating to 1/H = 0 one can easily determine M_s. Using the value for M_s measured that way, the initial susceptibility (2.13) provides information about the mean diameter of the magnetic particles. A more sophisticated analysis called magnetogranulometry (Weser and Stierstadt, 1985a; Maiorov, 1981) can even provide information on the size distribution of the magnetic particles, using the full shape of the magnetization curve. Fig. 2.8 illustrates how good a magnetization curve calculated using a size distribution from a magnetogranulometric analysis fits with the respective experimental data. The precision of the determination of the size distribution has recently been shown in a comparison of distributions obtained from electron microscopy and magnetogranulometry respectively (Wagener et al., 1999). The differences of the distribution curves shown in Fig. 2.9 are within the margins of error of the two methods.

Nevertheless, it should be mentioned that the distributions obtained by either of these methods have remarkably wide margins of error and thus just give a principle impression of the distribution of particle sizes in a ferrofluid. But remembering that concentrated ferrofluids are optically opaque (Taketomi, 1983; Inaba et al., 1989) one has to face the fact that the precise optical techniques for determination of size distributions commonly used in other colloids are not applicable for

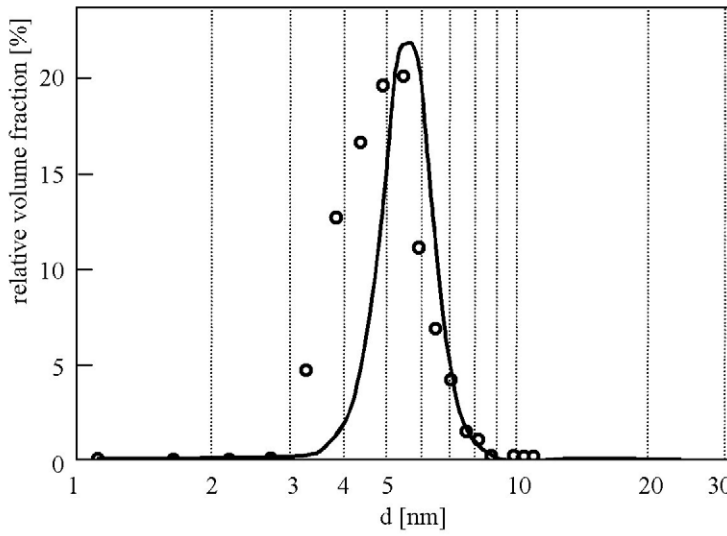

Fig. 2.9. Size distributions of magnetic particles obtained by electron microscopy (full line) and magnetogranulometric analysis (circles) for a Co-ferrofluid in silicone oil (after Wagener et al., 1999).

ferrofluids. Recently experiments using neutron and x-ray scattering have been performed to get insight into the sizes and size distributions of the magnetic core as well as of the surfactant layer (Wiedenmann, 2001; Wagner et al., 2000) but even here a determination of size distributions as precise as they are measured for optically accessible fluids is not obtained. Furthermore the real size of the magnetic core need not to be the size of the metallic particle since magnetic dead layers may reduce it.

As mentioned in the beginning, any interaction between the magnetic particles has been neglected up to this point. This leads to a relatively transparent description of the equilibrium magnetization of magnetic fluids and describes the magnetization curves qualitatively well. Nevertheless interparticle interaction is not *a priori* negligible and its importance rises with increasing volume concentration of the magnetic material as well as with higher values of dipolar interparticle interaction, as it appears e.g. for increasing particles size or for magnetic material with higher bulk magnetization – for instance for Co particles.

As will be seen in Chap. 4, this interaction is strong enough to produce significant effects in the fluid's rheological behavior. Thus it seems to be reasonable to consider it in the treatment of magnetization too. To account for magnetic dipolar interaction of the particles one has to determine the local field acting on a particle. To calculate this field, a virtual sphere is introduced around the particle being in the spheres center. In the Weiss model (O´Grady et al., 1983) the sphere does not contain any further particles and the internal field and the magnetization in the surrounding continuum are assumed to be constant. In a recently published model

(Huke and Lücke, 2000), this concept has been extended by dividing the influence of the fluid on the particle in the center of the sphere into two different parts. One coming from a region at higher distance, being described like in the Weiss model and a second one from closer distance, i.e. from the dipole field of particles inside the sphere which are explicitly taken into account. The problem of these models is always their experimental verification. As mentioned above, the determination of the size distribution shows wide margins of error. Thus fine effects of interactions may be covered by the errors even if an agreement of model and measurement is found (O´Grady et al., 1983). A real test of the models would therefore require well defined monodisperse ferrofluids.

2.2.2 Relaxation of magnetization

As shown in Sect. 2.2.1 the field dependence of the equilibrium magnetization of a ferrofluid provides valuable information about the fluid's make-up. For the dynamic properties of magnetic fluids the question of relaxation of magnetization has additional importance. Generally speaking there are two different processes determining the way how the magnetization of a ferrofluid can follow magnetic field changes. On the one hand we can assume, that the magnetic moment of the particle is fixed with respect to its crystal structure. This kind of particles are called magnetically hard. The relaxation of magnetically hard particles will take place by a rotation of the whole particle. On the other hand under certain material conditions, the magnetic moment may rotate inside the particle, i.e. relative to the crystal structure. This kind of relaxation of particles, called magnetically weak, can take place if the thermal energy is high enough to overcome the energy barrier provided by the crystallographic anisotropy of the magnetic material. Both processes can be characterized by a respective relaxation time. For the first one usually called Brownian Relaxation (Brown, 1963) this relaxation time is given by

$$\tau_B = \frac{3\widetilde{V}\eta}{k_B T} \quad , \tag{2.17}$$

where $\widetilde{V}$ denotes the hydrodynamic volume of the particle, i.e. including the surfactant layer, $\widetilde{V} = \pi (d + 2s)^3 / 6$ and η is the dynamic viscosity of the liquid.

For the relaxation of the moment inside the particle, called Néel relaxation, another characteristic relaxation time is to be used (Néel, 1949)

$$\tau_N = f_0^{-1} \exp\left(\frac{KV}{k_B T}\right) \quad . \tag{2.18}$$

Here K is the anisotropy constant of the particles and f_o is the Larmour frequency of the magnetization vector in the anisotropy field of the particle, being of the order $f_o \approx 10^9 s^{-1}$. It should be recognized that the Néel relaxation depends on the volume of the magnetic core of the particle, while the Brownian relaxation is influenced by its hydrodynamic size. The relaxation of magnetization in a monodisperse suspension will follow the process with the shorter relaxation time.

As seen from (2.17) and (2.18) both relaxation times grow with increasing particle size. But while τ_N increases exponential with particle size, τ_B grows only linear with the particle dimension. Thus for small particles τ_N will be smaller than τ_B and the relaxation will take place by rotation of the moment inside the particle (see Fig. 2.10). From a certain critical diameter the situation changes and the particles become magnetically hard. This critical diameter depends on the viscosity of the carrier liquid, on the thickness of the surfactant layer and in particular on the magnitude of the anisotropy constant K, which is for nearly spherical particles mainly given by the crystal anisotropy and thus by the material parameters of the magnetic component.

Table 2.1 gives an overview concerning the critical diameters calculated for various magnetic materials commonly used in the synthesis of ferrofluids. For a real ferrofluid the anisotropy constant will not only be determined by the crystal anisotropy but also shape anisotropies due to discrepancies from the spherical shape have to be considered. Thus Table 2.1 shows also the critical diameters for a magnetite ferrofluid with an ellipticity of particles of about 15 % – being a realistic value for commercial ferrofluids. For this fluid the anisotropy constant has been calculated using the demagnetization factors from (Osborne, 1945). The same assumptions have been used for the calculations in Fig. 2.10. The values are calculated for a surfactant layer thickness of s = 2 nm and for two different viscosities of the carrier medium; water and oil with a viscosity one order of magnitude higher than that of water.

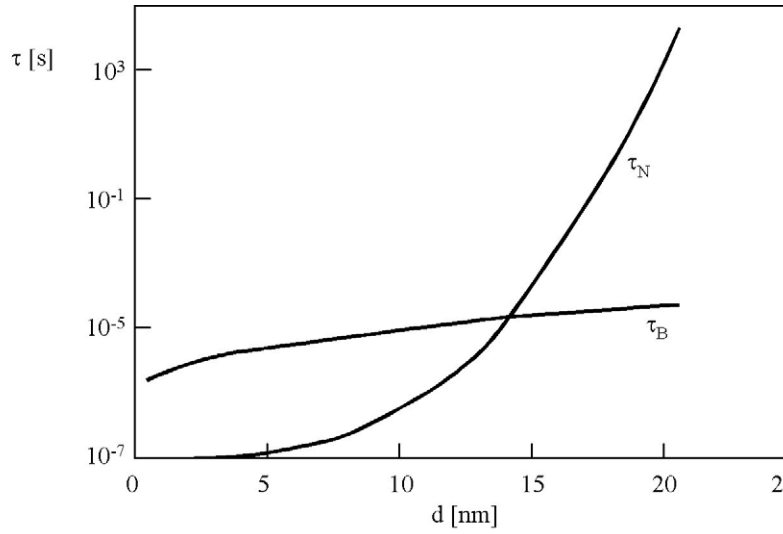

Fig. 2.10. Brownian and Néelian relaxation time for the magnetization of a magnetite ferrofluid with kinematic viscosity $\nu = 100$ mm^2/s as a function of particle size. The diameter d is the diameter of the magnetic core of the particle and a surfactant layer thickness of 2 nm has been assumed.

Table 2.1. The critical diameter d_{crit} for the transition from Néel to Brownian relaxation behavior for various materials

Material	K (kJ/m^3)	d_{crit} (nm) (η=10^{-2} kg/ ms)	d_{crit} (nm) (η=10^{-1} kg/ms)
Fe_30_4	14	18	19
Fe_30_4 with shape anisotropy	28	14	15
Co	485	5	6
Fe	50	12	13
$CoOFe_2O_3$	200	7	8
Ba- Hexaferrite	70	10	11

Close to the critical diameter the relaxation takes place by a mixture of both processes and Shliomis (Martsenyuk et al., 1974) showed that this situation can be described using an effective relaxation time combined from the Néel and Brown times for the relevant particle diameter

$$\tau_{eff} = \frac{\tau_B \tau_N}{(\tau_B + \tau_N)} \quad . \tag{2.19}$$

In a real ferrofluid the situation becomes more complicated due to the relatively broad size distribution resulting in a situation where a part of the particles relaxes mainly by the Néel process, while another part follows the Brownian process. Due to the lack of knowledge concerning the size distribution of concentrated ferrofluids a precise determination of the relaxation times requires direct experimental techniques. Fannin (see e.g. (Fannin et al., 1993; Fannin, 1994; Fannin and Coffey, 1996) showed, that the determination of the complex susceptibility is a suitable tool for the investigation of the relaxation behavior of the magnetization of ferrofluids. He obtained valuable information concerning the effective relaxation time and also on the size distribution, using position and shape of the resonance peak of the real part of the complex viscosity. Meanwhile this technique has not only its undoubted importance for the characterization of magnetic fluids but serves also as a diagnostic tool in biomedical applications (see e.g. (Hiergeist et al., 1999; Hergt et al., 1998).

2.3 Viscous properties in the absence of magnetic fields

For the discussion of the magnetoviscous effects, the knowledge of the viscous properties of a magnetic fluid in the absence of magnetic fields will be of serious importance. In particular its dependence on the amount of suspended particles and – for experiments even more crucial – on temperature will have to be known to enable well founded interpretation of experimental data.

Generally speaking one can state, that the viscosity of a suspension will vary from that of the carrier liquid due to the presence of the suspended particles. As

usual the first approach for a theoretical treatment of such changes has been given for highly diluted suspensions. Already in 1906 Einstein (Einstein, 1906, 1911) stated, that a linear relation

$$\eta_0 = \eta_c \left(1 + \frac{5}{2}\tilde{\phi}\right) \tag{2.20}$$

will hold for suspensions of noninteracting spherical particles. Here η_c means the viscosity of the carrier liquid, η_o the viscosity of the suspension in the absence of a magnetic field and $\tilde{\phi}$ denotes the volume fraction of all suspended material. It should be noted for ferrofluids, that $\tilde{\phi}$ does in principle not only account for the particles including their surfactant but also for possible excess surfactant often used to stabilize the fluid. Nevertheless for all practical means it is sufficient to use the volume fraction of the particles including their surfactant layer for $\tilde{\phi}$. Since the magnetic measurements discussed in Sect. 2.2.1 do only provide a knowledge of the volume fraction of magnetic material ϕ, $\tilde{\phi}$ has to be calculated from this using the thickness of the surfactant layer

$$\tilde{\phi} = \phi \left(\frac{d + 2s}{d}\right)^3 \quad . \tag{2.21}$$

The value of s needed to calculate $\tilde{\phi}$ is usually taken from the producers information, which has approximate character. Only few efforts have been undertaken till now to determine the real value of s in given samples of ferrofluids with higher precision (Wiedenmann, 2001; Lembke et al., 1999). Thus the error resulting form the lack of knowledge in s is usually larger than that from neglecting the excess surfactant.

As mentioned above, Einstein's formula (2.20) is only valid for highly diluted suspensions. If reasonably concentrated ferrofluids with magnetic volume concentration about $\phi = 0.1$ leading to $\tilde{\phi} = 0.27$ ($\bar{d} = 10$nm, $s = 2$ nm) are considered this condition is not longer valid. A first improvement of (2.21) has been given by Batchelor (Batchelor, 1970) adding a quadratic term into Einstein's equation

$$\eta_0 = \eta_c \left(1 + \frac{5}{2}\tilde{\phi} + \frac{31}{5}\tilde{\phi}^2\right) \quad . \tag{2.22}$$

But already for values of $\tilde{\phi}$ in the order of 0.3 this relation underestimates the real situation. This forced Rosensweig (Rosensweig, 1985) to extend this relation again using also an quadratic term in $\tilde{\phi}$. Under the assumption that the suspension's viscosity should diverge for a certain critical volume fraction of suspended material $\tilde{\phi}_c$ and writing the viscosity generally as $\eta_0 = \eta_c / (1 - 5/2\tilde{\phi} + b\tilde{\phi}^2)$ he obtained

$$b = \frac{\left(\frac{5}{2}\tilde{\phi}_c - 1\right)}{\tilde{\phi}_c^2}$$

and thus

$$\eta_0 = \eta_c \left(1 - \frac{5}{2}\tilde{\phi} + \left(\frac{5}{2}\tilde{\phi}_c - 1 \right) \left(\frac{\tilde{\phi}}{\tilde{\phi}_c} \right)^2 \right)^{-1} . \qquad (2.23)$$

Usually $\tilde{\phi}_c = 0.74$ is assumed when (2.23) is used for comparison with experiments. For a total volume fraction of up to 0.05 (2.23) coincides with (2.20) to an accuracy of better than 1%, while (2.22) and (2.23) differ for $\tilde{\phi} > 0.2$ for more than 1% for the value of $\tilde{\phi}_c$ mentioned above.

In Fig. 2.11 a typical dependence of the zero field viscosity of a magnetic fluid, – containing magnetite particles with a mean diameter of $\bar{d} = 10$ nm and a surfactant thickness of s = 2 nm (producers information) – on volume concentration is shown together with the relations (2.20) and (2.23). For (2.23) $\tilde{\phi}_c = 0.74$ has been used. Obviously Rosensweig's formula fits the experimental data to a high accuracy without additional fitting parameters in a concentration range up to $\tilde{\phi} = 0.3$.

If clustering of the magnetic particles appears, the critical volume fraction usually reduces dramatically, leading to more significant differences between Rosensweig's and Batchelor's approach (Rosensweig, 1985). Volume fractions up to $\tilde{\phi} \approx 0.3$, corresponding to $\phi \approx 0.11$, can be well described using Rosensweig's formula (2.23) if the critical volume fraction is chosen appropriately.

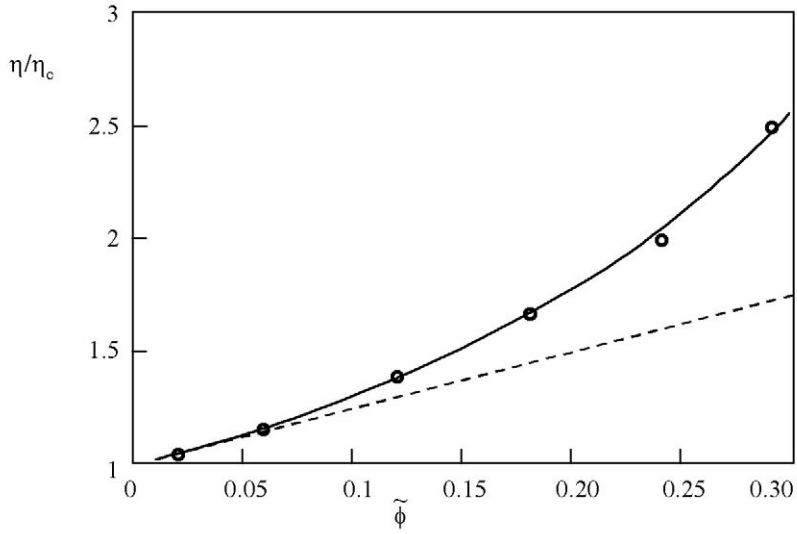

Fig. 2.11. The dependence of the zero field viscosity of ferrofluid as a function of the volume concentration of suspended material. The dashed line represents Einstein's viscosity relation (2.20) while the full line is calculated following Rosensweig's approach (2.23). The circles represent experimentally obtained data from a dilution series of a kerosene based ferrofluid containing magnetite particles.

Higher total volume content of suspended material requires even more complicated functional relations for a proper description. This has been shown by Pshenichnikov (Pshenichnikov et al., 1998) for fluids with volume concentrations of $\tilde{\phi}$ up to approximately $\tilde{\phi} = 0.6$. His approach, based on a modified Chong description (Chong et al, 1971), leads to a good approximation for the viscosity, especially for high values of ϕ .

The result in (Pshenichnikov et al., 1998) overestimates the viscosity for low concentration but for extremely high volume concentration of the suspended particles a good description of the dependence of viscosity on volume concentration is found as shown in Fig. 2.12 (Pshenichnikov et al., 1998). From the last equation and from the data shown in Fig. 2.12 it becomes obvious, that extremely high volume concentration of magnetic particles leads first of all to a strong increase of zero field viscosity. This is of serious importance for the discussion of magnetoviscous effects and their possible application that will be given later on in Chap. 4 and Chap. 5. One of the major questions in this context will be the treatment of the field influence on the viscosity of magnetic particle suspensions.

It will be discussed in detail, that particle-particle interaction plays a dominating role in this respect. One of the possibilities to increase this interparticle interaction is usually the increase of the volume fraction of magnetic material. The results on zero-field viscosity and its dependence on the particle volume fraction discussed above show clearly, that such an approach is strictly limited by the increase of η_o. Especially for later applications, but also for basic investigations, the relative change of viscosity will have major importance.

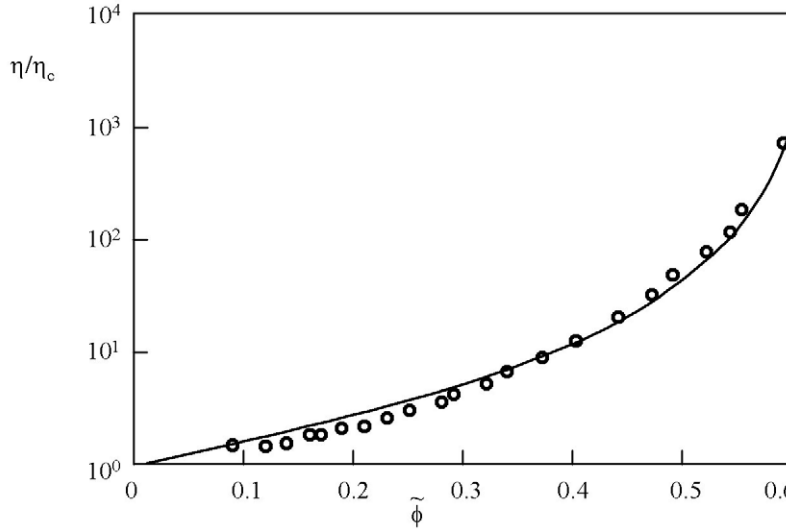

Fig. 2.12. The zero field viscosity of a highly concentrated ferrofluid (circles) (after Pshenichnikov et al., 1998). The full line represents the theoretical description given in (Pshenichnikov et al., 1998).

For example in applications a change from low viscosity to extremely strong viscous or even viscoelastic properties is usually required. Thus a high value of η_o reduces the importance of the magnetically induced changes of viscosity.

2.4 Applications of magnetic fluids

The possibility of magnetic control of flow and properties of ferrofluids has led to the development of a wide variety of possible applications of these liquids in various fields from mechanical engineering to biomedical employment. It is not within the frame of this work to give an extensive review of the application possibilities of magnetic fluids. This has already been done in a certain detail in various monographs (Berkovsky and Bashtovoy, 1996; Berkovsky et al., 1993), which the interested reader should consult for more details. Nevertheless we will give here a short outlook to the application possibilities to shed a light on the technological potential of ferrofluids. In addition it is the aim of this section to outline the qualitative difference between those applications already used in every day life, and those that may result from a proper magnetic control of magnetic fluids' viscosity by means of magnetic fields.

2.4.1 Mechanical applications

The most famous application of magnetic fluids is the sealing of rotating shafts. Consider a situation as it is shown in Fig. 2.13. A rotating shaft made of a material with high permeability is surrounded by a permanent magnet. If the gap between shaft and magnet is reasonably small, i.e. in the order of a few tenth of a millimeter, the magnetic field in the gap can easily reach values in the order of 1T. Outside the gap the field is more or less negligible, leading to an extremely high field gradient in the region of the gap. If a ferrofluid is placed into the gap, the magnetic forces acting on the fluid can be easily high enough to hold the fluid in this position even if a pressure difference is applied to both sides of this liquid seal. Using the ferrohydrodynamic Bernoulli equation as given in (Rosensweig, 1985)

$$\rho g h + p + \frac{\rho}{2} v^2 - \mu_0 \overline{M} H = \text{const} \quad , \tag{2.24}$$

where v is the velocity of the fluid flow, p the pressure and $\overline{M}$ is a mean magnetization defined by

$$\overline{M} = \frac{1}{H} \int_0^H M dH \quad ,$$

one can calculate the maximum differential pressure allowed.

Assuming that the shaft and thus the fluid is at rest, $v = 0$, and observing that the potential energy for points (1) and (2) in Fig. 2.13 is identical, one can write the pressure difference as

$$\Delta p = p_1 - p_2 = \mu_0 \overline{M} H \quad . \tag{2.25}$$

For realistic values of the saturation magnetization of the fluid $M_s = 56$ kA/m and the field in the gap $H = 1.5 \cdot 10^4$ kA/m one sees from (2.25) that the fluid can be hold easily against a pressure difference of approximately 1 bar. Since the fluid keeps its liquid properties even under the influence of such strong magnetic fields, the friction exerted to the shaft by this magnetic fluid seal is negligibly small compared to conventional mechanical sealing techniques like e.g. oil seals.

This advantage is commonly used in various technical applications like the sealing of hard disc drives, rotating x-ray tubes or rotary vacuum feedthroughs where reliable sealing at low friction is required. A combination of this sealing technique with the levitation of non magnetic materials in a ferrofluid under the influence of a magnetic field gradient (Rosensweig, 1966) enabled the design of a magnetic fluid bearing (Berkovsky et al., 1993), while the levitation phenomenon itself is used in magnetohydrostatic separation of ores (see e.g. Odenbach, 1998).

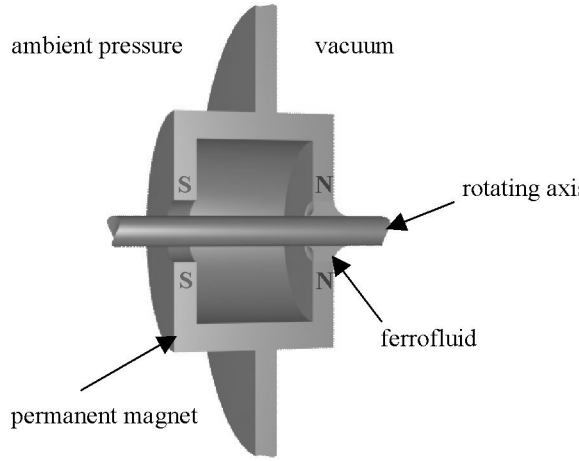

Fig. 2.13. Principle sketch of the sealing of a rotating axis with a magnetic fluid fixed in the small gap between the axis and a surrounding permanent magnet.

2.4.2 Thermal applications

The use of magnetic fluids as a heat transfer medium that may be magnetically hold in a certain position is nowadays the commercially most important branch of ferrofluid manufacturing. The major application in this field is cooling of loudspeakers, enabling a significant increase of the maximum acoustical power without any geometrical changes of the speaker system.

The problem occurring in high power loudspeakers is the transfer of the ohmic heat from the voice coil to the speaker's structure (see Fig. 2.14). Since the coil

has to move freely, no rigid connection is allowed and thus the heat transfer in conventional loud speakers is limited by the thermal conductivity of the air between coil and structure. Normal non-magnetic liquids can not be used to enhance the thermal conductivity in the speaker gap since they can not be reliably located in the gap. In contrast a magnetic fluid is spatially fixed by the strong field in the gap, holding the fluid in there, even if high amplitudes of the coil appear. The high thermal conductivity of the ferrofluid, being approximately eight times higher than that of air, enables a significant increase of the maximum acoustic power of the speaker as shown in Fig. 2.14 (Berkovsky and Bashtovoy, 1996). This concept is nowadays used for high power speakers as well as for speaker systems with small geometrical dimensions as they are used e.g. in car HiFi-systems.

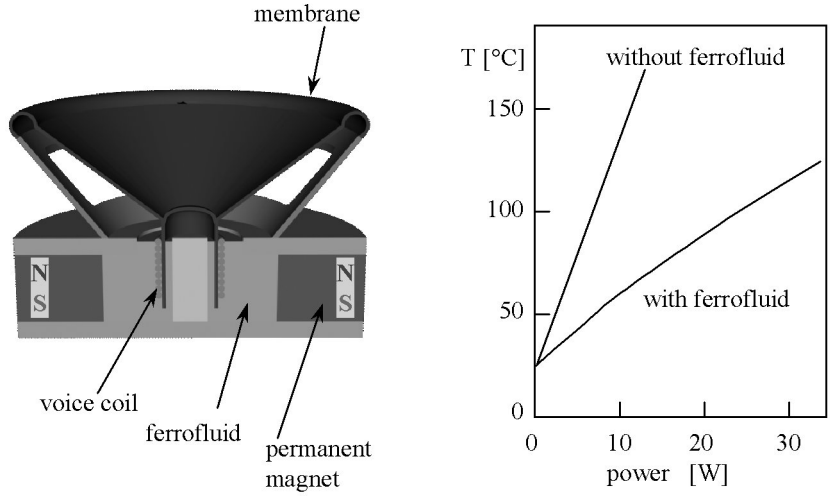

Fig. 2.14. Sketch of a loudspeaker cooled by a magnetic fluid kept in the magnetic gap around the voice coil. On the right side the temperature of the speaker is shown as a function of its power with and without the use of ferrofluid as cooling agent to illustrate the cooling efficiency (after Berkovsky and Bashtovoy, 1996).

2.4.3 Medical applications

The third important field of application of magnetic fluids that should be mentioned in this short overview, is their use in biomedical applications. For example, their use as a contrast medium in x-ray examinations (Papisov et al., 1993) or for positioning tamponade for retinal detachment repair in eye surgery (Dailey et al., 1999) has been reported. Furthermore the application of magnetic fluids for the purpose of cancer treatment either by hyperthermia (Chan et al., 1993; Jordan et al., 1993; Hergt et al., 1998; Hiergeist et al., 1999), using the change of mag-

netization in an AC-field to heat the tissue, or by drug targeting (Ruuge and Rusetski, 1993), are obviously challenging possibilities.

For the last mentioned application – the targeting of drugs in the body – the surfactant layer is functionalized with drugs or biological markers. Afterwards the fluid is injected to a vein and directed by magnetic fields towards the place the drug is needed in. There it is fixed with appropriately formed magnetic fields, enabling a targeted transport of the drug. In this way the amount of drugs necessary for a certain treatment can be dramatically reduced, and since the drugs are no longer distributed all over the organism, side effects can be widely diminished. The practical importance of this way of drug delivery is easily seen in chemotherapy for cancer treatment, usually giving rise to serious side effects. If the fluid is carrying the chemotherapeutics, only a comparably negligible amount of the substance has to be applied and the effect of it can be concentrated in the tumor. Adding not only the drugs but also biological markers, which are enriched in the tumor tissue, to the particles' surfactant results in a furthermore enhanced targeting of the drugs. First pre-clinical tests (Alexiou et al., 2001) have shown, that this method may provide fascinating new therapeutic possibilities.

2.4.4 Aspects for the design of future applications

The examples for applications for ferrofluids in various fields have shown exemplarily, that actually realized ways to use magnetic fluids for technical or other means usually rely on the possibility to fix the fluid at a certain spatial position. This focus is furthermore strengthened if one checks through the various application overviews (see e.g. Berkovsky and Bashtovoy, 1996).

Widely unused remains the possibility to exert an active control to the flow of magnetic fluids by magnetic fields or to change and control their basic properties by such means. Thus the focus of future development of applications of magnetic fluids will have to concentrate on the aspects of "flow control" and "change of properties". The first of these aspects can be illustrated with an example from the field of heat transfer applications. As described in Sect. 2.4.2 ferrofluids are widely used as a magnetically positioned heat transfer medium in loudspeaker cooling. A more advanced kind of transfer techniques may be employed by using the thermomagnetic convection to drive a magnetically controlled thermal flow in the liquid. The phenomenon is based on the change of magnetization of the fluid with temperature. As seen from (2.12) the magnetization of a magnetized ferrofluid decreases with increasing temperature. Thus, in a situation as shown in Fig. 2.15, a temperature gradient applied to a magnetized liquid will give rise to a magnetization gradient antiparallel to the temperature gradient. If in addition a magnetic field gradient parallel to the temperature gradient is applied a destabilizing magnetic force will appear in the fluid. This force can drive a convective flow that is purely controlled by the strength and direction of the applied magnetic field (Odenbach, 1995a).

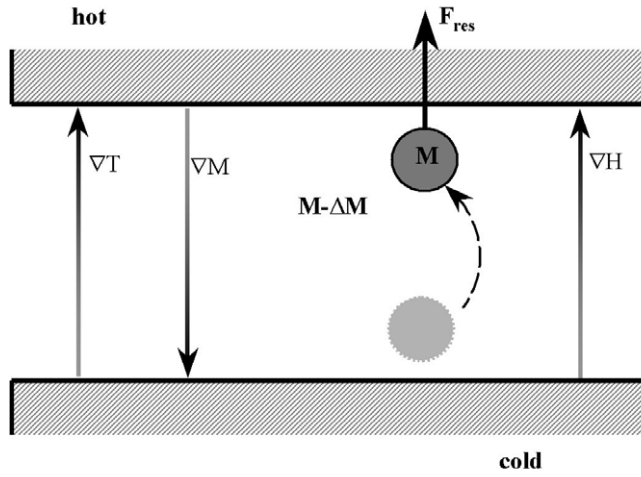

Fig. 2.15. On the driving force of thermomagnetic convection. If a volume element of the fluid is displaced adiabatically in the direction of the field gradient it will be surrounded by hotter fluid in the shown arrangement. Thus the volume element will have higher magnetization than its surrounding and will thus experience a force in the direction of the initial displacement.

Looking for technical devices, in which such a flow could be established for cooling purposes, one can e.g. focus on high power transformers. These are usually cooled with a cooling agent pumped by means of an external pump. As shown in Fig. 2.16 such transformers provide an ideal situation for the establishment of thermomagnetic convection, since parallel temperature and field gradients are naturally present in the system. Therefore a detailed knowledge of thermomagnetic convection processes may lead to a transformer design, in which a ferrofluid is used as cooling agent, pumped by the magnetic forces present in the system. Such a kind of cooling would reduce the maintenance effort, since no moving parts are needed for the establishment of the convective flow.

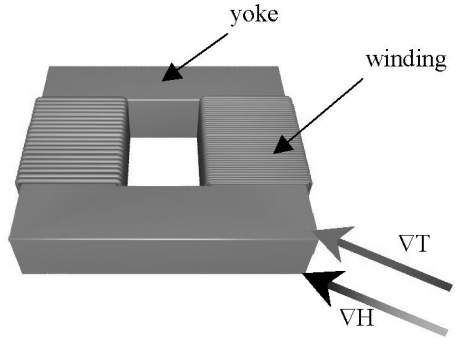

Fig. 2.16. Temperature and field gradient in a transformer system. The relative alignment of temperature and magnetic field changes correspond to the situation of thermomagnetic convection shown in Fig. 2.15. Thus thermomagnetic convection may be used to pump a ferrofluid employed as cooling agent in a high power transformer.

2.4.5 Applications and the magnetoviscous effect

The second aspect for future applications mentioned above is the change of the properties of the fluids by means of magnetic fields. In the context of the present work especially the magnetically induced change of their viscous properties will have to be discussed. During the past 30 years strong effort has been undertaken to produce liquid materials which undergo strong changes in their viscous properties under the influence of an electronically controllable signal. The best results up to the present have been achieved with electrorheological fluids (Lemaire et al., 1992; Wen et al., 1999; Chu and Lee, 2000). The disadvantage of these systems are the extremely high electric fields needed to induce the viscosity changes. These fields lead to serious difficulties if technical devices using the fluids have to be designed.

As a second route to obtain a fluid that might be used e.g. in electronically controlled damping systems, suspensions of magnetic particles have been considered. The most important technical approaches have been made with so called magnetorheological fluids (see e.g. Carlson et al., 1996) containing micron sized particles.

With such fluids clutches, brakes and dampers have been designed, exhibiting an electronically controllable performance. This should shortly be illustrated by a damper designed for damping of seats in large trucks. Such seats consist of a spring, a mass – the seat with the driver – and a damping unit and are therefore a relatively simple oscillation system (see Fig. 2.17). Using a damper with a damping coefficient constant in time will result in a resonance frequency with relatively large oscillation amplitude as it is shown for a magnetic fluid damper in the absence of a magnetic field in Fig. 2.17. Increasing the damping constant will reduce the resonance but lead to higher oscillation amplitudes at higher frequencies. If a feedback loop controls the damping coefficient of a MR-damper, the resonance can be damped out without an increase of the high frequency oscillations – an improvement of the overall performance of the device.

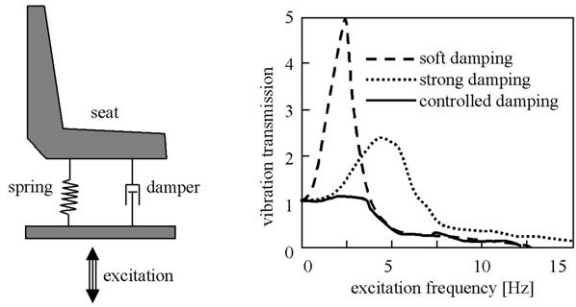

Fig. 2.17. A possible application of magnetoviscous effects is the damping of objects like truck seats as shown in the scheme on the left side. The right side documents the damping performance of a controlled magnetorheological damper (full line) together with the behavior of non controlled dampers, i.e. dampers with constant damping coefficient, with two different damping coefficients (after Carlson, 1994).

Magnetorheological fluids as they've been used in the example given in Fig. 2.17 will be discussed – for comparison with ferrofluids – in Chap. 5. The disadvantage of these systems is the sedimentation of the particles in the gravitational field, leading to a quick destabilization of the suspensions. Nonetheless the performance of the mentioned damping system is so challenging, that an improvement of the liquids would be an interesting research goal to make such devices available in standard application areas. A way to do that is a proper understanding of the reasons for the appearance of magnetoviscous effects in ferrofluids, leading to an enhancement of these properties that may be achieved by appropriate changes of the fluids composition.

Besides this, the appearance of magnetoviscous effects has importance for the standard applications of magnetic fluids too. Looking for example to the sealing of rotary shafts in Sect. 2.4.1 it is clear, that a strong increase of viscosity of the used fluid in the strong magnetic field in the sealing gap may result in serious effects concerning the overall performance of the device. Thus the knowledge about the magnetoviscous behavior of the fluid is an important part of the information needed for the proper design of many kind of ferrofluid applications.

In the following two sections we will now discuss the magnetically induced changes of the viscous properties of ferrofluids – containing nanosized particles not affected by gravitational sedimentation. As mentioned, changes of the microscopic make-up of these fluids may lead to liquid systems combining the advantages of magnetorheological fluids and ferrofluids. Such an improvement can finally enable the production of long term stable fluids used in devices like the damping system described above.

3. The magnetoviscous effect in highly diluted ferrofluids

As outlined in Chap. 2, the most specific property of magnetic fluids is the possibility to exert a significant influence to their flow and physical properties by means of moderate magnetic fields. Focusing on the change of physical properties in presence of magnetic fields, the change of the fluid's viscous behavior due to the action of an appropriate magnetic field seems to be the most prominent effect and still one of the most challenging topics of ferrofluid research.

Stepping back in history, the first paper dealing with viscosity changes in colloidal suspensions of magnetic particles in the presence of magnetic fields was published by Rosensweig et. al. (Rosensweig et al., 1969). In this paper Rosensweig and his co-authors report the investigation of a viscosity increase observed in ferrofluids containing nanosized magnetite particles in magnetic fields up to 25 kA/m. The investigations were carried out in a cone-plate viscometer with the magnetic field perpendicular to the shear planes in a concept similar to the one described in Sect. 4.2.3 By a dimensional analysis they argue, that the viscosity of the fluid should be a function of the ratio (SR) of viscous to magnetic stress

$$\mathrm{SR} = \frac{\dot{\gamma}\,\eta_o}{\mu_o M_o H} \quad , \tag{3.1}$$

the ratio of magnetic to thermal energy – the well known Langevin parameter $(\mu_o mH)/(k_B T)$ – as well as of the volume concentration of particles ϕ. Here $\dot{\gamma}$ denotes the shear rate, η_o the viscosity of the solvent, M_o the spontaneous magnetization of the magnetic material, H the magnetic field, m the particles' magnetic moment and $k_B T$ its thermal energy.

By reducing the discussion to diluted fluids and under the assumption, that the thermal motion of the particles will affect the magnetization M of the liquid only, they come to the conclusion, that the ratio of the fluid's viscosity under influence of the magnetic field H to that of the fluid for H=0 is only a function of the stress parameter SR

$$\frac{\eta}{\eta_{(H=0)}} = F(\dot{\gamma}\,\eta_o/\mu_o M_o H) \quad . \tag{3.2}$$

With this they argue that the viscous behavior should be at a constant minimum level for large values of the stress parameter, i.e. for high shear rate or vanishing field, and that it should reach a maximum for high fields or low shear, i.e. for the

S. Odenbach (Ed.): LNP m71, pp. 33–57, 2002.

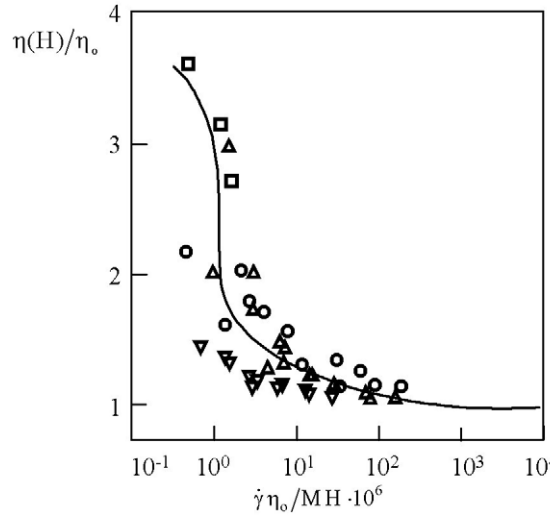

Fig. 3.1. Measured viscosity changes for various magnetic fluids as a function of the stress ratio between shear stress and magnetic stress (after (Rosensweig et al., 1969)). The full line is a guide to the eye.

stress parameter tending towards zero. In the intermediate range the viscosity is assumed to depend on shear and field.

The high field limit, and thus in general the appearance of field-induced changes of viscosity is explained in this paper already by the hindrance of rotation of the particles in the field – an argument that we will discuss in more detail in Sect. 3.1.

In principle – as we will see later – this simple argumentation gives already a good idea concerning the field-dependent changes of viscosity. Nevertheless, the approach does not account for interaction of the particles and the inclusion of thermal motion is not sufficient as will be discussed later on. The experimental proof given in (Rosensweig et al., 1969) is carried out with four magnetic fluids, with distinctively different microscopic make-up. The scatter of the results shown in Fig. 3.1 is accounted to the effects of different surfactant shells, but as we will discuss in Chap. 4, the microscopic make-up concerning particle size and concentration may have been of much greater importance for the different behavior of the fluids. Therefore the assumption, that they all show similar behavior can not necessarily be hold that way. Nevertheless one should recognize that this publication has been the first to discuss magnetoviscosity at all. The approach, coming from an interest concerning applications of ferrofluids and focusing to a technically valuable classification of the fluids' field-induced viscosity changes by means of the stress parameter, is a highly interesting and still up to date idea.

Thus even under the aspect that some of the conclusions of the paper may not hold, and that the description of magnetoviscosity is not complete, it is extremely astonishing, that this paper has been more or less forgotten in the forthcoming

literature. All further work just refers to a paper by John P. McTague (McTague, 1969) which appeared just 8 weeks later. Both works were prepared absolutely independent (Rosensweig, 2001) and they stressed two different aspects of the same phenomenon. While Rosensweig focused on technically interesting problems in fluids used for applications, McTague dealt with a highly diluted model system. While the later problem was well defined enough to find a theoretical explanation shortly after, Rosensweig's fluids were of much more complex nature and thus touched problems which are now reaching a status where a microscopic explanation becomes possible. Following this twofold structure we will discuss the results obtained in relatively concentrated magnetite suspensions in Chap. 4, while the focus of Chap. 3 will be on the more simple questions related to dilute model systems. Thus we will now start with the discussion and explanation of the so called rotational viscosity – a concept being the basis for all further attempts of interpretation of magnetoviscous behavior.

3.1 Rotational viscosity

In July 1969 McTague (McTague, 1969) published an article dealing with the changes of viscosity in a diluted suspension of cobalt particles. This paper was followed by a first theoretical explanation by Hall and Busenberg (Hall and Busenberg, 1969) in the same issue of the Journal of Chemical Physics. The final theoretical explanation by Shliomis (Shliomis, 1972) published about two years later was not only the explanation of magnetoviscosity in diluted magnetic fluids, but also the basis for the development of ferrohydrodynamics. Before we cross the way from McTague's experiment over the approach for explanation by Hall and Busenberg to Shliomis' concept of rotational viscosity we will first discuss the physical reason for the appearance of magnetic field-induced changes of the viscosity of a ferrofluid.

Assuming a suspension of magnetic nanoparticles under the influence of a shear flow, it is obvious that the particles will rotate in the flow with their axis of rotation parallel to the vorticity of the flow (Fig. 3.2).

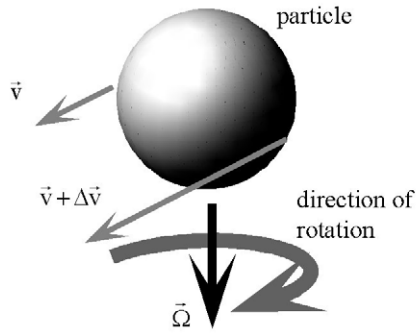

Fig. 3.2. A magnetic particle in a ferrofluid under shear forcing the rotation of the particle in the flow.

For the following we will now consider that the magnetic moment of the particles is fixed within the particle. In the terms of magnetic relaxation as discussed in Sect. 2.2.2, this means that the Brownian relaxation time is shorter than the Néel time and thus the particles are magnetically hard.

If a magnetic field is applied to the suspension under shear, we have to distinguish two different extreme situations.

First we can consider that the applied field is perpendicular to the vorticity of the flow. In this situation the magnetic field will try to align the magnetic moment with the field direction while the viscous torque exerted by the flow tries to rotate the particle and thus – since the moment is fixed in the particle – will force a misalignment of magnetic moment and field. This misalignment will give rise to a magnetic torque trying to realign the moment and thus counteracting the viscous torque (see Fig. 3.3 (a)). This torque counteracts the free rotation of the particle in the flow and thus gives rise to an increase of the fluid's viscosity.

As second variant the field can be applied collinear with vorticity as shown in Fig. 3.3 (b). In this case the magnetic moment will be aligned in the direction of the field and since this is identical with the axis of rotation of the particle no field influence on the rotation of the particle will appear. Thus, in this situation no change of viscosity of the fluid will be observed.

From the model discussed, we see immediately that an anisotropic change of viscosity of the fluid, depending not only on the strength but also on the direction of the field relative to the flow, should appear. In addition it is clear, that the viscosity change should reach a maximum at high magnetic field strength, when the rotation of the particles in the flow is completely inhibited.

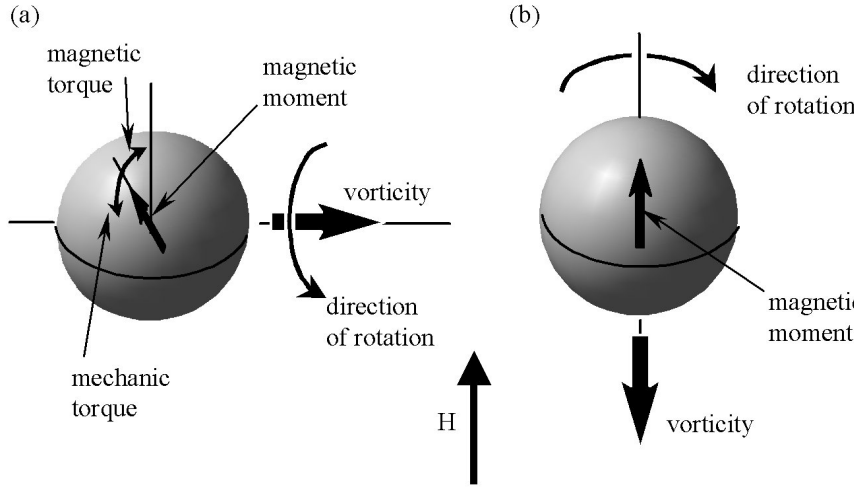

Fig. 3.3. The origin of rotational viscosity in a ferrofluid. Explanations are given in the text.

It should be recalled, that this discussion is based on two major assumptions concerning the particles in the suspension. First of all it is required that the magnetic moment is fixed in the particle, i.e. the particle is magnetically hard. In addition no interaction of particles is considered, thus the suspension is assumed to be highly diluted.

Both conditions were well satisfied in McTague's experiments (McTague, 1969) using suspensions of cobalt particles with a mean diameter of at least 6 nm. As discussed in Sect. 2.2.2 the Néel relaxation time for such particles is longer than the relaxation for the Brownian mechanism. Furthermore the suspensions used contained only about 0.05 vol. % of magnetic material and can thus be assumed to be highly diluted, reducing the probability of the appearance of cooperative phenomena due to interparticle interaction. The fluid has been investigated in a capillary viscometer placed into the gap of a permanent magnet. Two different directions of the flow relative to the magnetic field have been chosen. Assuming that the flow is directed along the z-axis in cylindrical polar coordinates with the origin of the coordinate system on the symmetry axis of the tube, the flow profile of a laminar tube flow is given by $v_z = v_{oz}\,(1\text{-}r^2/a^2)$. Here v_{oz} denotes the maximum velocity of the flow and a the tube diameter. Thus the vorticity of this flow

$$\Omega_{tube} = \frac{v_{oz}\, r}{a^2} \tag{3.3}$$

is directed in azimuthal direction only. With the field parallel to the flow (H||v) a perpendicular alignment of H with the vorticity has been arranged. In contrast the situation with the field perpendicular to the flow direction leads to the necessity to average over the angle between field and vorticity since it varies over the cross section of the tube. This averaging leads to the fact that the viscosity increase for the situation with H⊥v should be half as strong as in the situation H||v. Fig. 3.4 shows the results of the change of viscosity as a function of magnetic field strength for both field directions. An obvious increase of viscosity is observed, and the expected relation for the two different field directions, and thus the anisotropy of the magnetoviscous effect, is found too.

It should be noted, that in contrast to (Rosensweig et al., 1969) no effects of shear rate are considered and not even an information concerning its absolute value is given. Furthermore effects of the field, and of field gradients on the flow as they are mentioned in (Rosensweig et al., 1969) and discussed in detail in Sect. 4.2 are also not considered at all.

A first theoretical approach – based on the physical model of hindrance of rotation of the particles – has been given by Hall and Busenberg (Hall and Busenberg, 1969).

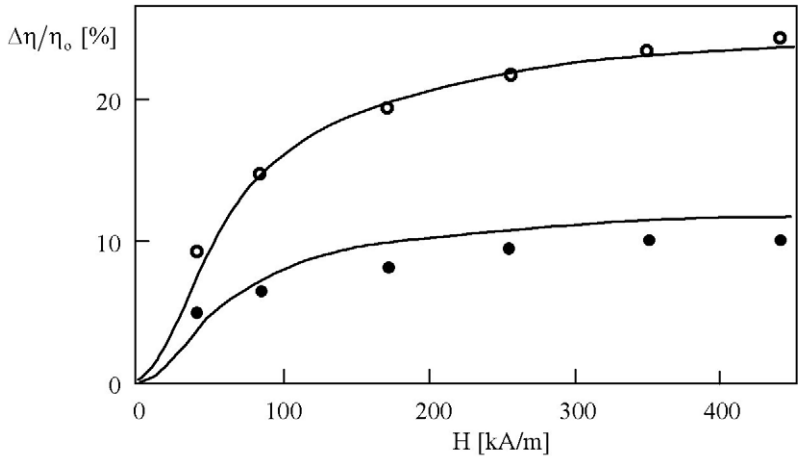

Fig. 3.4. Rotational viscosity in a Co-ferrofluid after (McTague, 1969) with theoretical curves as calculated from Shliomis' theory.

They end up with an extension of Einstein's expression for the viscosity of a suspension including a new term depending on strength and direction of the applied magnetic field

$$\eta_{(H)} = \eta_0 \left(1 + \frac{5}{2}\tilde{\phi} + \frac{3}{2}\phi' \sin^2\varepsilon \right) \tag{3.4}$$

where ϕ' denotes the volume fraction of the particles including the surfactant – in contrast to $\tilde{\phi}$ being the volume concentration of all suspended material, i.e. including dispersants or free surfactant molecules. The term $\sin^2\varepsilon$ contains the magnetic part in the form

$$\sin^2\varepsilon = \frac{1}{2}\left(1+\xi^{-2}\right) - \left[\frac{1}{4}\left(1+\xi^{-2}\right)^2 - \xi^{-2}\sin^2\beta\right]^{\frac{1}{2}} \quad . \tag{3.5}$$

Here β denotes the angle between the vorticity of the flow and the magnetic field direction, while the parameter ξ represents the ratio between the magnetic torque and the viscous torque acting on a particle

$$\xi^{-1} = \frac{\mu_0 \, m H}{4\pi\eta_0 \, d^3 \, \dot{\gamma}} \quad . \tag{3.6}$$

For large field, i.e. for $\xi \to 0$ (3.5) reduces to

$$\sin^2\varepsilon = \sin^2\beta \tag{3.7}$$

and thus (3.4) provides a two times higher increase of viscosity for a fluid under influence of a field parallel to the flow than in the case of H⊥v. Thus for the high field limit experiment and theory agree qualitatively well.

In contrast, for low field strength the theory predicts a too strong increase of viscosity, a discrepancy which is forced by the neglection of any thermal motion of the particles in the flow. Again – as in (Rosensweig et al., 1969) – the thermal effects just enter by the magnetization of the fluid, while the influence of the Brownian motion of the particles on the counteraction of viscous and magnetic torque and its effects to the fluid's viscosity is neglected. This point of criticism to Hall and Busenberg's model is the starting point for the development of the theory of ferrohydrodynamics which – up to date – gives an excellent basis for the description of hydrodynamic processes in ferrofluids. Shliomis (Shliomis, 1972) states that the condition of equilibrium of magnetic and viscous torque, leading to a complete hindrance of the particles' rotation, as given in (Hall and Busenberg, 1969) without accounting for thermal motion of the particles

$$\mu_0 m H \geq 8 \pi d^3 \eta_o \Omega \tag{3.8}$$

where $\vec{\Omega} = 1/2\ \mathrm{rot}(\vec{v})$ is the vorticity of the flow, leads to too small field values for the complete blocking of rotation. For typical values for the cobalt particles as used in (McTague, 1969) ($m = 7 \cdot 10^{-19}$ Am^2; $\eta_o \approx 10^{-3}$ kg/ms, $d \approx 10^{-8}$ m) one obtains for a flow with $\Omega \approx 10^2$ s^{-1} a limiting value of $H \approx 30$ A/m, being approximately three orders of magnitude smaller than the experimentally observed values. Shliomis' conclusion is, that the real condition for the hindrance of rotation of the particles must be dominated by thermal motion and must thus be written as

$$\mu_0 m H \geq k_B T \quad . \tag{3.9}$$

To solve the problem of a correct description of the hydrodynamics of a suspension of magnetic particles, Shliomis introduces the variable of internal angular momentum density S given by the product of the sum of the moments of inertia of the particles per volume I and their averaged angular velocity ω

$$\vec{S} = I\vec{\omega} \quad . \tag{3.10}$$

To describe the fluids behavior he sets up a set of equations consisting first of all of the ferrohydrodynamic Navier Stokes equation

$$\rho \frac{d\vec{v}}{dt} = -\nabla\left[p + \frac{1}{2}\mu_o \left(\vec{M}\vec{H}\right) + \frac{\vec{S}}{I}\left(\vec{S} - I\vec{\Omega}\right)\right] + \eta\nabla^2\vec{v} + \mu_o\left(\vec{M}\nabla\right)\vec{H} + \frac{1}{2\tau_s}\mathrm{rot}\left(\vec{S} - I\vec{\Omega}\right) \tag{3.11}$$

where τ_s is the rotational relaxation time of the suspended particles in the carrier liquid. In addition he employs an equation for the relaxation of the internal angular momentum under the influence of a flow and a magnetic field

$$\frac{d\vec{S}}{dt} = \mu_0 \vec{M} x \vec{H} - \frac{1}{\tau_s}\left(\vec{S} - I\vec{\Omega}\right) \quad . \tag{3.12}$$

Here the first expression on the right side introduces the magnetic action due to the field interacting with the particle's magnetic moment, while the second one accounts for the relaxation of the angular velocity of the particles in the flow due to viscous friction. Unknown at this point is the magnetization M in a system of particles rotated relative to the field direction. To obtain this equation one can introduce (Shliomis, 1972) a reference frame connected to the rotating particle, in which the relaxation of magnetization reads

$$\frac{d'\vec{M}}{dt} = -\frac{1}{\tau}\left(\vec{M} - M_E\hat{H}\right) \quad , \tag{3.13}$$

where τ is the typical relaxation time for magnetization in the system, M_E the equilibrium magnetization, $\hat{H}$ a unit vector in field direction and the dash indicates the moved reference frame. It should be noted, that τ can be in principle either the Brownian relaxation time or the Néelian one as discussed in Sect. 2.2.2. For the further discussion, since the model for the appearance of a field-dependent enhancement claims magnetically hard particles, it will be assumed that $\tau = \tau_B$.

Retransforming the equation of relaxation of magnetization to the usual reference frame by means of $(d\vec{M}/dt) = (d'\vec{M}/dt) + \vec{\omega}\times\vec{M}$ one obtains the required equation by

$$\frac{d\vec{M}}{dt} = \frac{1}{I}\vec{S}\times\vec{M} - \frac{1}{\tau_B}\left(\vec{M} - M_E\hat{H}\right) \quad . \tag{3.14}$$

This equation, together with (3.11) and (3.12) provides a complete set of equations for ferrohydrodynamics. To proceed with the problem of magnetic field-induced viscosity changes, Shliomis choose the special case of planar Couette flow for the further discussion and we will here follow this argumentation to get a sufficient insight into the background of the resulting equation for the viscosity changes. Assuming a stationary flow, $d\vec{S}/dt = 0$ in a constant magnetic field, leading to $d\vec{M}/dt = 0$ we obtain from (3.12)

$$\vec{S} = I\vec{\Omega} + \tau_s\mu_0\vec{M}\times\vec{H} \tag{3.15}$$

and from (3.14)

$$\frac{1}{I}\left(\vec{S}\times\vec{M}\right) = \frac{1}{\tau_B}\left(\vec{M} - M_E\hat{H}\right) \quad . \tag{3.16}$$

With (3.15) in (3.16) one ends up with

$$\vec{\Omega}\times\vec{M} = \frac{1}{\tau_B}\left(\vec{M} - M_E\hat{H}\right) - \frac{\tau_s}{I}\mu_0\left(\left(\vec{M}\times\vec{H}\right)\times\vec{M}\right) \quad . \tag{3.17}$$

Furthermore, one can eliminate S with (3.15) also from the antisymmetric part of the general form of the stress tensor, given also by Shliomis (Zaitsev and Shliomis, 1969) as

$$\sigma_{ik} = -\left(p + \frac{\vec{S}}{I}\left(\vec{S} - I\vec{\Omega}\right)\right)\delta_{ik} + \eta\left(\frac{\partial v_i}{\partial x_k} + \frac{\partial v_k}{\partial x_i}\right) + \frac{1}{2\tau_s}\left(S_{ik} - I\Omega_{ik} + \left[H_i B_k - \frac{1}{2}\left(\vec{H}\vec{B}\right)\delta_{ik}\right]\right) \tag{3.18}$$

leading to

$$\sigma_{ik} = -\left(p + \frac{\vec{S}}{I}\left(\vec{S} - I\vec{\Omega}\right)\right)\delta_{iK} + \eta\left(\frac{\partial v_i}{\partial x_k} + \frac{\partial v_k}{\partial x_i}\right) + \frac{1}{2}\mu_o\left[M_i H_k - M_k H_i\right] + H_i B_k \quad . \tag{3.19}$$

To obtain the missing value of M in (3.19) we assume that shear rate is relatively low and that the relaxation of magnetization takes place rapidly. So one can expand the magnetization around its equilibrium value with a small disturbation $\tilde{\vec{M}}$

$$\vec{M} = M_E \hat{H} + \tilde{\vec{M}} \quad . \tag{3.20}$$

Then (3.17) becomes – linearized in $\tilde{\vec{M}}$ –

$$\tau_B \frac{M_E}{H}\left(\vec{\Omega} \times \vec{H}\right) = \tilde{\vec{M}} + \mu_0 \frac{\tau_s \tau_B}{I}\frac{M_E}{H}\left(\vec{H} \times \left(\tilde{\vec{M}} \times \vec{H}\right)\right) \tag{3.21}$$

from which we easily obtain the value of $\tilde{\vec{M}}$ to be

$$\tilde{\vec{M}} = \frac{M_E \tau_B}{H\left(1 + \mu_0 \tau_s \tau_B M_E \frac{H}{I}\right)}\left(\vec{\Omega}\, x\, \vec{H}\right) \tag{3.22}$$

Equations (3.20) and (3.21) provide the value of M needed in (3.19) which now becomes

$$\sigma_{ik} = -\left[p + \frac{\vec{S}}{I}\left(\vec{S} - I\vec{\Omega}\right)\right]\delta_{ik} + \eta\left(\frac{\partial v_i}{\partial x_k} + \frac{\partial v_k}{\partial x_k}\right) + H_i B_k - \frac{M_E \tau_B}{2H\left(1 + \mu_0 \tau_S \tau_B M_E \frac{H}{I}\right)}\varepsilon_{ikl}\mu_0\left[\Omega_l H^2 - H_l\left(\vec{\Omega}\, x\, \vec{H}\right)\right] \quad . \tag{3.23}$$

With this expression we can obtain the force per surface unit in x-direction on a surface at z = 0 to be

$$f_x = \sigma_{xz} - \sigma'_{xz} = \eta\left(\frac{\partial v_x}{\partial z} + \frac{\partial v_z}{\partial x}\right) + \frac{M_E \tau_B \mu_0 \left[\Omega_y H^2 - H_y\left(\vec{\Omega}\times\vec{H}\right)\right]}{2H\left(1+\mu_0\tau_s\,\tau_B\,M_E\frac{H}{I}\right)} \quad . \qquad (3.24)$$

If we now come back to the example of a planar Couette flow $\vec{v}=(2\Omega z,0,0)$; $\vec{\Omega}=(0,\Omega,0)$ with a magnetic field in z-direction perpendicular to $\vec{\Omega}$, (3.24) leads to

$$f_x = 2\Omega\left[\eta + \frac{1}{4}\mu_0 M_E H \tau_B \left(1+\mu_0\tau_s\,\tau_B M_E\frac{H}{I}\right)^{-1}\right] \quad . \qquad (3.25)$$

The additional portion summed to the usual viscosity η is called rotational viscosity and is the field-dependent part of viscous friction in a ferrofluid

$$\eta_r = \frac{\mu_0 M_E\, H\, \tau_B}{4\left(1+\mu_0\tau_s\,\tau_B\,M_E\,\frac{H}{I}\right)} \quad . \qquad (3.26)$$

To get an expression allowing the comparison of experimental data with the theory we have to replace the variables M_E, τ_B, τ_s and I by measurable quantities. Shliomis showed in (Zaitsev and Shliomis, 1969) that

$$\tau_s = \frac{d'^2\rho'}{45\eta} \quad I = \frac{1}{10}\,d'^2\,\rho'\,\phi' \quad , \qquad (3.27)$$

where the dashed quantities regard to the particles including their surfactant and ρ' is thus the mean density of the whole solid fraction.

From Sect. 2.2.1 we know that

$$M_E = M_s\left(\mathrm{ctgh}\alpha - \frac{1}{\alpha}\right) \quad \alpha = \frac{\mu_0 m H}{k_B T} \qquad (3.28)$$

and that τ_B can be written as

$$\tau_B = \frac{\pi\, d'^3\,\eta}{2\,k_B\,T} \quad . \qquad (3.29)$$

With (3.27) and (3.29) the rotational viscosity becomes

$$\eta_r = \frac{3}{2}\phi'\,\eta_o\,\frac{\alpha - \tanh\alpha}{\alpha + \tanh\alpha} \quad . \qquad (3.30)$$

For the derivation of (3.30) we have considered the field being perpendicular to vorticity. For an arbitrary orientation (3.30) has just to be extended by a factor accounting for the angle β between field and vorticity, becoming

$$\eta_r = \frac{3}{2}\,\phi'\,\eta_o\,\frac{\alpha-\tanh\alpha}{\alpha+\tanh\alpha}\,<\sin^2\beta> \quad , \tag{3.31}$$

where <…> denotes the spatial average of the respective quantity.

The change of viscosity in the fluid can also be written in a more intuitive way based on the initial model of hindrance of rotation of a particle in a magnetic field. As mentioned, two torques are acting on the particles – a magnetic torque, macroscopically written as torque density $\mu_0 \vec{M}x\vec{H}$ and a viscous torque, being present as soon as the rotation speed of the particles ω_p differs from the vorticity of the flow. The equilibrium of both torques, which leads to the hindrance of particle rotation can thus be written as

$$\mu_0\,\vec{M}\times\vec{H} = 6\,\eta\phi'\left(\omega_p-\Omega\right) \quad . \tag{3.32}$$

Therefore the change in viscosity can directly be related to the difference in the speed of rotation leading to (Bacri et al., 1995)

$$\eta_r = \frac{3}{2}\,\eta\,\phi'\,\frac{\Omega-\omega_p}{\Omega} \quad , \tag{3.33}$$

where the particle's angular velocity would have to be calculated. A detailed calculation will finally lead back to expression (3.31). The above given (3.31) describes in a good form the experimental results by McTague as shown in Fig. 3.4.

It should be noted again in this context that the experiments by McTague fulfill the requirements of a diluted suspension of magnetically hard particles quite well, and that they are thus preferable for a quantitative test of the theory.

We will now get an idea of the consequences of (3.31) and will try to find experimental validation for some of the predictions of this relation for magnetoviscosity.

First of all we can have a look to the limits of high and low strength of the applied magnetic field. To make our further discussion independent from the fluids' zero field viscosity we define the relative field-induced change of viscosity R as

$$R = \frac{\eta_{(H)}-\eta_{(H=0)}}{\eta_{(H=0)}} = \frac{\Delta\eta}{\eta_0} = \frac{\eta_r}{\eta_0} \quad . \tag{3.34}$$

For large values of H, the Langevin parameter $\alpha = (\mu_o mH)/k_BT$ becomes large and thus for the limit $H\to\infty$, tanh(α) goes to zero leading to a high field limit of rotational viscosity only determined by the volume fraction of solid material in the suspension

$$R_{(H\to\infty)} = \frac{3}{2}\,\phi'<\sin^2\beta> \quad . \tag{3.35}$$

Thus for perpendicular alignment of field and vorticity we end up with an absolute maximum of the relative change of viscosity

$$R^{max} = \frac{3}{2}\phi' \quad . \tag{3.36}$$

This means, that in a suspension of noninteracting magnetically hard particles with a volume fraction of magnetic material about 7 vol.%, mean particle diameter of about 10 nm and a surfactant thickness of about 2 nm, the relative change of viscosity in a field can not exceed about 40%. A value that one should keep in mind for the later discussion of results obtained with commercial ferrofluids having fluid parameters close to the mentioned values. In addition to the large field limit, one can have a glance on the behavior of the fluid in the presence of weak fields. In this case tanh(α) can be expanded and for small values of α one obtains

$$\tanh\alpha = \alpha - \frac{1}{3}\alpha^3 + O(\alpha^5) \quad . \tag{3.37}$$

Using this in (3.31) the expression (α -tanh(α))/(α +tanh(α)) can be approximated by

$$\frac{\alpha - \tanh\alpha}{\alpha + \tanh\alpha} \approx \frac{1}{6}\alpha^2 \quad . \tag{3.38}$$

Thus we can state that the relative rotational viscosity will increase with the square of the applied magnetic field for weak fieldstrength, i.e. for H < 20 kA/m

$$R \approx \frac{1}{4}\phi'\alpha^2 \sim H^2 \quad , \tag{3.39}$$

as it is proved in Fig. 3.5 for a commercial ferrofluid.

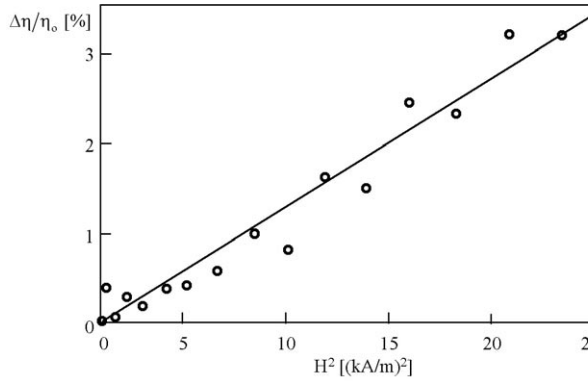

Fig. 3.5. Rotational viscosity of ferrofluid APG513A containing 7.2 vol.% of magnetite particles (d = 10 nm) as a function of the square of the applied magnetic field.

Besides the limits discussed before, Shliomis' description of rotational viscosity as given in (3.31) does also provide a quantitative information about the anisotropy of the magnetic field-dependent changes of the viscosity of a ferrofluid.

As explained in the introduction of this section, the effect of rotational viscosity vorticity of the flow determining the axis of rotation of the magnetic particles in the flow. McTague´s experiments (McTague, 1969) proved two different situations, a field perpendicular to vorticity and another one with spatially varying angle have been studied. Rosensweig's experiments (Rosensweig et al., 1969) considered a perpendicular alignment only. From (3.31) one can see that the spatial mean of the sine of the angle between field and vorticity is assumed to describe the anisotropy effect. So one of the predictions made in Shliomis' theory (Shliomis, 1972), is the variation of the rotational viscosity with $\langle \sin^2\beta \rangle$ a prediction that should be subject of test by use of appropriate flow and field directions. In a series of experiments using the transition from Couette to Taylor vortex flow in a fluid between concentric cylinders we've tried to validate this $\langle \sin^2\beta \rangle$-law (Ambacher et al., 1992; Odenbach and Gilly, 1996; Odenbach, 2000). In these experiments a magnetic fluid is contained between two concentric cylinders, the outer cylinder being at rest while the inner one is rotating. For this situation it is well known, that a laminar flow profile – the so called circular Couette flow – is established for sufficiently low rotation frequencies of the inner cylinder. An increase of the rotation speed over a certain critical value leads to a transition from the laminar flow profile to a flow structure consisting of toroidal, pair wise counterrotating vortices (see Fig. 3.6), called Taylor vortex flow (Taylor, 1923).

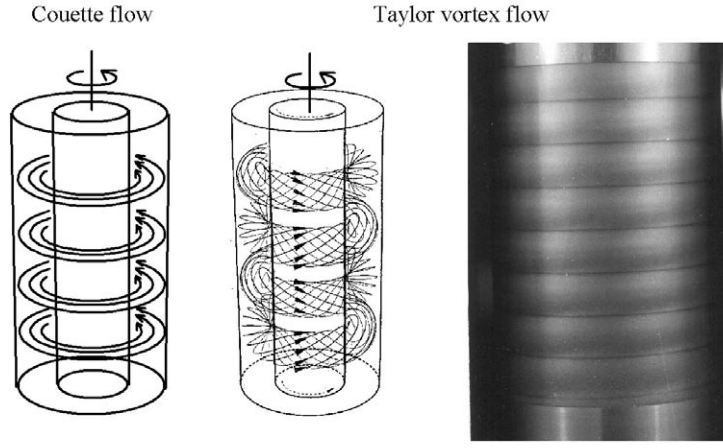

Fig. 3.6. The flow between concentric rotating cylinders. If the outer cylinder is at rest, a laminar Couette flow will be established for low rotation rate of the inner cylinder (left drawing), while for higher rotation speed a transition to Taylor vortex flow appears (right drawing (after Rehberg, 1981) and left photography of the flow profile obtained in a silicone oil with aluminium particles for visualization).

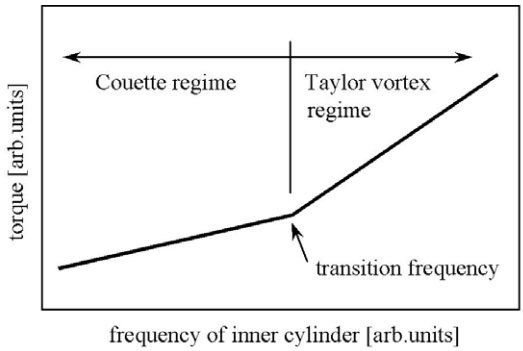

Fig. 3.7. The change of torque between Couette and Taylor vortex flow indicates the transition frequency between the flow states in a plot of torque vs. frequency.

The status of the system can be described by the Reynolds number

$$\mathrm{Re} = \frac{2\pi f R_i w}{\nu} \quad , \tag{3.40}$$

where f denotes the rotation frequency of the inner cylinder, R_i its radius, w the gap width between the cylinders and ν the viscosity of the fluid contained in the gap. If the Reynolds number exceeds a certain critical value, the transition between the two states of flow appears. This critical value can be calculated from the geometry of the cylinder arrangement (DiPrima and Swinney, 1981). Since the actual Reynolds number depends on frequency and the fluid's viscosity only, while the critical value is constant as long as the geometry of the system is fixed, the transition between the flow states may be used as a measure of the actual viscosity of the fluid under investigation. An increase of viscosity will lead to an increase of the frequency of the inner cylinder needed to induce the change from Couette to Taylor vortex flow. To observe this transition in a magnetic fluid, special measuring techniques are necessary, since the opaqueness of the fluids prohibits a direct optical observation of the flow profile as it is undertaken in usual investigations of Taylor Couette flow. A way out of this problem is the detection of the torque necessary to drive the inner cylinder. This torque depends linear on frequency for the regimes of Couette as well as of Taylor vortex flow. But an additional portion of torque is necessary to keep up the vortex flow. This additional torque results in an enhanced slope of the linear dependence of torque on frequency as shown in Fig. 3.7. The frequency for which the change in the slope appears is the transition frequency between the flow states. Therefore a change of this frequency provides a measure for a change of viscosity in the system. If a magnetic field is applied to a magnetic fluid contained between the cylinders, the transition frequency will change with field strength and one can calculate the relative field-dependent change of viscosity by

$$R = \frac{\nu_{(H)} - \nu_{(H=0)}}{\nu_{(H=0)}} = \frac{f^*_{(H)}}{f^*_{(H=0)}} - 1 \quad , \tag{3.41}$$

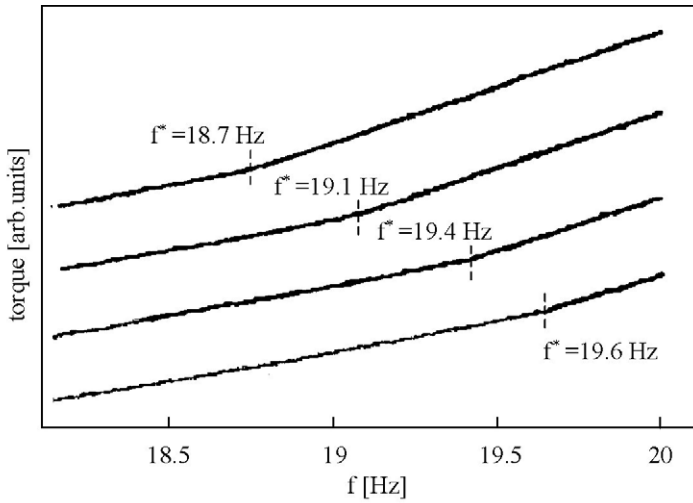

Fig. 3.8. The appearance of rotational viscosity forces a change of the transition frequency in a Taylor-Couette system under influence of a magnetic field.

where f* denotes the transition frequency. The field-dependent variation of the transition is shown in Fig. 3.8 for a commercial ferrofluid (APG513A) containing about 7 vol.% of magnetite particles with a mean diameter of about 10 nm. We will discuss the full curve of the change of viscosity of this fluid and questions related to its quantitative interpretation later on in Sect. 4.1. Here we will just focus on two qualitative questions - the quadratic increase of the viscosity change with field strength and the $<\sin^2\beta>$-law. As it was already clearly seen from Fig. 3.5, the relative field-dependent change of viscosity R rises linear with the square of the strength of the applied magnetic field. Thus we can assume here that – for weak field – the theory resulting in (3.31) fits qualitatively well to the results obtained in APG513A using the Taylor Couette set up. Thus we can use this data to get an idea of the validity of the $<\sin^2\beta>$-law. In the axial-symmetric set up of Taylor Couette flow three natural field directions are possible to be applied to the system (Fig. 3.9).

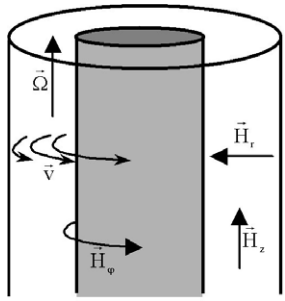

Fig. 3.9. Basic magnetic field geometries matching the symmetry of a Taylor-Couette system.

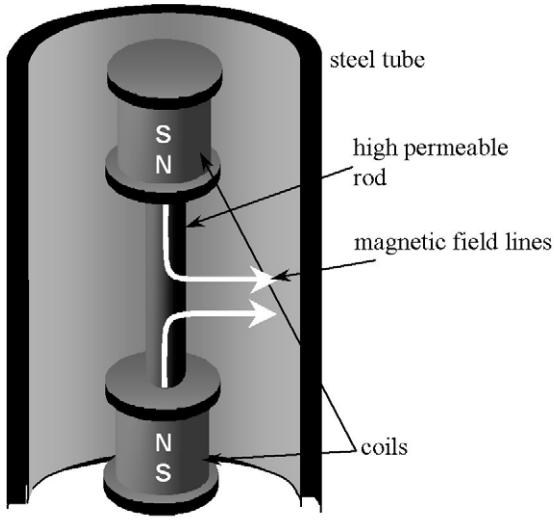

Fig. 3.10. Set up to generate a radial magnetic field for a Taylor-Couette apparatus (after Ambacher et al., 1992).

First of all an axial field H_z parallel to the cylinder axis can be applied. To obtain a homogenous field over the whole fluid gap, an arrangement of four coils on a spherical shell – a so called Fanselau arrangement (Fanselau, 1929) has been chosen. By an appropriate choice of the coil sizes, this arrangement allows the generation of a magnetic field with a homogeneity of better than 0.1 % over the whole fluid volume (Ambacher et al., 1992).

The second possible field direction is an azimuthal magnetic field, which can be generated by a current leading wire along the cylinder axis. In this case the generation of a field of appropriate strength requires the use of electric currents of up to approximately 1000 A resulting in a severe generation of Ohmic heat. Thus the current leading wire has to be designed as water cooled tube and serious attention has to be paid to the control of the temperature influences on the experimental results (Odenbach and Gilly, 1996). The third natural field direction is a radial magnetic field H_r directed from the inner to the outer cylinder of the Taylor Couette arrangement. To generate such a field, two coils have been placed on a high permeable rod. The coils generate antiparallel magnetic fields. If an appropriate outer connection for the magnetic flux is established by a steel tube, the direction of the field in the central region of the rod is radial as depicted in Fig. 3.10 (Ambacher et al., 1992). The two later arrangements allow only the generation of relatively weak fields of up to about 10 kA/m. But this is sufficient for the weak field test of the $<\sin^2\beta>$-law discussed here. The three different field directions provide three different mean angles between field direction and vorticity of the Taylor vortex flow. The value of $<\sin^2\beta>$ has been calculated using numerical data for the flow profile of the vortex flow (Lücke, 1992). The resulting values are 0.63 for the axial field, 0.69 for the azimuthal field and 0.68 for the radial field.

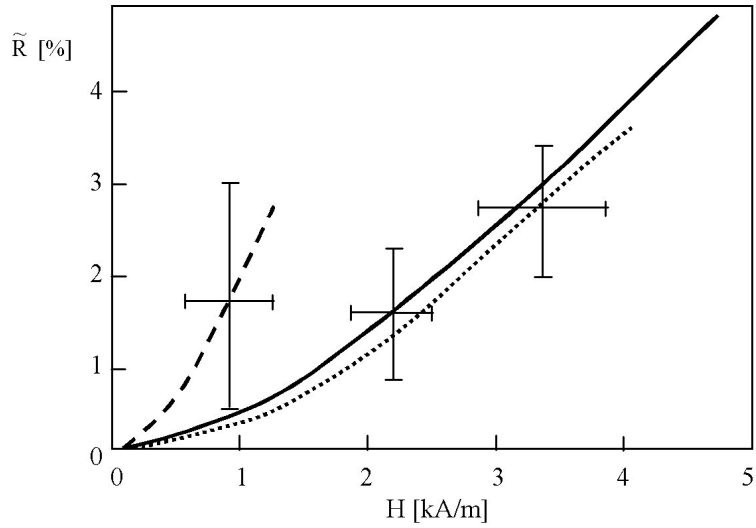

Fig. 3.11. The change of the reduced rotational viscosity in APG513A as a proof of Shliomis' $<\sin^2\beta>$-law. (full: axial field, dashed: azimuthal field, dotted: radial field)

To enable a comparison of the experimental data with the $<\sin^2\beta>$-law, we introduce the reduced relative change of viscosity

$$\widetilde{R} = \frac{1}{<\sin^2\beta>} R \quad , \tag{3.42}$$

which makes the field-dependent viscosity changes independent from the field direction. This value is plotted in Fig. 3.11 for the three different fields for the fluid APG513A (Odenbach, 2000). Within the margins of error the three curves coincide, providing a sufficient test of the validity of the $<\sin^2\beta>$-law. Concerning the scatter of data one should keep in mind, that the values for the different field directions have been obtained over many years using the same kind of fluid but different samples. As it will become clear from the discussion in Sect. 4.3.2 slight production dependent changes in the microscopic make-up of the fluid would be able to give rise to the observed scatter of the data. In principle another possible explanation for the slight observed discrepancies might be caused by an influence of the magnetic field to the flow structure itself. As already mentioned in (Shliomis, 1972) such changes might influence the measure of viscosity in the fluid. For the Taylor Couette arrangement used for the determination of the data shown in Fig. 3.11, such changes have been theoretically investigated (Niklas, 1987; Vislovich et al., 1986). The change of the flow profile is established as a variation of the wavelength of the instability, i.e. of the axial size of the flow vortices. It should be mentioned here, that this effect is a result of the appearance of an anisotropic change of viscosity in the fluid. For example an axial field will not hinder a rotation of the particles caused by the azimuthal component of the flow,

while the radial and azimuthal component are influenced. On the other hand radial and azimuthal fields will hinder – to a different amount – all three flow directions. A detailed analysis (Niklas, 1987) shows, that an axial field leads to a decrease of the axial vortex size, a radial one generates an increase while an azimuthal field does not change the wavelength of the flow at all. Due to the problems of observation of flow profiles in magnetic fluids, a quantitative experimental test of the phenomenon is still pending. Fig. 3.12 shows a qualitative prove to give an idea of the real existence of the predicted flow changes. In this test, we've attached a small permanent magnet to the outer cylinder, generating an inhomogeneous field with radial and axial components in the fluid. The flow profile has been observed by means of an ultrasound Doppler velocimeter (Takeda et al., 1991). The shown time dependence of the flow profile indicates flow towards the flow sensor in black and counter directed flow in white. Thus the distance between two white or two black stripes indicates the axial size of the vortices. It is seen in Fig. 3.12, that for the instance of time where the magnet has been applied, a change of the flow profile in the field region appears. At places where the radial component dominates, an increase of the vortex size is observed while a decrease appears in the region where the axial field component is dominant. Obviously this is only a crude qualitative test since the inhomogeniety of the field will have important influence on the flow too. Nevertheless it shows that the predicted changes in the flow profiles really exist. But since their magnitude depends on the change of viscosity (Niklas, 1987), the weak field measurement performed for the $<\sin^2\beta>$-test will not seriously be affected by these changes.

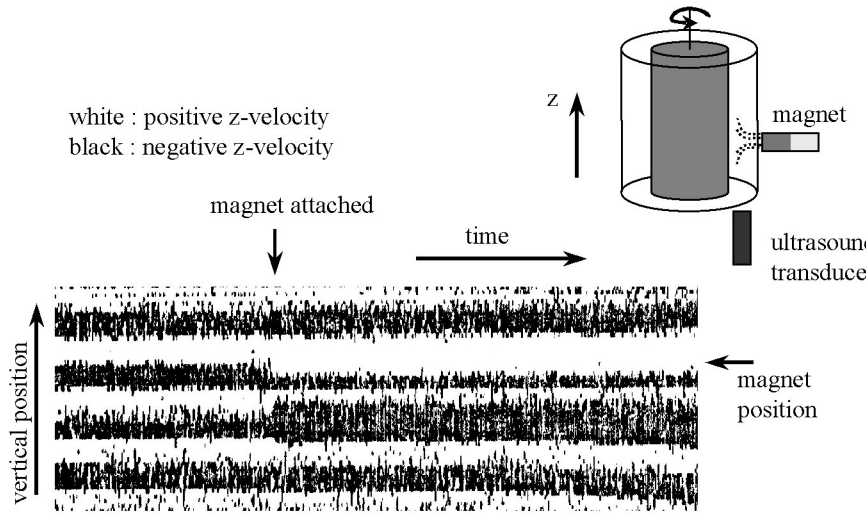

Fig. 3.12. The change of the flow profile of Taylor vortex flow in a ferrofluid in the presence of a magnetic field as measured by ultrasound Doppler velocimetry. In the time evolution flow towards the sensor is indicated in black, flow in the counter direction in white.

At this point one should mention, that the field-dependent viscosity changes obviously provide a tool for flow control in magnetic fluids, since flow components with vorticity perpendicular to the field direction will be suppressed. This has been used e.g. in (Schwab, 1989; Odenbach, 1995a) to align the flow of thermomagnetic convection in certain directions.

Stepping back to Shliomis´ theory we should finally recognize, that it does not contain any shear dependence of the magnetoviscous effect. With other words it is – in principle – only valid for vanishing shear rate. This is neither valid for McTague's experiments (McTague, 1969), where no information on shear rate is provided, nor for the experiments in the Taylor-Couette arrangement, where the shear rate has been about 500 s^{-1}. Just one single experiment has been carried out to provide a shear free measurement of magnetically induced changes of the viscosity of a ferrofluid (Embs et al., 2000). In this experiment a cylindrical vessel filled with ferrofluid has been used as the weight of a torsional pendulum (see Fig. 3.13). The vessel is internally segmented to avoid any flow of the fluid in the vessel. This guarantees that the fluid performs a solid body oscillation. If a magnetic field is applied perpendicular to the axis of oscillation of the pendulum, a situation is generated where the vorticity of the flow is perpendicular to the field. The resulting hindrance of rotation of the particles in the fluid due to the action of the field leads to an additional damping term for the oscillation of the pendulum, which can directly be related to the field-dependent viscosity increase in the fluid. The advantage of the system is, that no shear flow appears in the fluid. Thus the magnetoviscous effect can be measured shear free. In principle this should be an excellent basis for a comparison of the experimental data with Shliomis' theory. In (Embs et al., 2000) the experiments have been carried out with a highly purified commercial magnetic fluid containing 3.3 vol.% of magnetite particles. The results for the rotational viscosity obtained from the damping of the pendulum appear to fit with Shliomis´ theory of rotational viscosity. Taking this into account the measured magnetoviscous effect in this experiment is significantly higher than the theory of rotational viscosity would predict if only the small portion of larger magnetically hard particles being present in the fluid would be taken into account.

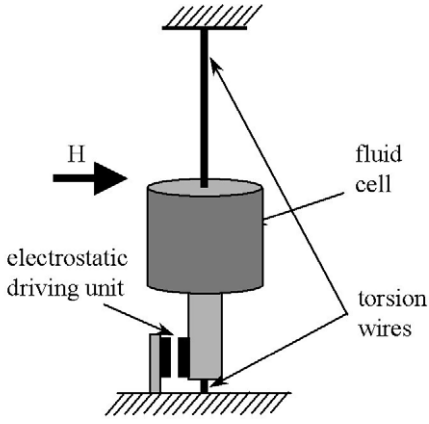

Fig. 3.13. A torsional pendulum for the determination of rotational viscosity (after Embs et al., 2000).

This immediately sheds a different light to the discrepancies between the results in (Embs et al., 2000) and those for other commercial fluids e.g. in (Weser and Stierstadt, 1985b; Ambacher et al., 1992; Odenbach et al., 1999a) discussed in (Embs et al., 2000). We will come back to this question at the end of Sect. 4.3.2, showing that it is mainly based on problems in the interpretation of a macroscopic measurement of magnetoviscous effects on the basis of assumptions concerning the microscopic make-up of the fluids.

Before ending this section one should recall, that – as already mentioned – parts of Shliomis' theory have been subject to criticism over the years. In particular the question of entropy production has been risen several times and different approaches concerning the stress tensor (Felderhof and Kroh, 1999; Müller and Liu, 2001) and the equation for relaxation of magnetization (Liu, 1995; Müller and Liu, 2001) have been made. It is not within the scope of this work to discuss these different theoretical approaches for rotational viscosity in detail. In particular not, since the principle concept of hindrance of rotation of magnetic particles as it has been used in (Shliomis, 1972) has never lost its importance in the understanding of the behavior of ferrofluids. As we will see, only the microscopic model will have to be modified leading from single particles to chains and agglomerates determining the magnetoviscous behavior. Readers interested in the theoretical discussion concerning the basis of the theory of rotational viscosity are particularly referred to an article by Engel (Müller and Engel, 1999), comparing Shliomis´ approach (Shliomis, 1974; Shliomis, 1972) with that of Liu (Liu, 1995).

3.2 "Negative" viscosity

Up to now we have always assumed, that a static magnetic field is applied to the ferrofluid, hindering the magnetic particles' free rotation, and leading to an increase of the fluid's viscosity. For the reason of completeness, and since interesting new effects will appear, we should have a short glance at the effect of an alternating magnetic field on the viscous behavior of magnetic fluids. As in Sect. 3.1 we will assume that the magnetic particles are noninteracting – the question of interparticle interaction and its importance for magnetoviscosity will be in the focus of Chap. 4.

If one assumes a ferrofluid under shear being exposed to a static magnetic field, it is clear that a situation where the viscous torque slightly exceeds the magnetic hold will result in an inharmonic but hindered rotation of the particles. In the case of an alternating magnetic field the influence of the field may have a different characteristic. If the fields frequency equals that of the particle rotation, no influence of the field on the particle rotation will be observable any more and field frequencies slightly higher than the frequency of particle rotation induced by the shear flow may speed up the rotation of the suspended particles. Even from this simple argument it is directly seen, that an oscillation of the field will reduce the magnetoviscous effect.

Such phenomena were first considered by Shliomis and Morozov (Shliomis and Morozov, 1994). Obviously the ferrohydrodynamic equations discussed in

Sect. 3.1 do not distinguish between static and alternating magnetic fields. Thus they are suitable to calculate the effective viscosity of a ferrofluid as well in the static as in a time dependent situation. In (Shliomis and Morozov, 1994) this approach is separated into two parts – the discussion of weak fields and that of fields of arbitrary strength. We will focus here on the first part giving the principle of the occurring effects, while for the second part only the results and their comparison with experiments will be discussed. The advantage of the weak field approximation is the possibility to use a linearized equation – $M = \chi H$ – for the magnetization of the fluid. For an alternating field polarized in the x- direction

$$H_{x(t)} = H_0 \cos(\omega t) \quad , \tag{3.43}$$

with the field's amplitude H_o and its oscillation frequency ω, (3.12) and (3.14) lead to a magnetization component in x-direction

$$M_x = \chi H_0 \cos(\omega t - \delta) \tag{3.44}$$

if a quiescent state, i.e. $\Omega = 0$ is assumed. Here δ denotes the phase angle between magnetization and field, which is determined by the relevant relaxation time of the magnetization. For magnetically hard particles with relaxation time τ_B for the Brownian relaxation process, it is then (Shliomis and Morozov, 1994)

$$\tan\delta = \omega\tau_B \quad . \tag{3.45}$$

If a flow is applied to the fluid, the magnetization will be tilted against the field direction and additional components of M in y- and z-direction will appear. For a flow with vorticity in z-direction only the y-component of $\vec{M}$ will remain for the discussion of the problem and with $\tilde{M}_y$ being the amplitude of this time dependent magnetization component, which will oscillate with the same frequency as $H_{x(t)}$ but with a phase delay θ, one obtains

$$M_y = \tilde{M}_y \cos(\omega t - \theta) \quad , \tag{3.46}$$

which can be used in (3.12) and (3.14) again, leading to (Shliomis and Morozov, 1994)

$$\begin{aligned} \tilde{M}_y &= \Omega\tau_B \chi H_0 \cos^2\delta \\ \theta &= 2\delta \end{aligned} \quad . \tag{3.47}$$

This y-component of M is responsible for the magnetic torque acting on the particles in a field polarized in y-direction and one obtains

$$\vec{M}\times\vec{H} = M_y H_x = \Omega\tau_B \chi H_o^2 \cos^2\delta \cos(\omega t)\cos(\omega t - 2\delta) \quad . \tag{3.48}$$

Using this in (3.12) for the steady state (dS/dt = 0) and averaging over the fast time scale of the problem given by the magnetic field frequency and thus by the relaxation speed of magnetization one can calculate the rotation frequency of the particles ω_p to be (Shliomis and Morozov, 1994)

$$\omega_p = \Omega \left(1 - \frac{\alpha^2}{6} \frac{\left(1 - \omega^2 \tau_B^2\right)}{\left(1 + \omega^2 \tau_B^2\right)^2} \right)$$

$$\alpha = \frac{\mu_0 mH}{k_B T} \quad . \tag{3.49}$$

This expression can now be used to obtain the field-induced viscosity change by means of (3.33) as

$$\Delta\eta = \frac{1}{4} \eta \phi' \alpha^2 \frac{1 - \omega^2 \tau_B^2}{\left(1 + \omega^2 \tau_B^2\right)^2} \quad . \tag{3.50}$$

This result transfers immediately to the weak field approximation for rotational viscosity (3.39) for $\omega = 0$, thus the classical form of rotational viscosity (Shliomis, 1972) can be seen as a special case of the results in (Shliomis and Morozov, 1994). For $\omega\tau_B = 1$ we reach the case of a match of the field frequency with the relaxation of the magnetization and thus, as argued earlier, the field effect on viscosity will vanish. For even higher frequencies we see, that the viscosity change in (3.50) can become negative – the particles rotation is driven by the field and this driving spins up the fluid resulting in a decrease of viscosity (see Fig. 3.14). This part of the field-dependent viscosity contribution leads to the name "negative viscosity" introduced in (Shliomis and Morozov, 1994).

It should be noted, that a second approach to calculate the frequency dependence of the viscosity of a ferrofluid has been undertaken at the same time as Shliomis published his work on negative viscosity (Shliomis and Morozov, 1994). A month prior to publication of (Shliomis and Morozov, 1994; Salueña and Rubí (Salueña and Rubí, 1995) handed in a calculation based on a Smoluchowski equation of the correlation of the magnetic moments of the particles and thus taking into account a certain interparticle interaction. They also find a decrease of viscosity with increasing magnetic field, but in contrast to (Shliomis and Morozov, 1994), a direct comparison with tailored experiments is still missing.

Measurements to check the predictions of (Shliomis and Morozov, 1994) have been performed shortly after the appearance of the theory in Bacri's group in Paris (Bacri et al., 1995).

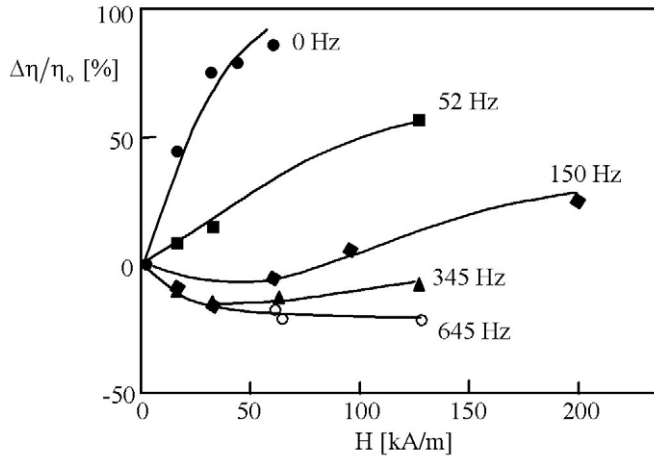

Fig. 3.14. The dependence of the relative viscosity changes of a ferrofluid in an alternating magnetic field (after Bacri et al., 1995).

They used Co-ferrite particles with a mean diameter of about 10 nm, being charge stabilized in water. Co ferrite has the advantage of a high crystal anisotropy leading to reliable blocking of the Néel relaxation process (see Table 2.1). The fluid’s viscosity has been investigated by means of a capillary viscometer placed in a solenoid allowing to apply a magnetic field with an amplitude of 80 kA/m, using a frequency range from 0 to 1 kHz. With this setup they obtained the viscosity changes shown in Fig. 3.14 for different frequencies of the magnetic field. Obviously one observes the well known increase of viscosity for $\omega = 0$ and for increasing frequency the expected reduction of the field-dependent component of viscosity appears. Finally at sufficiently high frequencies, one finds a negative contribution of the field-induced viscosity changes with a functional behavior being comparable to the theoretical prediction shown in Fig. 3.14.

To get a direct comparison with (Shliomis and Morozov, 1994) Bacri’s group measured the relaxation time τ_B by means of a transient birefringence experiment (Neveu-Prin et al., 1993) leading to τ_B=1.6 ms for the fluid investigated. To obtain a good overview of the field strength and frequency dependence of the viscosity changes, isolines of the relative field-dependent viscosity changes are plotted in Fig. 3.15. The left side shows calculations following (3.50) using the measured value of τ_B, while the right side gives the values measured in (Bacri et al., 1995). Good qualitative agreement between theory and experiment has been found here, and in particular the appearance of the “negative” viscosity effect has been experimentally verified.

A second set of experiments has been performed using a commercial ferrofluid containing magnetite particles (Zeuner et al., 1998) with a volume fraction of

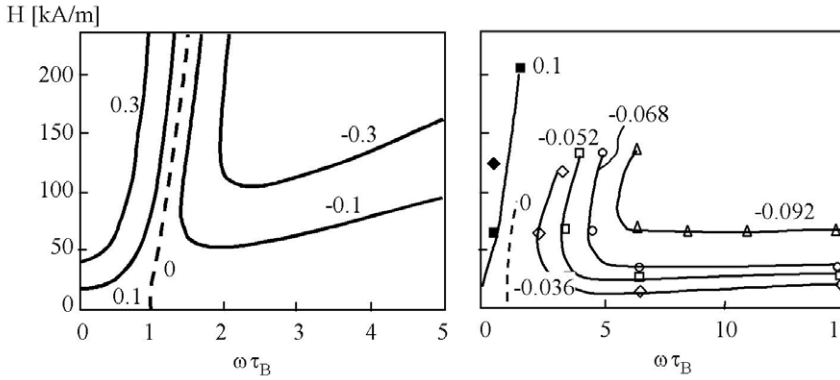

Fig. 3.15. Isolines of the viscosity changes as a function of magnetic field strength and frequency. Left side: experimental results; right side: theory by Shliomis (after Bacri et al., 1995).

about 3.6 vol.% and a mean particle diameter obtained from electron microscopy of approximately 12 nm. The experiments uses – as Bacri's work (Bacri et al., 1995) continuous flow through a capillary pipe. The special feature of the setup used here is the employment of a reference pipe placed in the fluid loop just behind the solenoid pipe which can be subjected to a magnetic field polarized in flow direction (see Fig. 3.16). By measuring the pressure drops over the reference and the solenoid pipe with and without applied magnetic field, the authors can determine the relative field-induced viscosity changes. The advantage of the reference pipe is given by the exclusion of temperature effects and other disturbing changes in the experimental parameters since the zero field reference viscosity is measured always together with the field-dependent value and thus under identical

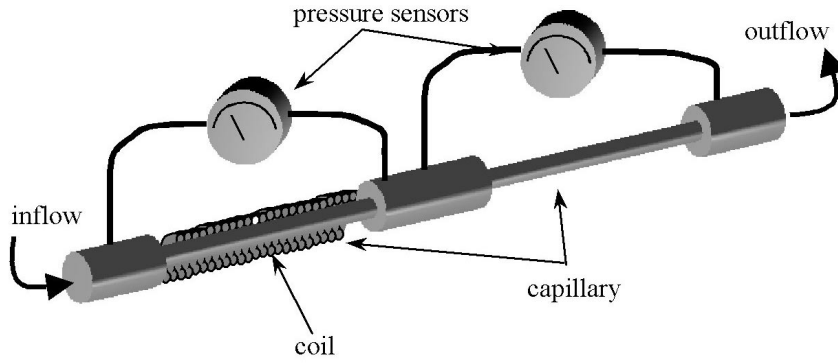

Fig. 3.16. Experimental set up to measure "negative viscosity" effects in a capillary viscometer with reference tube (after Zeuner et al., 1998).

experimental boundary conditions. In these experiments again a good qualitative agreement with the theoretical predictions (Shliomis and Morozov, 1994) has been found. At low frequencies a reduction of the field-dependent viscosity part occurs and for frequencies above approximately 6 kHz a negative viscosity effect is observed. Problems appear here in the quantitative comparison of the experimentally determined values with the extended model given in (Bacri et al., 1995). A fit of the data to the equation for the viscosity changes leads to serious problems concerning the interpretation of the results obtained for the fit parameters. The authors decided to use the relaxation time of magnetization, the hydrodynamic volume fraction and the magnetic moment of the particles as free parameters since for all three no satisfying values from other measurement had been available.

For the determination of all three parameters the lack of knowledge concerning the size distribution and the thickness of the surfactant layer is crucial. But fitting the parameters leads first of all to a frequency dependence of all three values, being most pronounced for the relaxation time. In addition the value obtained for the hydrodynamical volume fraction is so close to that of a close packing, that it is obviously physically not reasonable. Since on the other hand a reasonable qualitative agreement with the theory has been found, the authors come to the conclusion, that – besides effects due to errors in the determination of the size distribution – in particular interaction of the particles may have influenced the experimental results. A situation quite similar to the results for the viscosity changes obtained in an even higher concentrated fluid in (Ambacher et al., 1992), which will be quantitatively discussed in the next section.

Thus, as a conclusion of the effect of rotational viscosity, we can state two major points. First it has been seen in very different experiments, using a wide variety of magnetic fluids, that the concept of hindrance of rotation of magnetic units in a shear flow due to the action of a magnetic field is well suitable for the qualitative explanation of the appearance of field-induced viscosity changes. On the other hand the quantitative comparison of experimental data with the theory based on the assumption of non–interacting particles leads to significant differences in particular for relatively high concentrated fluids. This point leads to the assumption, that the interparticle interaction has great importance for the magnetoviscous effects. Evidence for this assumption and resulting consequences will be the subject of the following discussion.

4. Magnetoviscosity in concentrated ferrofluids

In Sect. 3.1 it has been discussed, that a magnetic field exerts a torque to the magnetic particles in the fluid, influencing their free rotation in a shear flow. The theory used to describe the related phenomena explicitly excludes any interaction of the magnetic particles to allow a treatment in form of a single particle model.

As a consequence, experiments performed to provide a quantitative proof of the above mentioned theoretical approaches have to deal with highly diluted ferrofluids. This leads to the fact, that the changes of viscosity induced by the magnetic field are in the order of a few percent in maximum (McTague, 1969). Such small changes of viscosity are obviously of no technical importance at all. Nevertheless, as mentioned in the discussion of future applications in Sect. 2.4, the change of the properties of the fluids due to the influence of magnetic fields, and in particular the reversible variation of their viscous behavior, is one of the most challenging fields in this respect. To allow for a technically reasonable strength of field-induced viscosity changes an increase of the concentration of magnetic particles is doubtlessly unavoidable. If the magnetic volume fraction is increased, particle-particle interaction will increase too and may become the most significant parameter for the magnetic changes of the fluid's viscosity. Besides opening the door to new application areas, the introduction of particle interaction increases also the possibilities for basic research due to the externally variable strength of this particle interaction. Furthermore all fluids used for typical technical applications have a magnetic volume concentration in the order of 10 vol.%. At such high concentration interaction can not be excluded and a knowledge of the resulting viscous changes is of importance for the design of the applications. Since interaction is not included in Shliomis' model (Shliomis, 1972) the single particle model for rotational viscosity used there will not longer be sufficient to give a quantitative description of the occurring effects. To avoid confusion we will denote from here all field-induced changes of viscosity in concentrated suspensions as magnetoviscous effects to provide a clear discrimination from the rotational viscosity observed in diluted systems in the absence of particle interaction.

4.1 Magnetoviscous effects in commercial fluids at high shear rate

In Sect. 3.1 we have shortly discussed the qualitative agreement of experimental data, obtained using the transition frequency from Couette to Taylor vortex flow,

S. Odenbach (Ed.): LNP m71, pp. 59–84, 2002.

with the $<\sin^2\beta>$-dependence in Shliomis´ theory (3.31). The related experiments have been carried out with a commercial magnetite based magnetic fluid having a volume concentration of magnetic material in the order of 7 vol.%. Thus it is to be expected that particle interaction may influence the results concerning the magnetoviscous properties. For small magnetic field the discussion in Sect. 3.1 showed clearly, that qualitative agreement with the theory (3.31) is given. Now we will focus on the quantitative aspects of the fluid's behavior and on the magnetoviscosity at higher magnetic field strength. Fig. 4.1 shows the dependence of the relative change of viscosity $R=(\eta_{(H)}-\eta_o)/\eta_o$ obtained in an axial magnetic field with a strength of up to 40 kA/m (Ambacher et al., 1992). The shear rate $\dot{\gamma} = dv/dr$ applied in the experiment is about $\dot{\gamma}$ =500 s^{-1}. Obviously a strong increase of viscosity with field strength is observed.

As mentioned, the fluid used contains magnetite particles with a total volume concentration of magnetic material of 7.2 vol.%. The size distribution of these particles obtained from a magnetogranulometric analysis is shown in Fig. 4.2. The mean size, as obtained from the initial susceptibility of the fluid is $\bar{d}$ =10 nm, corresponding well to the data of the size distribution.

A first step to compare the experimental data on the magnetoviscous effect with (3.31) is to calculate the rotational viscosity using the size distribution and the volume concentration known form magnetization measurement.

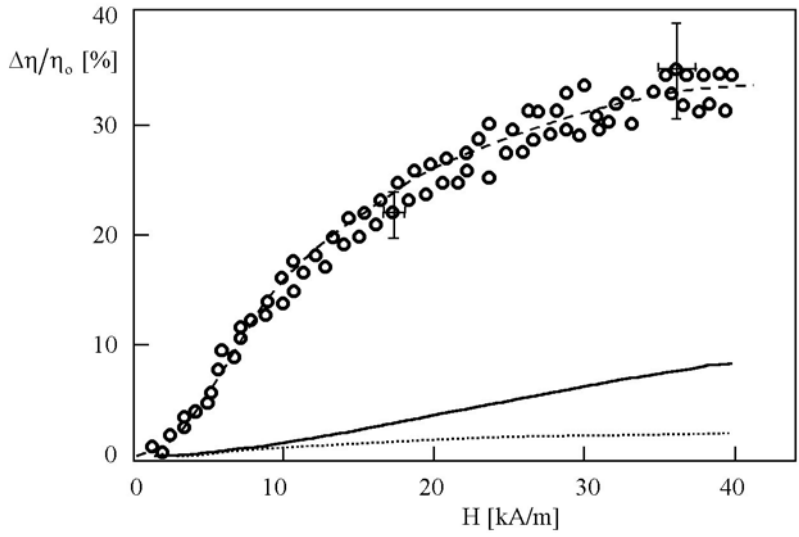

Fig. 4.1. The relative change of viscosity in a magnetite based ferrofluid (APG513A) measured at $\dot{\gamma}=500 s^{-1}$. The full line represents the calculated values from Shliomis' theory assuming $\bar{d} = 10\,nm$ and $\phi' = 0.18$, i.e. all magnetic material contributing to the effect. The dotted line is calculated by (3.31) too, but accounts only for the large magnetically hard particles (i.e. the shaded fraction in Fig. 4.2.) The dashed line represents a fit ($\bar{d} = 16\,nm$, $\phi' = 0.18$) of (3.31) to the experimental data.

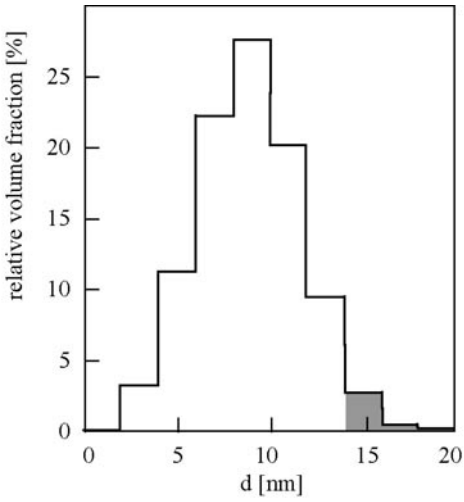

Fig. 4.2. Size distribution of the fluid used for the experiments shown in Fig. 4.1 as obtained from magnetogranulometric analysis.

The resulting full line in Fig. 4.1 shows a significant quantitative discrepancy with respect to the experimental data. In addition it has to be observed, that only particles being magnetically hard should contribute to the viscosity changes (see Sect. 3.1). As discussed earlier (Sect. 2.2.2) the magnetic relaxation behavior depends strongly on the particle size. For magnetite, the critical diameter for the transition from Néel-relaxation to magnetically hard behavior is about 13 nm. Therefore only particles larger than this critical diameter should contribute to the change of viscosity discussed here and might thus be taken into account in calculations following (3.31). From Fig. 4.2 it is obvious, that these particles represent only a very small fraction of the total magnetic mass suspended in the fluid. Thus, a correct interpretation of (3.31) using the relevant part of the fluid data will lead to an even stronger discrepancy between experimental data and theory (dotted line). On the other hand a fit of (3.31) to the experimental data, leaving the particle size as a free fit parameter leads to a good agreement of the fitted values with the measured data if a mean diameter of about $\bar{d}$ =16 nm is assumed. Obviously this fit is not a realistic physical description of the situation since the magnetization measurement leads to significantly different values for the particle sizes. Nevertheless it leads to two starting points for the understanding of the magnetoviscous behavior. First of all the possibility to fit (3.31) to the data allows the assumption that the changes of viscosity are driven by the hindrance of free rotation of structures carrying a magnetic moment which is spatially fixed within the structure. Furthermore it becomes clear at this point that particle-particle interaction plays an important role for the appearance of the magnetoviscous effects in concentrated ferrofluids. The problem, which has to be solved now, concerns the question, what kind of microstructural changes give rise to the observed effects and which interactions are important for the related phenomena. Since magnetic fluids are complex systems, and since many parameters related to the microstructural make-up of the suspensions will influence their magnetoviscous properties, it is *a priori* extremely difficult to give

tremely difficult to give a reliable prediction how a real suspension would behave. Therefore the historical evolution of the field required a subsequent development of experiments and models to get an insight into the related phenomena. In these experiments single parameters were changed and the resulting variation in the magnetoviscous behavior has been used as input for new models leading to new starting points for further experimental proofs. In the following we will first discuss the experimental techniques available for the investigation of field effects on viscosity of ferrofluids. After this the experimental data and the related models will be presented in detail.

4.2 Experimental techniques for the investigation of magnetoviscous properties in ferrofluids

4.2.1 Capillary viscometers

In the first experiments on rotational viscosity carried out by McTague in 1969 (McTague, 1969) a capillary viscometer has been used. The details of these experiments have already been described in Sect. 3.1. Thus we will here only discuss the advantages and problems of this technique for an investigation of magnetoviscous effects in general. Normal capillary viscometers are characterized by a parabolic flow profile (see (3.3)) in the measuring section. As discussed in Sect. 3.1 this allows the application of two different magnetic field directions with respect to the flow. A solenoid producing a field in direction of the flow will maintain an angle of $\beta = 90°$ between field direction and vorticity of the flow, while placing the capillary into the gap of an electromagnet with $\vec{H} \perp \vec{\vartheta}$ provides a value for $\langle \sin^2\beta \rangle = 0.5$.

An arbitrary alignment between field direction and vorticity can not be achieved in a suitable form with this technique. Thus an experimental test of the $\langle \sin^2\beta \rangle$-behavior predicted in (Shliomis, 1972) required a more complex flow (Ambacher et al., 1992) as discussed in Sect. 3.1.

An extension of the capillary method has been described by Maiorov (Maiorov, 1980) using a flat channel instead of the capillary (see Fig. 4.3). The break of symmetry in the flow profile compared with the tube flow in normal capillary viscometers, leading to

$$v_x = v_0(a^2 - y^2);\ v_y = 0;\ v_z = 0 \tag{4.1}$$

allows to obtain one additional field direction with respect to the flow profile providing a possibility to obtain additional information on the fluids' properties. Here a denotes the gap width between the parallel plates of the channel as depicted in Fig. 4.3. The vorticity for the flow profile in (4.1) is given by

$$\Omega_z = v_0 y \quad . \tag{4.2}$$

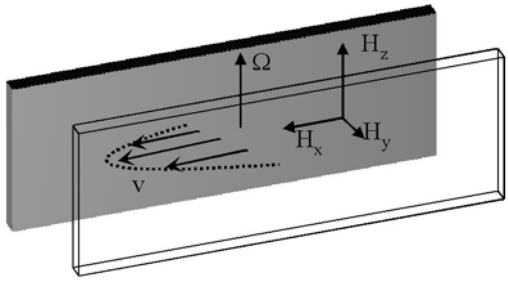

Fig. 4.3. A flat channel arrangement for the investigation of magnetoviscous effects as used in (Maiorov, 1980).

Thus obviously a field in z-direction leads to $\beta = 0$ while fields in x- and y direction provide $\beta = 90°$.Thus no further information concerning the $<\sin^2\beta>$-law can be obtained. Nevertheless the field direction in x- and y-direction are different since H is perpendicular to Ω and v for H || y and it is perpendicular to Ω but parallel to v for H || x. For a colloid containing spherical particles no difference of the magnetoviscous behavior will appear for the two directions, but an ellipsoidal particle shape will lead to a reduction of the viscosity increase for the field parallel to the flow direction (Maiorov, 1980; Grants et al., 1990). In addition a viscosity change for H || Ω is expected for non spherical particles too (Grants et al., 1990). Thus the mentioned reduction of symmetry allows an insight into the sphericity of the particles in addition to the normal determination of the magnetoviscous effect.

Besides the mentioned problem concerning the choice of the angle β between field and vorticity, two further backdraws appear if a capillary viscometer is used in experiments on magnetoviscosity in ferrofluids. The first one concerns the proper alignment of flow and field in general and the possibility of appearance of disturbing magnetic forces.

If a field is applied to the capillary one has to pay special attention to the effects appearing at the edges of the capillary as well as at the end of the magnetic field region. Usually the capillary and the in- and outflow regions are placed completely in a region of constant magnetic field. This leads to a constant field all over the measuring region, but the respective alignment of field and vorticity is not well defined in the in- and outflow region. The lack of knowledge of β in these regions leads to a systematic error in the interpretation of the experimental results. Furthermore Shliomis (Shliomis, 1972) already stated, that magnetic influences on the flow profile may severely affect the experimental results. This problem has to be considered for the in- and outflow regions as well as for the regions of inhomogeneous magnetic field appearing in solenoids as well as in magnetic fields produced by electromagnets with pole shoes. The field gradients appearing in these regions will give rise to magnetic forces which will influence the flow profile too.

If the field region is restricted to the measuring capillary, the problem will even rise since now the region of magnetic field gradients will affect the in- and outflow to the capillary directly resulting in unpredictable flow profiles and therefore in serious problems for the interpretation of the experimental data.

These problems have been negligible in McTague's experiments, since highly diluted ferrofluids have been used. If concentrated fluids are to be considered, the magnetic forces and therefore their influence on the flow profile will rise, limiting

the applicability of this method of viscosity determination in an unpredictable way.

The experiments on negative viscosity discussed in Sect. 3.2, which were performed using capillary viscometers, reduced these problems by differential measurement (Zeuner et al., 1998) and restriction to relatively small magnetic fields.

Furthermore a capillary viscometer will usually provide only a single shear rate for the investigation of the viscosity changes. If non-newtonian effects are to be investigated, a variation of shear rate becomes unavoidable. Therefore other techniques have to be considered to enable a detailed investigation of magnetoviscous effects in ferrofluids.

In Sect. 3.1 the use of the transition from Couette to Taylor vortex flow for the determination of rotational viscosity has been presented. As mentioned there, this technique provides the possibility to apply magnetic fields with different angles relative to the vorticity of the flow.

The influence of magnetic fields on the flow profile in this geometry has been theoretically predicted (Niklas, 1987; Vislovich et al., 1986) and is restricted to a change of wavelength of the instability, which does not affect the results for the range of viscosity changes observed in (Ambacher et al., 1992; Odenbach and Gilly, 1996) since the change of wavelength of the instability is less than 1 % and thus its influence can be neglected in comparison to the overall accuracy of the experiment. Nonetheless this geometry is not preferable for a detailed investigation of magnetoviscous effects, since it does not allow a continuous change of shear rate. Such changes would have to be performed by a variation of the cylinder geometry, requiring an exchange of the cylinders themselves.

4.2.2 Rheometers

The problems discussed above made clear, that an investigation of magnetoviscous effects in ferrofluids does not only require the possibility of application of variable magnetic fields of sufficient field strength, but also the variation of shear rate over a certain range.

If we additionally assume that – as we will see later on – non Newtonian effects can appear in ferrofluids under influence of magnetic fields, it becomes obvious that techniques from the field of rheology have to be employed to enable adequate investigations. For a non-Newtonian liquid the flow function

$$F_{(\dot\gamma)} = \eta_{(\dot\gamma)}\ \dot\gamma \tag{4.3}$$

is the characterizing quantity providing the information on the flow properties of the liquid which appear in stationary laminar flow. For a Newtonian liquid (4.3) obviously reduces to $F_{(\dot\gamma)} = \eta_{(\dot\gamma)}\ \dot\gamma$ with the shear viscosity η being independent of shear rate. For non-newtonian liquids the viscosity can change with shear rate, an effect that will be discussed for ferrofluids in Sect. 4.3. As mentioned, the flow function $F_{(\dot\gamma)}$ describes fluid properties which become visible in stationary laminar flows and thus the investigation of $F_{(\dot\gamma)}$ requires such a kind of flow. For example the determination of the dropping time of a sphere in a liquid would not be suit-

able since the flow around the sphere is a flow with non constant dilatation history and thus additional effects like memory phenomena would be able to influence the measurement. A good approximation of a stationary laminar flow can be obtained e.g. in a fluid between concentric rotating cylinders or between two plates or a cone and a plate (see Fig. 4.4). If in these geometries the gap between the cylinders or the opening angle of the cone are small, the shear rate can furthermore assumed to be constant all over the fluid sample. Since the stress depends on shear rate $\dot{\gamma}$ only, it is thus constant everywhere in the fluid too. In particular its value on the surface of the bounding material components - i.e. the cylinders or the cone or the plate - is the same as in the fluid and therefore the torque acting on one of the bounding components can be used as a measure for the stress.

For the cone–plate situation, the torque acting on the cone can be easily calculated to be (Whorlow, 1992)

$$N_{(\dot{\gamma})} = \int_0^{r_o} 2\pi r^2 \sigma_{(\dot{\gamma})} dr = \frac{2\pi}{3} r_o^3 \sigma_{(\dot{\gamma})} \tag{4.4}$$

where r_o denotes the radius of the cone and σ the stress in the fluid.

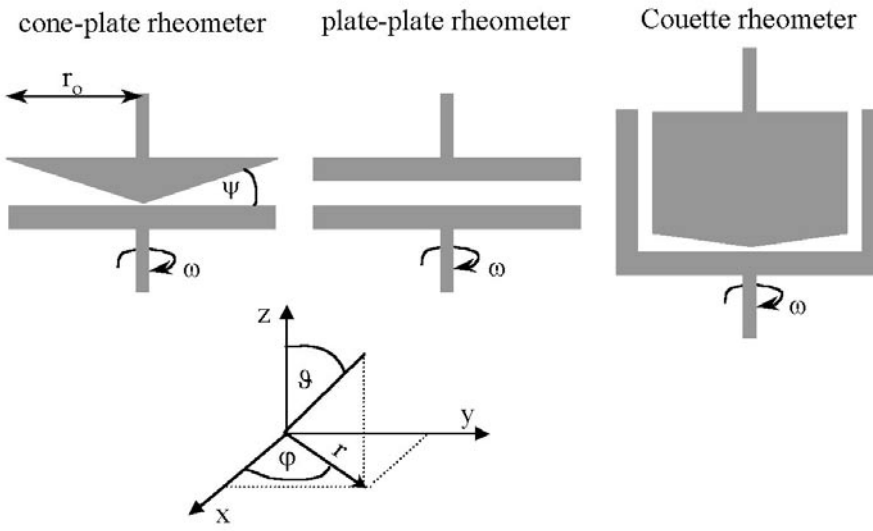

Fig. 4.4. Different geometries for the generation of stationary laminar flow used for rheometric investigations.

In the cone plate geometry the flow profile can be denoted in spherical polar coordinates to be

$$v_r = 0 \; ; \; v_\varphi = r \, (\sin \vartheta) \, \omega_{(\vartheta)} \; ; \; v_\vartheta = 0 \tag{4.5}$$

where r, φ, ϑ denote the usual coordinate directions (see Fig. 4.4). Thus, in this geometry, the shear rate acting on the fluid can be written as

$$\dot{\gamma} = \sin \vartheta \, \frac{d\omega}{d\vartheta} \quad . \tag{4.6}$$

With the assumption of a small opening angle ψ of the cone, $\sin \vartheta \approx 1$ and $d\omega/d\vartheta$ can be replaced by $\Delta\omega/\psi$ leading to an expression for the shear rate in the form

$$\dot{\gamma} = \frac{\Delta\omega}{\psi} \quad , \tag{4.7}$$

where $\Delta\omega$ is the difference in angular velocities of cone and plate. Together with (4.4) and the known relation between shear rate and stress $\sigma = \eta\dot{\gamma}$ we obtain for the viscosity

$$\eta = \frac{3\psi}{2\pi r_0^3} \, \frac{N_{(\dot{\gamma})}}{\Delta\omega} \quad . \tag{4.8}$$

Thus the flow function in this system can be written as

$$F_{(\dot{\gamma})} = \frac{3}{2\pi r_0^3} \, N_{(\dot{\gamma})} \quad , \tag{4.9}$$

and it is therefore directly proportional to the measured torque, where the proportionality constant is just a geometry dependent quantity given by the properties of the rheometer.

To use these techniques for the investigation of magnetoviscous effects in ferrofluids one has to be able to apply a magnetic field to the flow. This can be done either by a modification of commercially available rheometers or by the design of a specialized system for ferrofluid investigations. The choice between both possibilities is determined by the particular research goal. The first alternative is often used in application oriented research, where strong magnetic fields are required to obtain high magnetoviscous effects suitable for technical application. In these cases, where the fluid is magnetized close to saturation, the accuracy of field direction and homogeneity is not of first importance since only the maximum of the magnetoviscous effect is in the focus of the investigation.

For detailed parameter studies, needed for the exploration of the physical background of the effects, specially designed systems have to be considered. In the following we will first describe the modified commercial systems and afterwards a specialized rheometer for ferrofluid investigations, which has been used for most of the experiments discussed in this section.

To allow controlled magnetic field influences on a magnetic fluid, the flow cell of commercial rheometers has to be modified. First of all it has to be made of nonmagnetic materials like brass or aluminum instead of the commonly used stainless steel. Since the experiments using such rheometers are usually focused to the high field region, it has to be observed, that the field is not allowed to be perpendicular to a free surface of the fluid, since elsewhere the appearance of the spike like structure of normal field instability would influence the measurement. This problem will be discussed in more detail in the frame of the discussion of the specialized ferrofluid rheometer.

Due to this restriction concerning the direction of the magnetic field the usual modification of a rheometer for use with magnetic fluids consists of a Couette geometry with a four sector field as shown in Fig. 4.5 (Spur et al., 2001; Kormann et al., 1996a). The Couette cylinder is placed between two 90° pole shoes and the inner cylinder contains a soft iron piece to minimize the gap width between the pole shoes. The pole shoes have to be formed in a way that stray fields outside the fluid region are minimized. This is necessary, since the torque sensors are commonly based on inductive measurement techniques which may be influenced by external fields.

A coil on the yoke produces a strong magnetic field, which is led through the fluid cell by the pole shoe arrangement. In this way strong magnetic fields are obtained in two sectors of the fluid gap. In the center of these sectors the field is perpendicular to the shear plane and therefore to vorticity, leading to a maximal change of viscosity due to the hindrance of rotation of particles and agglomerates in the fluid. The disadvantage of the arrangement is the inhomogeniety of the field over the fluid gap. In the two sectors perpendicular to the pole shoe arrangement a significantly lower field is obtained. Thus a magnetic field gradient in the fluid influences the measuring results.

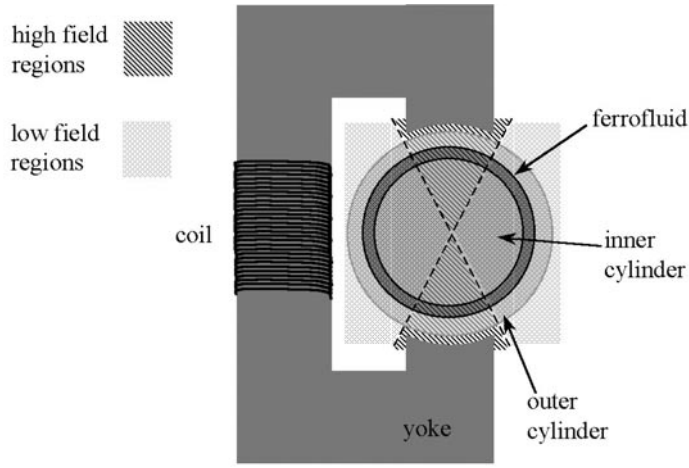

Fig. 4.5. High field magnetization stage for a modified rheometer used in magnetic fluid investigations (Kormann et al., 1996a).

This inhomogeniety is further enforced by the finite height of the pole shoes, leading to a field gradient in axial direction over the fluid volume.

In addition the angle between vorticity and flow changes over the fluid gap too, again influencing the results and increasing the difficulties in a comparison of the experimentally obtained data with theoretical approaches describing magnetoviscous effects. Nevertheless for parameter studies of fluids being determined for technical use, this technique leads to valuable results concerning yield stress and the overall magnetoviscous behavior. This is in particular true, since magnetic fields in real technical applications will neither fulfill the condition of homogeneity nor will have constant angle with respect to the flow. In such cases only the overall change of the viscosity of the fluid is of importance.

4.2.3 A specialized rheometer for the study of magnetoviscous effects in ferrofluids

As discussed above the modification of commercial rheometers for use with magnetic fluids leads to a system that does not allow a direct comparison of experimental data with theoretical approaches to a microstructural explanation of the magnetoviscous phenomena, since field direction and homogeneity are not good enough defined. The microstructural understanding of magnetoviscosity is nevertheless the essential key to the development of new fluids with stronger and therefore technologically interesting influence of magnetic fields on their viscous behavior. Thus a specialized rheometer for magnetic fluids had to be designed (Odenbach et al., 1999a), allowing proper alignment of a highly homogenous magnetic field with the flow structure. We will spend this section to the description of this rheometer, since most of the data on magnetoviscous properties discussed later on in this section has been obtained with this system. Thus its technical make-up and measuring accuracy is of serious importance for the interpretation of those results.

As mentioned already, a constant angle between vorticity and magnetic field direction, as well as the homogeneity of the field, are the most important requirements for quantitative investigations of magnetoviscosity. Taking this into account, it becomes obvious that the combination of a cone-plate system with a homogenous field in direction of the axis of rotation of the cone-plate arrangement is preferable here. The flow profile in the cone-plate geometry has been given in (4.5). From this we can calculate the vorticity of the cone-plate flow by

$$\vec{\Omega} = \frac{1}{2}\,\mathrm{rot}\,\vec{v} = \frac{1}{2}\begin{pmatrix} 2\cos\vartheta\ \omega_{(\vartheta)} + \sin\vartheta\ \dfrac{\partial\omega}{\partial\vartheta} \\ -\sin\vartheta\ \ \omega_{(\vartheta)} \\ 0 \end{pmatrix} . \qquad (4.10)$$

Again assuming a small opening angle ψ of the cone we can replace $\cos\vartheta \approx 0$; $\sin\vartheta \approx 1$ and $\partial\omega/\partial\vartheta \approx \Delta\omega/\psi$ (see Fig. 4.6). Thus we obtain the vorticity of the flow as

$$\vec{\Omega} = \frac{1}{2}\begin{pmatrix} \Delta\omega/\psi \\ -\omega \\ 0 \end{pmatrix} \approx \frac{1}{2}\begin{pmatrix} \Delta\omega/\psi \\ 0 \\ 0 \end{pmatrix} = \frac{1}{2}\begin{pmatrix} \omega/\psi \\ 0 \\ 0 \end{pmatrix} \quad , \qquad (4.11)$$

where it has been used that ψ is small and $\Delta\omega = \omega$ since only one part of the system is rotating. Assuming ψ to be small one can neglect the azimuthal component of $\vec{\Omega}$ since $\Delta\omega/\psi >> \omega$. As an example one can calculate, that for a system with an opening angle of $\psi \approx 3°$, $\Delta\omega/\psi$ is more than an order of magnitude larger than ω.

Thus obviously the vorticity of the flow has a dominant radial component and thus lies always in the x-y-plane. Therefore a field in z-direction is perpendicular to Ω all over the flow cell. In addition one can see from (4.3) that the shear rate in this geometry is independent from the position in the flow. Thus shear effects on e.g. cluster formation of magnetic particles are equal everywhere in the flow eliminating the problem of definition of an appropriate mean shear rate under consideration of the influence of shear rate gradients to particle chains or clusters.

A problem of this geometrical arrangement results from the fact, that a free fluid surface appears in a real technical design of the system in the gap between cone and plate (see Fig. 4.8.) This surface is perpendicular to the field direction. As it is well known from literature (Cowley and Rosensweig, 1967; Rosensweig, 1982) a surface instability forming spikes of magnetic fluid in a regular pattern appears in this geometry if the magnetic field strength exceeds a certain critical value (see Fig. 4.7).

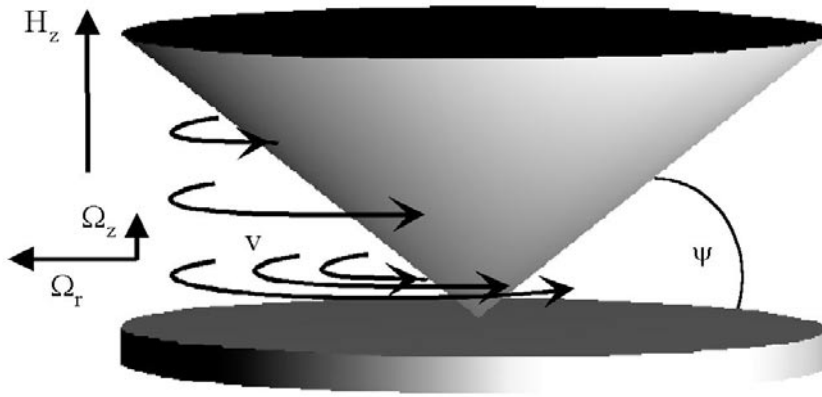

Fig. 4.6. Flow profile, vorticity and field direction in a cone plate arrangement used for ferrofluid investigations. Geometry is distorted for reasons of clearness.

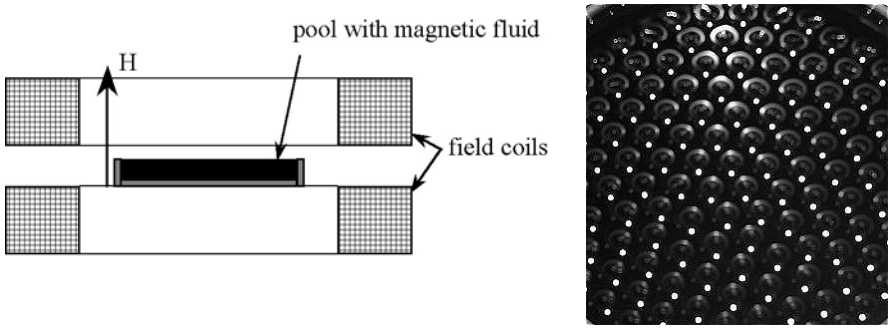

Fig. 4.7. The appearance of fluid spikes in a ferrofluid subjected to a homogeneous magnetic field perpendicular to the free fluid surface. The left side of the figure shows the principle set up of the experiment, the right side the typical hexagonal spike pattern in a top view on the fluid layer. The white dots are light reflections between the spikes.

The wavelength of the instability, given by the distance between two spikes, is in the order of 1 cm for common ferrofluids. If this instability takes place on the free surface of the cone plate system, a dewetting of the cone would appear (see Fig. 4.8). This dewetting would result in a reduction of the torque transmitted and thus in an influence on the measurement which is obviously not tolerable.

From Rosensweig's analysis (Rosensweig, 1982) one gets the critical magnetization of the fluid for the onset of the instability in the form

$$M_c^2 = \frac{2}{\mu_o}\left(1+\frac{1}{\mu}\right)\left(\rho g \sigma_s\right)^{\frac{1}{2}} \quad , \tag{4.12}$$

where ρ denotes the density, σ_s the surface tension and μ the permeability of the fluid.

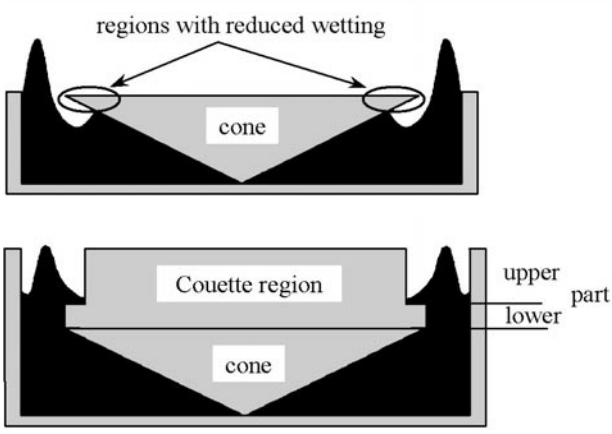

Fig. 4.8. In a cone plate arrangement the appearance of fluid spikes due to the normal field instability can force a disturbing dewetting of the cone which can be avoided by a combination of cone plate and Couette geometry.

For a standard ferrofluid with typical properties as given in Appendix A, one can easily calculate that even weak fields of about 20 kA/m are sufficient to drive the normal field instability. Thus this problem has to be seriously accounted in the design of the rheometers flow cell. A way out of this problem is the combination of the cone plate region with a Couette part as shown in Fig. 4.8.

In the transition region from the Couette to the cone-plate part the Couette region has to have a gap width chosen in a way, that the shear rate in the gap and in the cone plate region are identical. In this way flow instabilities and modified shear boundary conditions are avoided at the edge of the cone. The second part above this transition region is characterized by a significantly wider gap. This ensures, that changes of the torque transmitted in this region are negligible compared to the torque transmitted from the cone plate measuring region. Thus changes of the wetting of the cylinder in this region due to the appearance of normal field instability do not longer affect the measurement. As long as the fluid volume in this region is large enough to avoid that the spikes of normal field instability affect the lower Couette region, an axial field of relatively high strength can be applied.

For the actual case of the ferrofluid rheometer discussed here, a plate with angular frequency ω and a cone at rest have been chosen. The cone has an opening angle of 3° and a diameter of 80 mm. With the shear rate of the cone plate region

$$\dot{\gamma}_{CP} = \frac{\omega}{\psi}$$

and that of the Couette region

$$\dot{\gamma}_{CO} = \frac{R_1 \omega}{R_2 - R_1} \quad , \tag{4.13}$$

with R_1 and R_2 being the radii of the inner and outer cylinder respectively, one obtains the necessary gap width of the lower part of the Couette region to be 2 mm. The gap width in the upper part of the Couette geometry has been chosen as $d_2 = 7$ mm. Thus the ratio of the torque transmitted to the cone from this part to that from the cone-plate region can be calculated from

$$N_{CO} = \frac{2\pi R_1^3 h}{R_2 - R_1} \omega\eta \quad N_{CP} = \frac{2\pi}{3} R_1^3 \frac{\omega\eta}{\psi}$$

to be

$$\frac{N_{CO}}{N_{CP}} = \frac{3\psi h}{R_2 - R_1} \quad , \tag{4.14}$$

with h denoting the filling height of the Couette region.

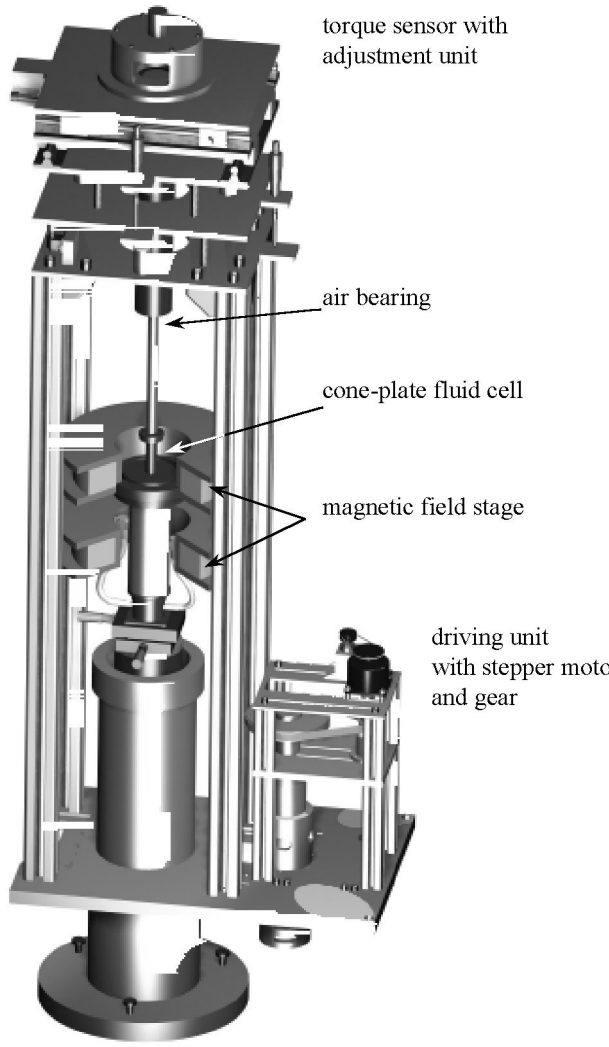

Fig. 4.9. The specialized rheometer for the investigation of magnetoviscous effects in ferrofluids used in the experiments. A detailed description is given in the text.

Thus, with the data given above, changes of the torque from the Couette part due to changes of the filling height of about 1 mm, e.g. due to dewetting forced by the normal field instability are approximately two orders of magnitude smaller than that from the measuring region. Therefore they are negligible within the range of accuracy of the whole system.

The cone is connected to an inductive torque sensor. To avoid any influence of the magnetic field applied in the fluid region to the torque determination, the sen-

sor has been placed about 80 cm above the fluid cell (see Fig. 4.9). It is mounted to the cone by means of an axis, which is held in an air bearing. The air bearing ensures, that no additional torques due to friction in bearings is added to that transmitted by the fluid. The system consisting of sensor and cone can be adjusted in the x-y-plane to an accuracy of 1 μm relative to the axis of rotation of the rheometer. In addition the adjustment unit at the top of the rheometer allows an adjustment of the angle of the cone relative to the x-y-plane with an accuracy of better than 1 mrad. In a similar way the position of the moved plate in the x-y plane can be assured to the same accuracy. The distance between the tip of the cone and the plate is finally also controlled to an accuracy of about 10 μm. All together these adjusting possibilities ensure that the flow profile of the cone plate flow is not disturbed by unwanted vortices.

The moved plate is driven by a unit consisting of a stepper motor and a gear system. With this unit, rotating as well as oscillating motion of the plate can be generated. The ranges of shear rate as well as of oscillation amplitude and frequency are given together with other relevant technical data of the rheometer in Table 4.1. It should be noted, that special attention has been paid to reach shear rates as low as possible. Since the effect of chain formation is relatively weak in ferrofluids available nowadays, significant effects can only be obtained at low shear rate where a breakage of the chains is avoided. Moreover, small shear rate is preferable for theoretical modeling of the microstructural reasons of the fluids behavior, as will be discussed in a later part of this section. High shear rates as they are more sufficient for technical applications are not the goal of this device, being devoted to the understanding of the physical background of the observed effects. The technically relevant shear rates can be obtained in high field systems as they have been discussed in Sect. 4.2.2.

The magnetic field in the direction of the axis of rotation of the plate is generated by two Helmholtz-coils placed around the fluid cell. The coils can produce a magnetic field of up to 40 kA/m in the fluid region. Assuming the measuring region of the fluid between cone and plate in first approximation as thin plate, one can calculate the relevant demagnetization factor of the system to be 0.926 (Kneller, 1962).

Table 4.1. Technical data of the ferrofluid rheometer

Diameter of cone	76 mm
Diameter of moved cell	80 mm
Cone-plate angle	3°
Torque range	10^{-5} -10^{-2} Nm
Frequency range rotating	0.037-22 Hz
Frequency range oscillating	0.021-20 Hz

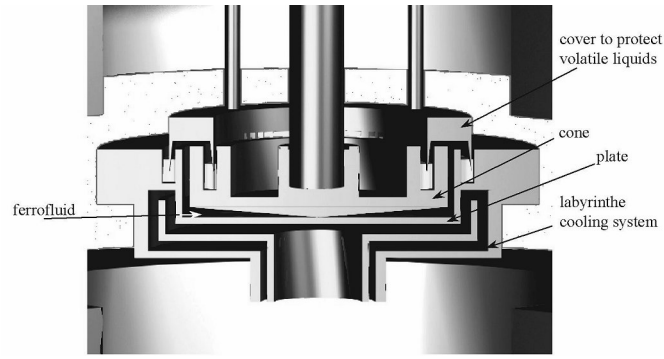

Fig. 4.10. The cooling system of the cone plate geometry of the ferrofluid rheometer. The frictionless cover is used for the investigation of fluids based on highly volatile carrier liquids.

Thus the field in the fluid H_i is given by

$$H_i = H_0 - 0.926\,M \quad , \tag{4.15}$$

where H_o denotes the strength of the applied field and $M = \chi H_i$ is the magnetization of the fluid, with χ being its susceptibility. For the standard fluid (Appendix A) the maximum field in the fluid can thus be calculated to be about 20 kA/m.

Particular effort has been devoted to the temperature stability of the system. Since the viscosity of the fluids depends strongly on temperature, and viscosity changes of several percent per degree are normal, it has to be assured that the temperature is maintained to an accuracy of better than 0.1 K over the whole sample. Therefore the plate of the fluid cell has been equipped with a labyrinth cooling system as shown in Fig. 4.10. Water from a precision thermostat reaches the plate in the center and is led around the plate towards the outflow. The stability of the thermostat is about 10 mK and since the cell is made of brass one can be sure that temperature homogeneity and stability is ensured by the water flow of about 12 l/min as long as the fluids is at rest. Nevertheless in the case of a rheometer one has to ensure that the temperature stability and homogeneity are also maintained in a sheared system even at the highest shear rate available.

Due to viscous friction heat is generated in the fluid under shear. This heat is transferred to the cell walls and can thus be removed by the cooling system. It can be shown (Böhme, 1981) that the heat flux can be written as $\phi_{Heat} = \tau\omega$ for the cone-plate system under assumption of a small opening angle of the cone, where t denotes the stress in the fluid and ? the angular velocity of the plate. From this we can calculate the temperature change with time in a sheared fluid with viscosity η under assumption of isolating walls to be

$$\frac{\partial T}{\partial t} = \frac{\eta\,\omega^2}{c\rho\psi} \tag{4.16}$$

with the specific heat capacity c and the density ρ of the fluid.

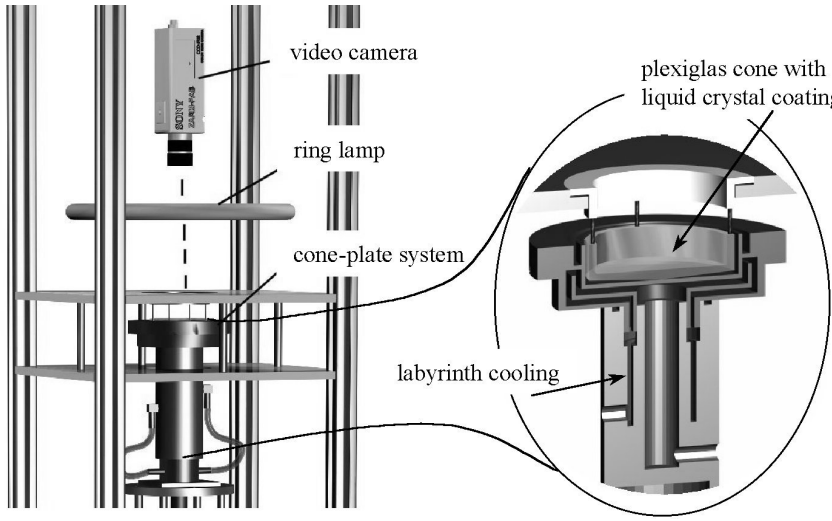

Fig. 4.11. A test set up to investigate the heat generation due to viscous friction and the efficiency of the cooling system in the fluid cell of the rheometer.

For a standard ferrofluid (Appendix A) this would lead for $\omega = 20s^{-1}$ to a temperature increase of about $5 \cdot 10^{-4}$ K/s and thus to an unacceptable change of viscosity of about 1 K in a usual experiment time of 30 minutes. The strong heat generation makes clear, that an optimal cooling system is required to maintain stable experiment conditions. This is an important point not only for the magnetoviscous investigations discussed here but for any kind of rheological measurement.

To test the cooling efficiency of the ferrofluid rheometer, a test stand using temperature sensitive liquid crystals as probe has been used. In the test stand, shown in Fig. 4.11, the driving system, the cooling loop and the plate of the original rheometer have been used to avoid modifications of the results due to changes in these parts. The cone has been replaced by a plexiglas cone of similar shape. This plexiglas cone is coated at the outer surface, i.e. in contact with the fluid, with temperature sensitive liquid crystals.

These substances are chiral nematic liquid crystals forming nematic phases - so called mesophases - in which the director, i.e. the orientation vector of the liquid crystal phase, changes its direction from plane to plane by a certain angle as shown in Fig. 4.12 (Vertogen and de Jeu, 1988). The spatial distance between two layers with identical direction of the director is referred to as the pitch of the liquid crystal system. If white light hits such a liquid crystal, only the wavelength corresponding to the pitch will be reflected. If the pitch length corresponds to a wavelength in the spectrum of visible light, this reflection results in a characteristic color of the liquid crystal system. For temperature sensitive liquid crystals the angle between the directors of the mesophases increases with increasing temperature, resulting in a decrease of the pitch and thus in a decrease of the reflected wavelength. With special liquid crystal mixtures the dependence of the pitch on

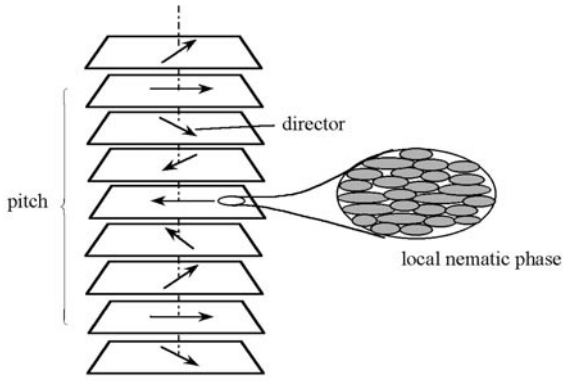

Fig. 4.12. Basic structure of a chiral nematic liquid crystal.

temperature, the starting point of visible light reflection as well as the high temperature end point can be precisely adjusted, leading to a temperature probe with adjustable range and resolution. By observation of the cone with a video camera from above, a color pattern can be obtained, visualizing the temperature distribution at the surface of the cone. Since the plexiglas cone has worse heat conductivity than the normal brass cone, the measured temperature changes will be higher than in the rheometer and give thus an upper limit for the temperature disturbances in a fluid under shear. The mixture used for the temperature tests of the rheometer had a total sensitivity range of 0.5 K over the color range from red (at 35°C) to blue (at 35,5°C). As seen from the color bar in Fig. 4.13 the used optical equipment thus allowed a resolution of temperature determination of 0.05 K.

In test experiments with a fluid with a kinematic viscosity $\nu = 100\ mm^2/s$, being at the upper margin of viscosities for modern commercial ferrofluids, no temperature changes could be observed, leading to the conclusion, that the cooling efficiency is high enough to ensure that the temperature stability of the fluid can be maintained to an accuracy of better than 0.05 K. The temperature homogeneity is better than 0.2 K over the fluid cell. Thus temperature effects can be neglected in the discussion of the magnetoviscous effects.

Table 4.2. Fluid data of the silicone oils used for the test of the cooling system (all data for 25°C) compared with relevant data of the standard ferrofluid

Fluid	ν [mm/s]	ρ [g/cm]	c [J/gK]	λ_T [W/Km]	$\partial\eta/\partial T$ [%/K]
APG513A	100	1.28	1.47	0.145	1.5
Baysilone 100	100	0.97	1.51	0.163	1.82
Baysilone 7000	7000	0.97	1.51	0.174	1.45

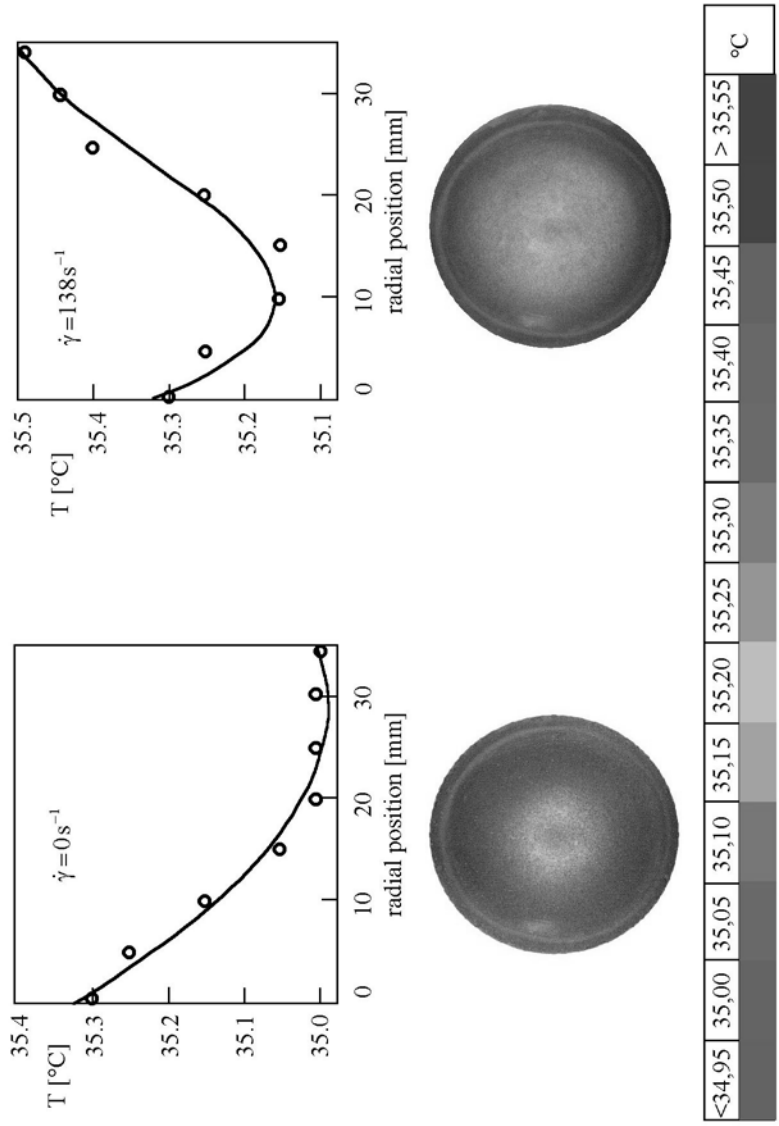

Fig. 4.13. The temperature distribution in the fluid cell at rest (left) and under shear with $\gamma = 138\ s^{-1}$ (right) in two dimensional liquid crystal representation and as averaged radial plot for a silicone oil with $\nu = 7000\ mm^2/s$.

To get an impression of the efficiency of the cooling system under more difficult conditions, similar experiments have been carried out with a high viscous silicone oil ($\nu = 7000$ mm^2/s) with a heat conductivity of 0.174 W/Km being comparable with the standard ferrofluid. The data of the fluid are given in Table 4.2.

Fig. 4.13 shows the temperature distributions for vanishing shear as well as for $\dot{\gamma} = 138$ s^{-1} in two dimensional liquid crystal representation as well as in the form of a radial temperature profile obtained from the liquid crystal image by means of digital image processing. The radial temperature change in the unsheared system is a result of the distance variation between cone and plate and of the resulting variation of the thickness of the fluid layer. The variation of 0.17 K around the mean temperature of 35.17 °C is small enough to be acceptable for rheological investigations. As seen from the curves, the mean temperature of the fluid rises by approximately 0.15 K due to the applied shear while the temperature distribution becomes even more homogenous due to the shear induced heating of the outer regions of the fluid. In conclusion one can state that even in this extreme situation the temperature control is good enough to allow high precision investigations of the rheological behavior of the fluids. The temperature induced changes of viscosity for all fluids investigated are below 0.05 % and will thus not have a disturbing effect on the investigations.

4.3 Shear dependence of the magnetoviscous effect

4.3.1 Results for a commercial ferrofluid and a first approach to a microscopic explanation

In Sect. 3.1 experiments using the commercial ferrofluid APG 513A in a situation with relatively high shear rate have been discussed (Ambacher et al., 1992). It had been shown there, that the strong magnetoviscous effect exhibited by this fluid can not be explained with the classical theory of non-interacting magnetic particles (Shliomis, 1972). It has been stated, that the discrepancies between experiment and theory may be forced by interaction of the particles which are expected to be not negligible in the concentrated fluid used. The assumption of the existence of a magnetic field supported interparticle interaction in a ferrofluid leads immediately not only to the statement that the magnetoviscous effect would be enhanced compared to the interaction free model. It also forces the assumption that the fluid should show non-newtonian behavior under the influence of magnetic fields of appropriate strength. Thus, rheological investigations using the rheometer described in Sect. 4.2.3 have been carried out, using a magnetic fluid of the same type as in the previous work (Ambacher et al., 1992).

As a first step in the search for non-newtonian behavior of a magnetic fluid the magnetoviscous effect has been measured for different shear rates. Therefore a fixed shear rate has been applied to the fluid and the increase of viscosity with magnetic field strength has been measured.

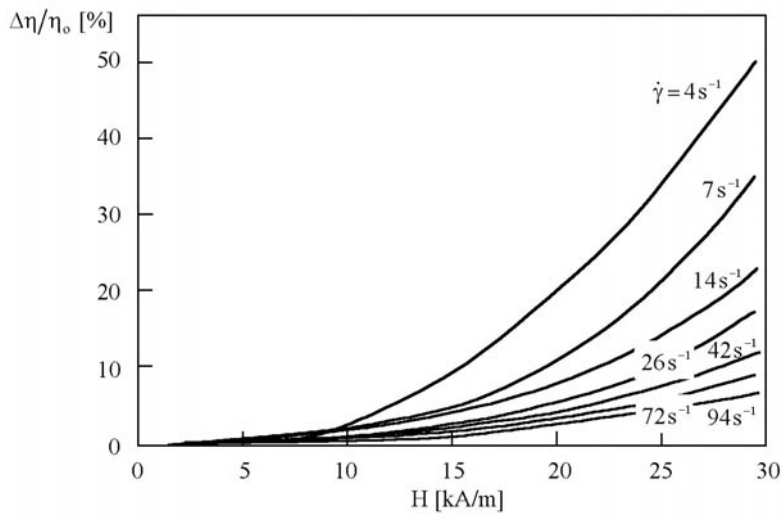

Fig. 4.14. The magnetoviscous effect in APG513A for shear rates between 4 s^{-1} and 94 s^{-1}.

Repeating this for different shear rates leads to an information upon the dependence of the viscosity change on field strength and shear rate. Fig. 4.14 shows a selection of measured magnetoviscous effects for different shear rates over a range of about two decades in shear rate. The fluid – APG513A – contains magnetite particles with a mean diameter of about 10 nm and a volume concentration of magnetic material of 7.2 vol.%. The thickness of the surfactant layer is 2 nm leading to a total concentration of suspended material of 28 vol.%. More details are given in Appendix A.

First of all a clear dependence of magnetoviscosity on shear rate is observed. As shear rate increases the magnetically induced increase of viscosity reduces significantly. Furthermore the measured increase at low shear rates – which are in principle much more suitable for a comparison since the theory is developed for vanishing shear rate and does not contain any shear effect – exceeds the maximum which can be calculated from Shliomis theory (see (3.36) to $\Delta\eta/\eta=0.42$ for small magnetic field strength already significantly. Thus, obviously the behavior of the fluid can not be described in terms of a noninteracting system of magnetic particles.

Nevertheless a plot of the viscosity change against the square of the field strength – as it is shown in Fig. 4.15 for different shear rates – confirms the $\Delta\eta\sim H^2$ law (see (3.39)) for weak magnetic fields resulting from (Shliomis, 1972) quite well for the whole shear rate range. Thus it can be assumed, that at least for weak fields, the theory is qualitatively suitable for the description of the effect. That means, that the increase of viscosity observed should be related to a hindrance of rotation of some magnetic structures due to the action of the magnetic field. The extremely strong effect leads immediately to the assumption that these structures have to be large compared with the single particles. Thus the relevant

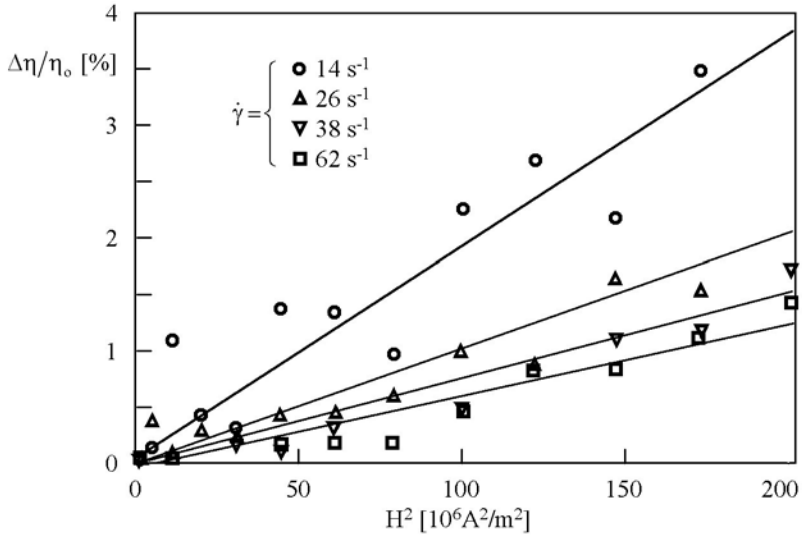

Fig. 4.15. The field-dependent viscosity changes in APG513A for 4 different shear rates plotted against H^2.

structures in the process can be assumed to be agglomerates of numerous single particles. The observed shear thinning strengthens this assumption. In the easiest cases the agglomerates can be assumed to be chains which are formed due to interparticle interaction in the presence of a magnetic field. These chains break up under the influence of shear, reducing the size of the structures determining the magnetoviscous effects. Thus the chain formation leads to the enhanced increase of viscosity while shear rate induced rupture of the chains gives rise to the observed field-dependent shear thinning.

Trying to follow this approach in more detail one has to deal with the question of chain formation of magnetic particles in a ferrofluid. The most important parameter for the description of this phenomenon is the interaction parameter λ given by (Rosensweig, 1985)

$$\lambda = \frac{\mu_0 M_0^2 V}{24 k_B T} \quad . \tag{4.17}$$

This dimensionless parameter describes the ratio between the magnetic interparticle interaction and the thermal energy of the particles. Obviously the formation of chains can only appear if the particle interaction is strong enough to keep up with the thermal motion of the particles, i.e. chain formation will only appear for values of λ significantly larger than unity. For 10 nm magnetite particles, like they are present in the fluid used in the shear thinning experiment, one can easily calculate from (4.17) using the data from Appendix A, that $\lambda = 1.3$, thus significant chain formation should not appear for such small particles. Obviously this

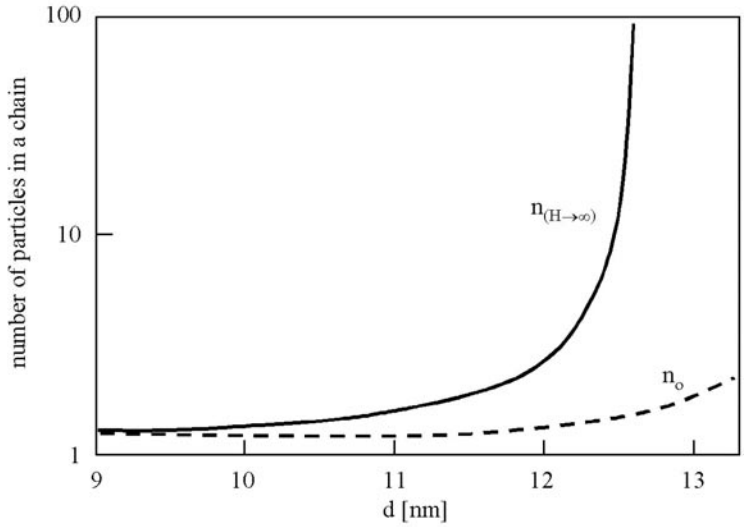

Fig. 4.16. The length of particle chains in a ferrofluid containing 5 vol.% of magnetite particles as a function of the particle diameter for vanishing field and for saturation calculated from (4.18).

agrees well with the stability requirement formulated in Sect. 2.1. From (4.17) one sees, that an efficient chain forming process should be observable for magnetite particles with diameters above 13 nm.

For particles of sufficient size de Gennes and Pincus (de Gennes and Pincus, 1970) and Jordan (Jordan, 1973) gave the earliest calculations concerning the length of magnetic particle chains. An approximation of Jordan's calculation for the limiting cases of vanishing as well as for infinitely high field, i.e. for saturation of the system, as given in (Rosensweig, 1985), leads to the analytic expressions

$$n_{(H=0)} = \left[1 - \frac{2}{3}\,\frac{\phi}{\lambda^3}\,e^{2\lambda}\right]^{-1} \qquad n_{(H\to\infty)} = \left[1 - \frac{2}{3}\,\frac{\phi}{\lambda^2}\,e^{2\lambda}\right]^{-1} \tag{4.18}$$

for the number n of particles in a chain, where λ is the above mentioned coupling parameter and ϕ as before the magnetic volume concentration.

Figure 4.16 shows the resulting dependence of the number of particles in a chain on the diameter of the single particles. Obviously in a vanishing field the suspension stays stable, i.e. the mean chain length is less than two particles over the whole diameter range shown. In contrast the tendency of chain formation increases dramatically if the single particle diameter exceeds the value of 13 nm for magnetite particles. The results of Jordan's calculations have been experimentally proved by Hayes (Hayes, 1975), where good agreement for sufficiently large particles has been found.

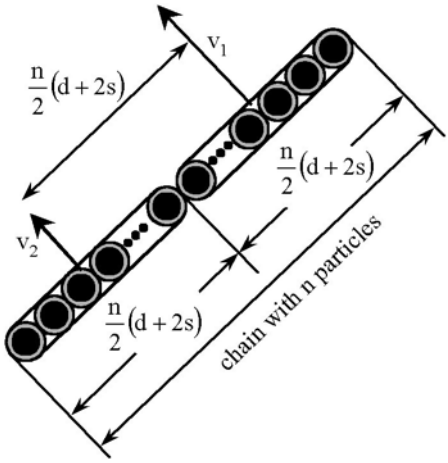

Fig. 4.17. A simple chain model to calculate the maximum stable chain length under the influence of shear. Explanations are given in the text.

The remaining problem in the explanation of the results on magnetoviscosity shown in Fig. 4.14 is thus the question whether sufficiently large particles exist in the commercial ferrofluid used. From the size distribution shown in Fig. 2.5 it is clear that the amount of large particles is very small and thus it will have to be clarified in the following whether this small amount of particles is sufficient to give rise to the observed strength of the magnetoviscous effects. To get a first impression whether the assumption of formation and breakage of chains of relatively large particles with mean size about 16 nm can be a reasonable approach for the further discussion, one can have a look on the following simple model of a chain of magnetic particles (Odenbach and Störk, 1998). As shown in Fig. 4.17 we assume that a chain consisting of n particles is subjected to a shear flow perpendicular to the chain axis. The particle chain is assumed to be rigid and straight. Further it is assumed that all magnetic moments in the chain are aligned parallel, i.e. we assume a situation of magnetic saturation.

To check the maximum length of a chain, being stable under shear flow, we assume that a break of the chain will appear in the middle leading to two chains consisting of n/2-particles.

The force keeping both parts of the chain together is given by the magnetic interaction force between the two particles in the center of the chain

$$F_m = \frac{\mu_o M_o^2 \pi d^6}{24(d+2s)^4} \quad . \tag{4.19}$$

The breakage is forced by viscous forces, which are different for both parts of the chain, since the chain is subjected to a shear flow. Thus one can write – following Stokes law - the force leading to disruption of the chains as

$$F_{vis} = 6\pi\eta_0 \frac{n}{2} \frac{(d+2s)}{2} (v_1 - v_2) \quad . \tag{4.20}$$

If one now expresses the shear rate $\dot{\gamma}$ by the velocity difference (v1-v2) and the spatial distance between the centers of the two chain parts n(d+2s)/2, one can obtain with

$$\dot{\gamma} = \frac{2\left(v_1 - v_2\right)}{n\left(d + 2s\right)} \tag{4.21}$$

the viscous force to be

$$F_{vis} = 6\pi\eta_0\,\dot{\gamma}\,\frac{1}{2}\left[\frac{n}{2}\left(d+2s\right)\right]^2 \quad . \tag{4.22}$$

Assuming now that a chain break will take place when viscous and magnetic forces become equal, the maximum number of particles in a chain n_{max} given by this simple model can be written as

$$n_{max} = \sqrt{\frac{\mu_0}{18\eta_0\,\dot{\gamma}}}\;M_0\,\frac{d^3}{(d+2s)^3} \quad . \tag{4.23}$$

Obviously the maximum number of particles in a chain reduces with increasing shear as it has been generally assumed in the model.

Figure 4.18 shows the variation of the maximum chain length with shear rate for a particle diameter of 16 nm. The chain length obtained is reasonable, especially if it is compared with the results by Jordan (Jordan, 1973) and Hayes (Hayes, 1975). The relative decrease with shear rate is furthermore comparable with the relative change of the magnetoviscous effect with increasing shear rate for a given magnetic field strength, as it is shown in Fig. 4.19 exemplarily for a field strength of H = 20 kA/m in the fluid, using the Ferrofluid APG513A.

Up to now the experimental results discussed were all obtained with the fluid APG513A. The first approach for an explanation of the magnetoviscous effects is clearly based on the microscopic properties of the fluid, especially on the size, size distribution and material of the magnetic particles. Furthermore it is to be expected, that changes in the volume concentration of magnetic particles will also significantly change the magnetoviscous behavior, even if the concentration is not part of the simple chain model discussed above. This shows, that experimental data for fluids with different microscopic make-up, as well as a much more detailed theory is required to enable a proper explanation of magnetoviscosity of ferrofluids. Thus in the following, we will first discuss experimental results for various fluids with varied constitution and then will have a glance at complex theoretical models allowing a comparison of experimental and theoretical results.

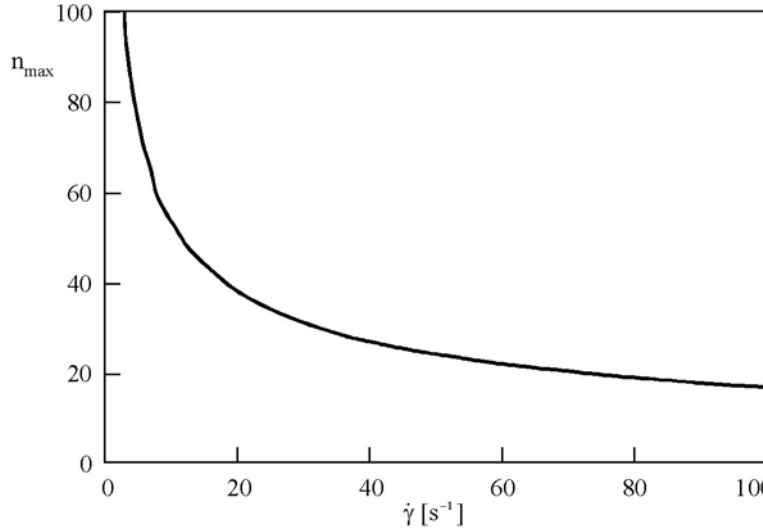

Fig. 4.18. The dependence of the maximum length of stable magnetic particle chains on shear rate for a particle size of 16 nm.

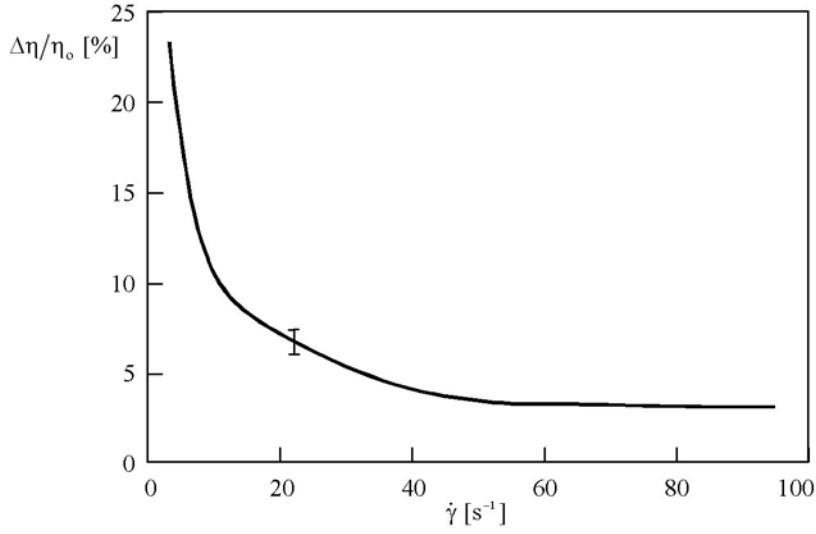

Fig. 4.19. Shear dependence of the magnetoviscous effect in APG513A for H = 20 kA/m.

4.3.2 Experimental results for fluids with different microscopic make-up

Looking for fluids with different microscopic make-up leads in principle to two different approaches. One possibility is given by the use of commercial ferrofluids available for different applications. These fluids contain commonly magnetite particles and differ concerning volume concentration and carrier liquid.

Their advantage is their long term stability but their general backdraw is a severe lack of information concerning their microscopic structure. As discussed in Sect. 2.2.1, the magnetization curve of a liquid gives some information concerning the mean diameter and the grain size distribution of the particles but the data – especially that concerning the size distribution – is connected with relatively large experimental errors.

This leads to obvious problems if experimental data for different commercial magnetic fluids is compared, since no information concerning the production process and thus no reliable data basis concerning their microscopic make-up – which can be significantly changed e.g. by different cleaning processes – is available. This is illustrated by the data given in Fig. 4.20 for different commercial magnetic fluids from various production lines, having an identical volume concentration of magnetic material of about 7 vol. %. Obviously the magnetoviscous behavior is significantly different. An effect that can be related to different purification processes changing the microscopic composition of the fluids as will be seen from the experiments discussed afterwards.

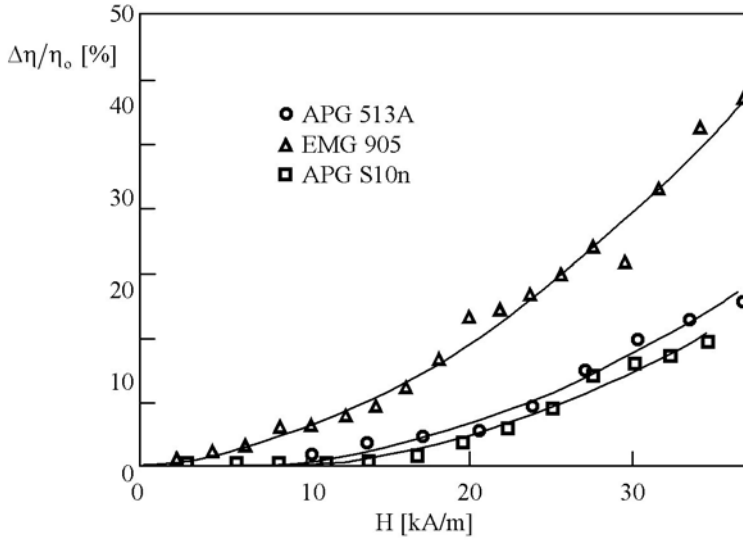

Fig. 4.20. The magnetoviscous behavior for three magnetic fluids with identical overall concentration of magnetic material, originating from different production lines.

S. Odenbach (Ed.): LNP m71, pp. 85–121, 2001.

A more systematic approach is based on the use of experimental fluids especially synthesized for particular investigations of the magnetoviscous behavior. Such fluids enable the controlled change of single parameters of the fluids' microscopic structure to get an insight into their importance for the overall properties of the fluid.

For example a change of the magnetic material would result in a change of the coupling parameter λ. Replacing magnetite with a spontaneous magnetization of $M_o = 4.5 \cdot 10^5$ A/m by cobalt with $M_o = 1.4 \cdot 10^6$ A/m would increase the coupling parameter from $\lambda = 1.3$ to $\lambda = 12.6$ for 10 nm particles. Thus the tendency to chain formation in the cobalt fluid would be significantly higher than in a fluid with magnetite particles - a behavior that was found as well experimentally (Charles, 1996) as in numerical models (Chantrell et al., 1982). Furthermore a change of the structure of the surfactant would influence the relation of magnetic and hydrodynamic diameter, resulting in a change of the particles' influence on the flow as well as on the tendency for chain formation.

Nevertheless, looking on the approach to an explanation of magnetoviscous effects in magnetite ferrofluids given in Sect. 4.3.1 one has to recover that the most important assumption in this approach has been, that magnetoviscosity and its change with shear rate and field strength is dominantly controlled by a small portion of large particles or primary agglomerates forming particle chains. The major portion of small particles is assumed to contribute not directly to the magnetoviscous effects. Thus the most important change of the microscopic structure of a fluid would be a change of the concentration of the large magnetic particles and agglomerates in the fluid. Such a change should give a direct impression whether these particles are of significant importance as assumed in Sect. 4.3.1 and thus whether it is reasonable to base a complex theoretical approach on a model assuming a small portion of large, chain forming particles in the presence of a magnetic liquid consisting of small particles in a carrier liquid.

Within a cooperation with K. Raj from Ferrofluidics Inc. we have thus measured the magnetoviscous effect for a series of fluids with variable content of large particles and agglomerates (Odenbach and Raj, 2000). During the synthesis of a magnetic fluid, particles and agglomerates are formed with a wide spectrum of particles sizes. To obtain a stable liquid, the larger magnetic structures have to be removed from the fluid. For the largest particles, being much larger than the mean diameter of 10 nm, being usual for commercial ferrofluids, this separation can be done by gravitational sedimentation in a centrifuge. From the Stokes law one can see immediately, that the difference in sedimentation velocity scales only with the square of the particle size

$$v = \frac{2}{9\eta} \rho g r^2 \tag{4.24}$$

and thus this technique is not very size sensitive and therefore not suitable for separation of particles in a size range around 16 nm or of primary agglomerates in dimer size from a ferrofluid. To separate such structures from the final fluid usually separation in strong magnetic field gradients is used. This technique allows a very sensitive choice of the size of the separated particles since the velocity of the

forced diffusion in a magnetic field gradient scales as d^6 (Odenbach, 1994b). This kind of purification is thus used as final step in the production process of a ferrofluid.

To obtain a series of fluids with variable content of large particles, samples were taken at various stages of the magnetic purification process. Two fluids were achieved at early stages, i.e. after a short exposure to the field gradient. These fluids contain a high content of large particles and agglomerates. A third fluid was purified in a normal way being usual for the production of a commercial ferrofluid while two further samples were taken after even longer purification, containing thus a lower portion of large magnetic structures. All samples were obtained from a common batch of ferrofluid ensuring, that no changes in other fluid parameters would affect the results. Furthermore it was observed, that all fluids have comparable overall content of magnetic material to avoid an influence of concentration changes on the particle-particle interaction.

Fig. 4.21 shows the normalized magnetization curves for all five fluid samples. The fluids are numbered consecutively (F1-F5) with the highest order number indicating the highest amount of large particles. From Fig. 4.21 it is obvious that significant changes in the shape of the magnetization curves appear. The steeper curve for F5 indicates the expected large amount of large particles. This can be quantified by a determination of the mean particle size from the magnetization curves as discussed in Sect. 2.2.1 The results for the five fluids are given in Table 4.3 together with their saturation magnetization also obtained from the magnetization curves and the related volume concentration.

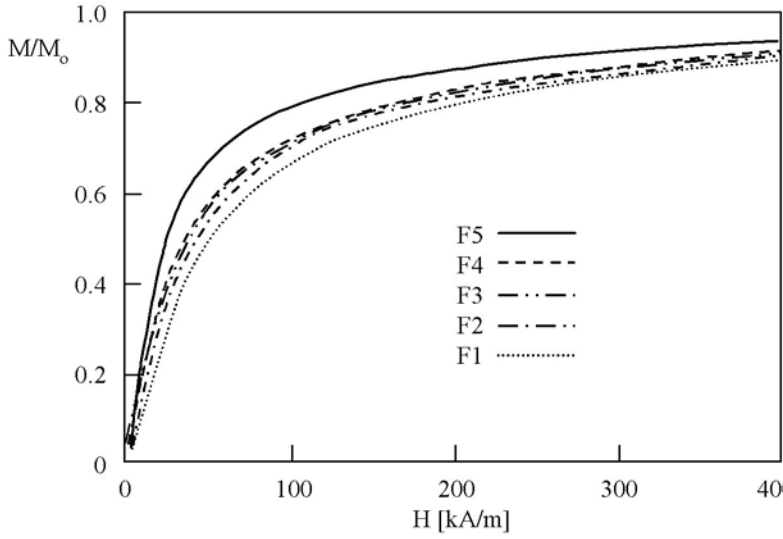

Fig. 4.21. Normalized magnetization curves for fluids F1-F5 containing different amount of large particles (increasing with ordinal number of the fluid).

Table 4.3. Mean particle diameter and overall magnetic content of fluids F1 – F5

Fluid	$\overline{d}$ (nm)	M_s (kA/m)	ϕ
F1	8.3	32.41	
F2	8.8	32.34	
F3	9.2	31.54	0.071 ±0.0008
F4	9.2	32.17	
F5	10.1	32.06	

Obviously the overall magnetic content of all 5 samples is identical within 1 % and thus an influence of concentration differences on the interaction of the particles can be excluded. In addition the mean particle diameter reduces significantly with increasing degree of purification showing the expected decrease of the content of large magnetic structures. As mentioned in Sect. 2.2.1 the magnetogranulometric analysis is not precise enough to quantify the differences in the content of large particles and agglomerates. For these five fluids the change of viscosity in the presence of a magnetic field of variable strength has been measured for different shear rates using the rheometer described in Sect. 4.2.3.

To check whether these fluids show a magnetoviscous behavior comparable to APG513A (see Sect. 4.3.1), Fig. 4.22 shows the change of viscosity of fluid F5 with the strength of the applied magnetic field for various shear rates. Obviously the field-dependent increase of viscosity as well as the shear thinning are observed here too.

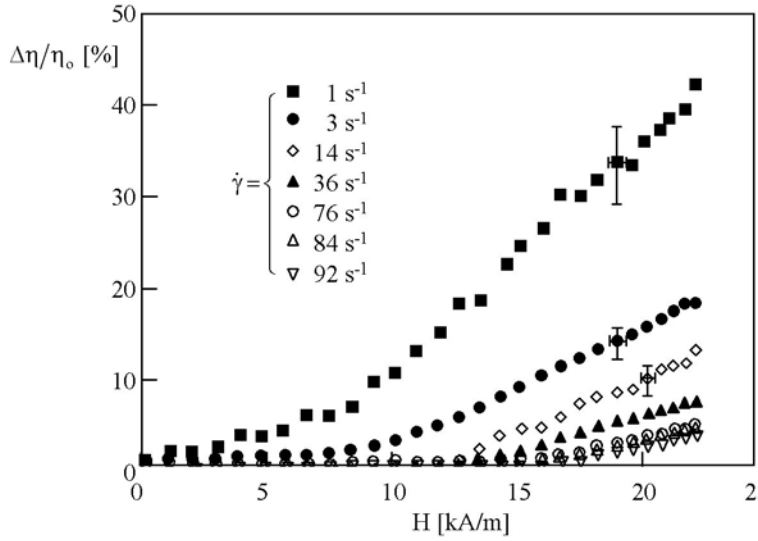

Fig. 4.22. The magnetoviscous effect for fluid F5 measured for 7 different shear rates.

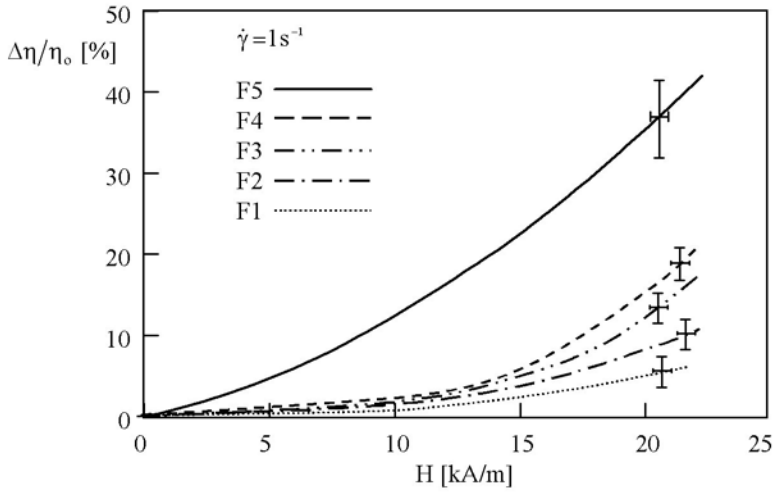

Fig. 4.23. The comparison of the magnetoviscous effect of fluids F1-F5 for $\dot{\gamma}=1s^{-1}$. The lines represent quadratic fits to the experimental data.

The most interesting point in the investigation of these fluids is now the comparison of the magnetoviscous effects in the different suspensions. In Fig. 4.23 the relative change of viscosity is plotted for all five fluids for $\dot{\gamma}=1s^{-1}$. It is clear from the experimental data, that the magnetoviscous effect diminishes with increasing degree of purification of the liquid.

This is strengthened by the data shown in the various graphs of Fig. 4.24. With increase of shear rate the magnetoviscous effect reduces for all fluids. Independent from shear rate, the different fluids show different strength of magnetoviscosity obviously connected with the amount of relatively large magnetic structures present in the liquid. With increasing shear rate the magnetoviscous effects fall below the detection limit of the rheometer successively starting with the most purified liquid F1. At high shear rates a magnetoviscous effect can only be measured for the fluids F4 and F5 containing a high degree of large particles.

Thus from the experimental data for the fluids F1-F5, having different content of larger particles and agglomerates, we can deduce that the most important contribution to the magnetoviscous effect in a magnetite based ferrofluid comes from the large particles.

Looking again to Fig. 4.22 one can try to quantify the content of large magnetic structures in the liquid. As shown in the figure, the change of the magnetoviscous effect reduces for high shear rates, or with other words, at high shear rates all chains of magnetic particles are broken and only the large single particles determine the magnetoviscous behavior. Their influence on the fluids viscosity can obviously just be based on the hindrance of their rotation in the flow due to the action of a magnetic field. Thus, neglecting the residual interaction between the large particles and between them and the magnetic liquid consisting of small

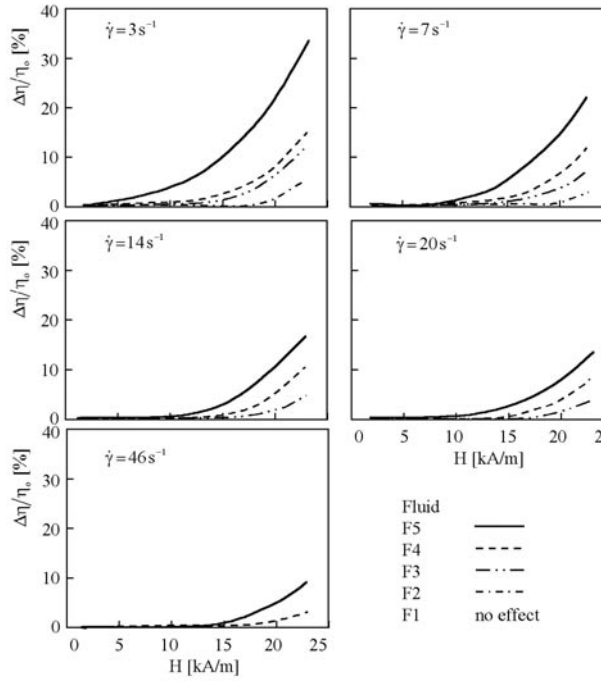

Fig. 4.24. The comparison of the magnetoviscous effect of fluids F1-F5 for various shear rates.

particles, the viscosity changes can be described as rotational viscosity exerted by the large particles in the field.

Thus – for this particular situation – Shliomis′ formula (3.31) can be used. Assuming that the mean particle diameter of the structures relevant for the magnetoviscous effect is about 16 nm one can thus fit (3.31) to the experimental data to obtain the volume concentration of the large particles. Fig. 4.25 shows the magnetically induced changes of viscosity for all five fluids for the highest shear rate obtained in the experiments. The shear rates are indicated for each curve. For fluids F3, F4 and F5 this shear rate comes directly from the region where the magnetoviscous effect does not significantly change with shear rate any more. Thus in these cases we can assume that the units interacting with the field are reduced to single particle size mainly. From the fit of (3.31) with the assumption of $\bar{d}$ =16 nm we can thus obtain here volume fractions of $\phi=8\cdot10^{-3}$ for fluid F5, $\phi=2.6\cdot10^{-3}$ for fluid F4 and $\phi=2.2\cdot10^{-3}$ for fluid F3. For the calculation a surfactant layer thickness of 2 nm has been assumed. The value for F3 seems to be reasonable since F3 is a fluid, being cleaned following the usual process for commercial fluids and the volume fraction obtained from the above described fit coincides with the results for the size distribution for commercial fluids as obtained from magnetogranulometric analysis.

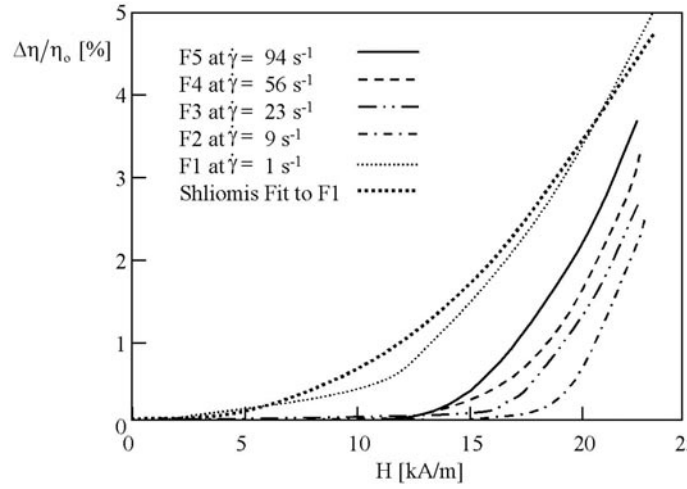

Fig. 4.25. The magnetoviscous effect for fluids F1-F5 for the highest shear rate available in the respective experiments. As example the data for F1 is shown together with a fit of Shliomis' theory (3.31) with $\bar{d} = 16\text{nm}$ and ϕ being the fit parameter to obtain an estimate for the concentration of large particles in the fluids.

Therefore the mentioned values for fluids F4 and F5 are good indications for the overall content of the large particles and agglomerates in these liquids too, since they are obtained from viscosity data which can also be assumed to be determined by single magnetic particles only.

For the fluids F1 and F2 the situation is somewhat different since the magnetoviscous effect could only be observed for few shear rates. Thus the values measured for the highest shear rate investigated can not definitely be assumed to be taken at a shear rate where all agglomerates were broken. Nonetheless the formation of chains and other large agglomerates becomes less probable with decreasing content of sufficiently large particles. Thus a volume fraction obtained from a similar fit as described for fluids F3 to F5 gives at least a valuable upper border for the content of large particles and primary agglomerates. From the respective fits one obtains $\phi=1.4\cdot10^{-3}$ for the fluid F2 and $\phi=9\cdot10^{-4}$ for fluid F1.

Table 4.4. Content of large agglomerates in F1 and F5 and measured viscosity changes

Fluid	ϕ_{large}	$\Delta\eta/\eta_o$ for H=23 kA/m; $\dot{\gamma}=1s^{-1}$
F1	$9\cdot10^{-4}$	0.07
F2	$1.4\cdot10^{-3}$	0.11
F3	$2.2\cdot10^{-3}$	0.17
F4	$2.6\cdot10^{-3}$	0.22
F5	$8\cdot10^{-3}$	0.42

The results for the volume concentration of large particles or primary agglomerates in the fluids collected in Table 4.4 show the successive reduction of such particles in the liquid due to the magnetic separation process as well as its influence on the achievable magnetoviscous effect for low shear rate and the highest magnetic field used.

The remaining question at this point is obviously whether the relatively small amount of large particles can form chains and agglomerates of sufficient strength and size to explain the observed magnetoviscous effects in commercial ferrofluids. In addition the results for fluids F1 and F5 force the question whether a controlled cleaning of fluids with a high magnetoviscous effect by means of magnetic separation can give more detailed insight into the microstructural reasons of magnetoviscosity in fluids with strong interaction. But before stressing these points a general remark concerning misinterpretation of experimental results on highly purified liquids should be made. As discussed in detail in Sect. 3.1, a basic assumption for the explanation of magnetoviscosity in the concept of rotational viscosity (Shliomis, 1972) is the demand of a fixed position of the magnetic moment of the particles relative to the crystal structure and thus the assumption that the Brownian relaxation time is smaller than the respective time for the Néel process. For commercial fluids containing magnetite particles this demand of magnetic hardness is equivalent to the demand that particles contributing to the magnetoviscous effect should be larger than approximately 13 nm as seen in Fig. 2.10. This is sometimes neglected in the interpretation of experimental results with help of Shliomis' theory on rotational viscosity. In highly purified liquids such an error may lead to serious misinterpretation of the experimental results.

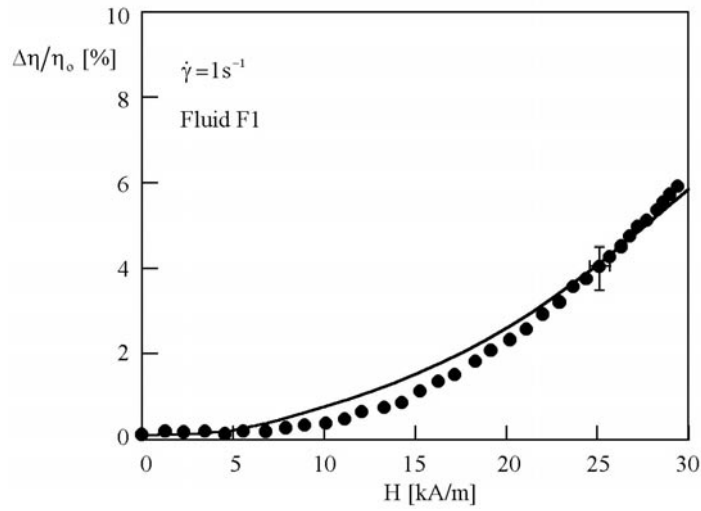

Fig. 4.26. The data obtained for fluid F1 for $\dot{\gamma} = 1s^{-1}$ together with a calculation of the magnetoviscous effect following (3.31) and using $\bar{d} = 8.5\,nm$, $s = 2$ nm and $\phi' = 0.22$, i.e. the total concentration of magnetic particles including their surfactant.

For example a calculation of rotational viscosity using (3.31) and taking the data of fluid F1 as given in Table 4.3 leads to the line shown in the Fig. 4.26. The dots in Fig. 4.26 are again the results for the measured magnetoviscous effect at $\dot{\gamma}=1s^{-1}$ for fluid F1. By chance these values coincide relatively well with the calculated curve. Thus one may run into the danger to charge the measured magnetoviscosity to a rotational viscosity forced by the hindrance of rotation of all particles in the fluid despite the fact that the majority of them is not able to contribute directly to magnetoviscous effects at all. Thus a fit of (3.31) to this data would lead to a misinterpretation in the way that the measured effect is pure rotational viscosity of single particles while, in reality, only a small portion of the suspended magnetic particles forms chains, leading to the observed increase of viscosity. Therefore any interpretation of magnetoviscosity should be carefully checked concerning a correct consideration of the relaxation process of the particles involved and of their resulting sizes.

4.3.3 Controlled change of the microscopic make-up of commercial ferrofluids

As mentioned above, fluids F1 to F5 were specially produced for the experimental investigation of magnetoviscous effects in ferrofluids. Since the purification process is part of the secret production process of ferrofluids, no detailed information about the strength of the magnetic field gradient used and the exposure time of the fluid to the field gradient is available. Therefore such data can not be used as input data for the interpretation of the rheological results. Furthermore, as Fig. 4.20 showed, commercial ferrofluids – as they are usually used for experiments – show significantly different magnetoviscous behavior, which – based on the results discussed above – can be related to different purification processes during their production. Thus it would be a valuable approach to build up a magnetic separation system allowing a controlled stepwise extraction of large particles from fluids to get a deeper insight into the connection between microscopic make-up and macroscopic behavior. To enable this, a magnetic separation stage consisting of specially designed pole shoes for a 1 T electromagnet and a trapezoidal fluid container (see Fig. 4.27) has been designed (Thurm and Odenbach, 2001). The pole shoe arrangement produces a vertical magnetic field gradient of up to $5\cdot10^7$ A/m^2 being constant within 3 % all over the fluid volume.

The change of concentration of magnetic particles as a function of time and spatial position in such an arrangement can easily be calculated from the diffusion equation (see e.g. Gerber, 1984; Blums et al., 1986; Odenbach, 1994b; Thurm and Odenbach, 2001)

$$\frac{\partial c}{\partial t} = D\left(\nabla^2 c\right) - \frac{1}{6\pi\eta r}\,\mu_o\, V\, M_{(H)}\,\nabla H \quad . \tag{4.25}$$

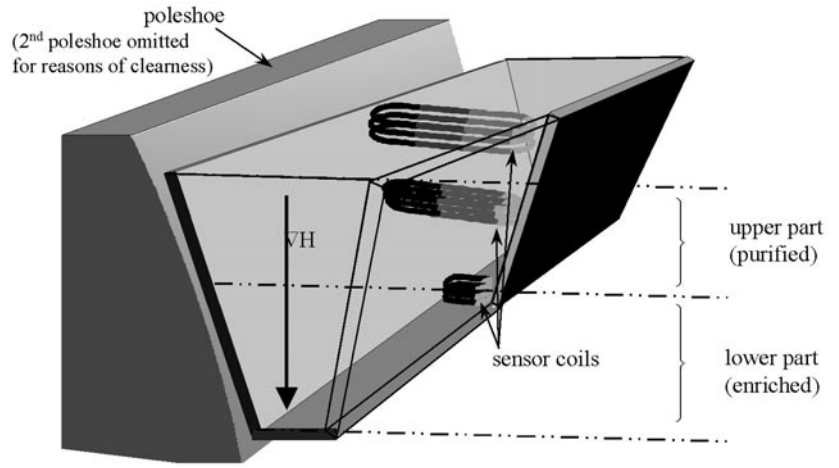

Fig. 4.27. Schematic sketch of the separation system for controlled purification of magnetic fluids. The fluid container is equipped with sensor coils to allow successive measurement of the evolution of concentration in the system. After the separation process the fluid sample is subdivided in an upper purified part and a lower portion enriched with large particles.

As shown in the simulation in Fig. 4.28, following (4.25), a gradient of the mentioned strength forces a change of the concentration distribution of the large particles in the container, while small particles with sizes about 10 nm remain unaffected. Thus a controlled separation of the fluid is possible.

Inductance measurement of small pick up coils mounted inside the fluid allows the online control of the separation process by measuring the temporal development of the concentration of the magnetic component of the fluid in three different depth' of the container. The inductance measurement system used (Völker et al., 2001) allows the determination of concentration changes as low as 10^{-4} vol.%.

In this system a ferrofluid can be exposed to a certain field gradient for a well defined instance of time up to several weeks. During this time particular effort is spend to keep the temperature of the fluid and the strength of the magnetic field constant to avoid any remixing effects due to flow effects, generated e.g. by thermal convection. After finishing the separation, the fluid is divided in two samples. The purified sample from the upper part of the container (see Fig. 4.27) contains a reduced amount of large particles. In contrast the second sample taken from the bottom of the container is enriched with large particles.

Both samples can then be characterized magnetically as well as rheologically. With this setup a first test experiment using APG513A has been performed (Thurm and Odenbach, 2001). The fluid has been exposed to a magnetic field gradient of $5 \cdot 10^7$ A/m^2 for two weeks.

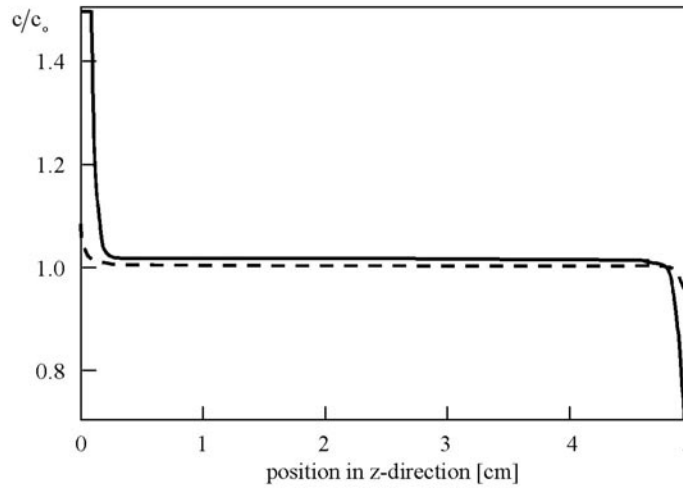

Fig. 4.28. The relative concentration change of magnetic particles in the container after two weeks of separation in a magnetic field gradient of $5 \cdot 10^7$ A/m^2 calculated for 10 nm particles (dashed line) and 16 nm particles (full line).

Magnetization measurement taken after the separation showed, that the upper sample contained about 7 vol.% of magnetic material, while the lower one was slightly enriched to 7.3 vol.% (7.15 vol.% original concentration). This difference is small enough to ensure that the concentration variation does not significantly influence the magnetoviscous behavior. The mean particle diameters were evaluated to be 9 nm and 11 nm respectively, compared to 10 nm in the original fluid. Figure 4.29 shows the results concerning the magnetoviscous behavior for the original fluid and the two separated samples. Obviously the enriched sample shows a stronger magnetoviscous effect than the original fluid. In contrast the purified liquid shows strongly reduced magnetoviscosity.

These results indicate again, that large particles dominate the magnetoviscous behavior and that their concentration is the most important parameter for the strength of chain formation and thus for the absolute strength of the magnetoviscous effect and its dependence on shear rate.

For the future systematic studies of various fluids using this system are planned, and it is foreseen to accompany the rheological measurement and interpretation by a modeling of the purification process that can be compared with the concentration data used to control the separation.

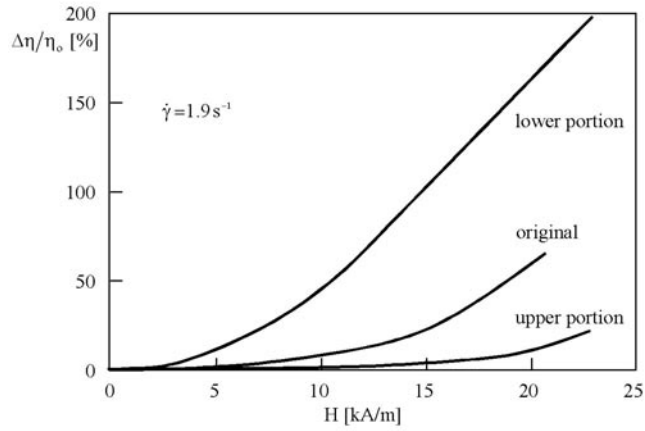

Fig. 4.29. The magnetoviscous behavior of APG513A compared with two samples of the fluids obtained from a two weeks separation process in a magnetic field gradient of 10^7 A/m^2. The curve indicated "upper portion" is measured with the purified fluid from the upper region of the separation chamber while the curve indicated "lower portion" is obtained with the fluid enriched with large particles during the separation process.

4.3.4 Microscopic explanation of magnetoviscosity in fluids with interparticle interaction

As discussed above, the single particle theory of Shliomis, neglecting the interparticle interaction is of great value for the interpretation of highly diluted ferrofluids, but it does not allow a sufficient explanation of effects found in concentrated suspensions where interaction between the particles becomes an important contribution. Furthermore a simple chain model gives a reasonable starting point for an interpretation, since formation and breakage of large magnetic structures could lead to a strong enhancement of magnetoviscosity as well as to the observed shear thinning. Nevertheless the amount of large particles, which may contribute to the effects is found to be small from magnetogranulometric size analysis as well as from high shear results in magnetoviscosity. Thus a theoretical approach describing the influence of chains on the magnetoviscous behavior is required to achieve a more detailed insight into the microscopic reasons for the field-induced increase of viscosity in concentrated magnetic fluids.

Thus on the basis of former work – especially by Andrey Zubarev see (Zubarev, 1992; Zubarev and Iskakova, 1995a,b; Zubarev and Yushkov, 1998) – a model has been developed, describing the rheological properties of magnetic fluids in the presence of chain like aggregates (Zubarev et al., 2001a). As it is well known, a full description of a polydisperse system with magnetic interaction and chain like aggregates is too complex for the existing methods of statistical physics. Thus a couple of assumptions had to be made, to allow a theoretical access to the problem. All these assumptions have been chosen in a way, that the model fluid

calculated, fits with the properties of the real fluid as good as possible. In detail, the assumptions are as follows:

First of all the polydispersity of the system is reduced to the model of a bidisperse liquid containing two fractions of particles with significantly different diameter. A general treatment of the effect of polydispersity is found in (Zubarev et al., 2001b) but without accountancy for chainlike aggregates. In the model discussed here, it is assumed, that one of the fractions consists of small particles with a diameter close to the mean diameter of the particles in the liquid and with a volume concentration also being close to the overall concentration of magnetic material in the suspension – values that can be obtained from magnetization measurement. The second fraction has thus to be highly diluted and it is assumed that the particle diameter of this fraction is considerably large compared to the mean particle diameter. In practice this means, that the fraction consists of the portion of large particles with diameters above 14 nm, seen e.g. in the size distribution given in Fig. 2.5. These particles can form chain like aggregates which are assumed to be straight and rigid. The magnetic interparticle interaction is considered for the particles in the chains but not between particles in different chains. Thus the formation of rod-like structures (see Fig. 4.30.) as they have been found for strongly interacting particles in Monte Carlo simulations (Satoh et al, 1996a; Satoh et al., 1996b) is not considered.

Furthermore interaction between particles of the different fractions is also neglected as it is small compared with the interaction of the particles with large diameter. Therefore the chain aggregates contain only these particles and not the ones of the major fraction with small diameter. These assumptions concerning the interaction are reasonable, since indeed a simple comparison of the interaction energies shows that the interaction of the large particles is about 3-times higher than that of the large with small particles and about 10-times higher than the interaction of the small particles with others of that fraction.

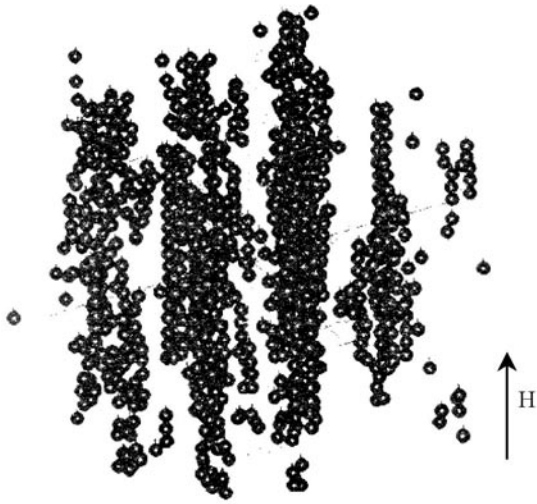

Fig. 4.30. Rod like structures formed by magnetic dipole interaction between magnetic particles and between particle chains (from Satoh et al, 1996b).

Concerning the interchain interaction, the simulations in (Satoh et al., 1996b) have shown that magnetite particles with diameters above 20 nm are necessary to make this interaction a significant contribution. Therefore it can be neglected in the present model being restricted to the particle size in normal ferrofluids, i.e. to particles up to 20 nm.

Finally it is assumed that the interaction of neighboring particles is stronger than that of the particles with the applied magnetic field leading to an alignment of the particles' magnetic moment in the direction of the chain axis. The validity of this assumption can also easily be proved. For 20 nm magnetite particles in a magnetic field of up to 25 kA/m as it has been used in all experiments discussed above, the energy in the field $E_H = \mu_o mH$ is about one order of magnitude smaller than the dipole-dipole interaction of particles of the same size as it can be calculated from (2.6).

With the given assumptions, first of all the properties of the concentrated system containing the small particles are estimated and then the interaction of the larger ones in the presence of a certain kind of magnetic background provided by the particles of the first fraction are calculated. The calculation is based on the fact that the distribution function of the particles in the chains, g_n, must provide a minimum in the systems free energy F_E.

$$F_E = k_B T \sum_n g_n \left[\ln \frac{g_n}{e} - \frac{1}{2k_B T} \mu_0 m_{chain} H \right] \quad . \tag{4.26}$$

Here the logarithmic part represents the normal entropic part of the free energy while the second term accounts for the energy of the chain in the field, where m_{chain} is the magnetic moment of the chain.

Following the methods in (Zubarev and Iskakova, 1995a,b) one obtains a complex expression for the mean number of particles in the chain <n> given by

$$< n > = \frac{\phi_l'}{V_l' \sum_n g_n} \tag{4.27}$$

with ϕ_l' and V_l' being the volume concentration and the particle volume of the large fraction including the surfactant and the distribution function g_n being a function of the interaction energies of the large particles with the field and with their nearest neighbor. Figure 4.31 shows <n> as a function of magnetic field strength as calculated that way in (Zubarev et al., 2001a). With this information about the mean length of the chains one can in principle calculate the components of the stress tensor of the liquid and thus its rheological properties for vanishing shear rate following the principles of statistical hydrodynamics of diluted suspensions of rigid ellipsoids (see e.g. (Brenner and Condiff, 1980)). This has been done in detail in (Zubarev et al., 2001a). The final equation for the viscosity of the fluid in the presence of chains interacting with the magnetic field has then been fitted to experimental data obtained for APG513A at an extremely low shear rate of $\dot{\gamma} = 0.1 s^{-1}$ being close to the theoretical limit of vanishing shear.

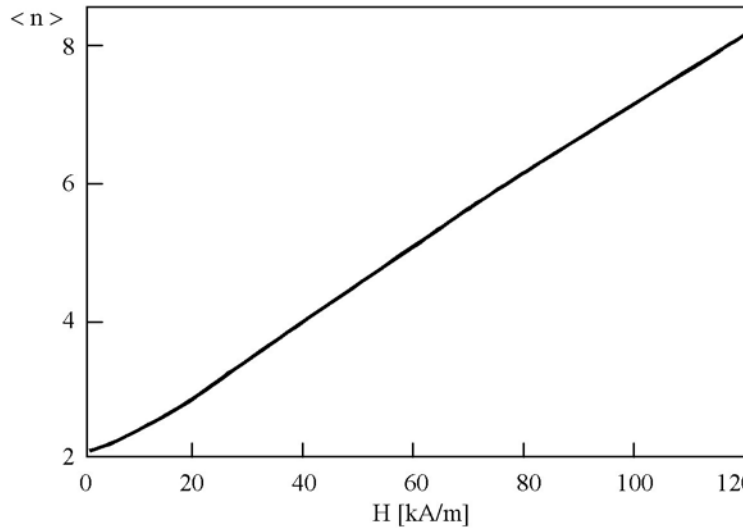

Fig. 4.31. The mean chain length <n> as function of the magnetic field strength.

Using the size d_{ml} of the magnetic core of the large particles and their volume concentration ϕ_1' as fit parameters, one obtains d_{ml}=16.5 nm and ϕ_1' = 0.017. Together with the overall volume concentration of particles ϕ' = 0.27, their mean diameter $\bar{d}$ = 9 nm, and the thickness of surfactant s=3 nm, this leads to a diameter of the small fraction of about 8,5 nm. The experimental data is shown together with the fitted values from (Zubarev et al., 2001a) in Fig. 4.32. It is obvious, that an excellent agreement of the chain model with the experimental data is obtained, giving another strong indication for the existence and importance of chains of magnetic particles. In addition, recalculating the volume fraction of magnetic material of the large particles, from the value for ϕ_1' given above, a volume fraction of ϕ_1=0.007 is obtained, which equals about 10 % of the total magnetic volume fraction. Comparing this with the size distribution of the magnetic particles obtained by a magnetogranulometric analysis for the fluid used in the experiment leading to the data in Fig. 4.32 (see Fig. 4.33) a good agreement for the large particle fraction is found. Furthermore the value for the amount of chain forming magnetic units obtained here from a detailed theoretical approach can be compared with the values obtained from the high shear rate limit for the fluids with varying content of large particles and agglomerates. Obviously the values are in the same order of magnitude and thus two independent methods lead here to the conclusion that the relatively small amount of large particles gives rise to the significant increase of the magnetic fluid's viscosity.

As a further proof for the fact that the large particle fraction forms chains which have dominant influence on the magnetoviscous behavior one can try to compare the theory with results for weak shear rates, i.e. $\dot{\gamma} \leq 1\ s^{-1}$. For this case a numerical solution of the theory in (Zubarev et al., 2001a) leads to shear dependent values

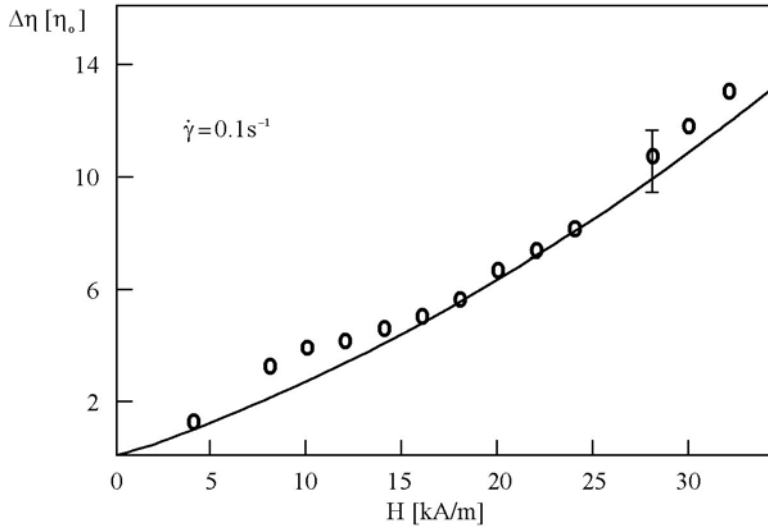

Fig. 4.32. Experimental data for the magnetoviscous effect in APG513A measured at $\dot{\gamma} = 0.1s^{-1}$ together with a fit following the chain theory in (Zubarev et al., 2001a).

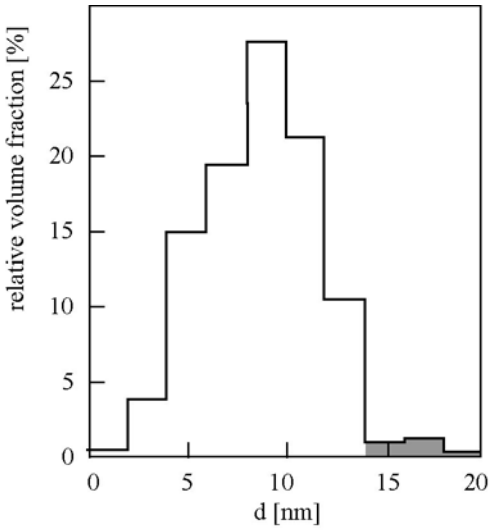

Fig. 4.33. The size distribution of particles for the batch of the fluid APG513A used in the experiments leading to the data in Fig. 4.32.

of the field dependence of the fluid's viscosity. As discussed above, shear will lead to a break of the chains and thus to a maximum length of the chains stable in the shear flow. This has been considered in the numerical calculation by using the maximum value, determined by a force equilibrium as it was discussed in the chain model in Sect. 4.3.1 (see (4.23)), as maximum for all summations over the particle number in the chains like in (4.26). The results were obtained using the data for the sizes and volume fractions for the large and small particle fraction in the fluid as obtained from the fit of the theory for vanishing shear to the experimental data for $\dot{\gamma}$ =0.1 s^{-1} (see above and Fig. 4.32). Figure 4.34 shows the comparison of the experimental data for $\dot{\gamma}$ =0.5 s^{-1} and 0.9 s^{-1} together with the numerical values calculated that way. It should be mentioned, that the theoretical values are not fitted but directly calculated using the data obtained for the case of vanishing shear which is shown for comparison in Fig. 4.34 too. Obviously good agreement concerning the order of magnitude of the viscosity changes is found between theory and experiment.

Thus one can finally state here that a bidisperse model, describing a concentrated commercial magnetic fluid as a system consisting of a relative small fraction of particles with magnetic diameters about 16 nm and of a magnetic fluid consisting of small particles can be the basis for a microstructural explanation of the magnetoviscous behavior.

In this model the large particles interact and the interaction leads to the formation of chains. The influence of these chains and their interaction with external fields dominates the magnetoviscous behavior. Breakage of the chains due to shear flow results in a reduction of magnetoviscous changes of the overall viscosity of the fluid. In addition a reduction of the volume fraction of the large magnetic particles also results in a decrease of the magnetoviscous effect.

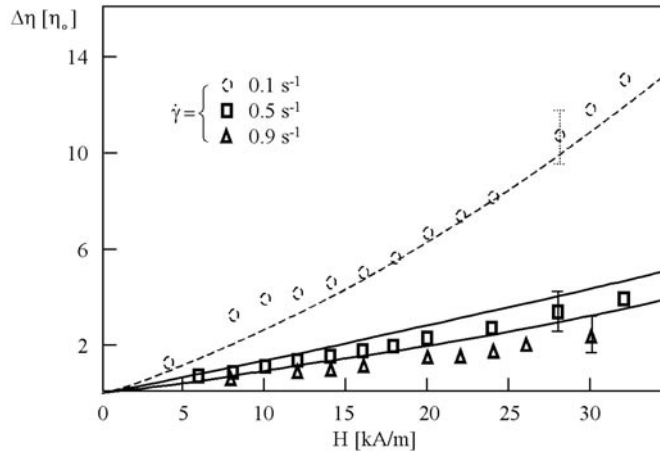

Fig. 4.34. The magnetoviscous effect for APG513A for various shear rates below $1s^{-1}$ together with calculations based on an extended chain theory for small shear rates and using the fit parameters obtained for $\dot{\gamma} = 0.1 s^{-1}$.

4.3.5 Rheological description of magnetoviscosity

As it has been shown in the various examples above, ferrofluids exhibit significant changes in their viscous behavior under the influence of magnetic fields. Till now we've tried to explain these phenomena by microscopic models to analyze the field influence on viscosity in terms of structural changes in the fluids' microstructure. Besides this approach, a rheological description of the fluids' behavior can be a helpful tool in the analysis and description of the behavior of different liquids.

One possible approach for a more general macroscopic description is the expression of viscosity of a ferrofluid under field influence as a function of the stress ratio (Rosensweig et al., 1969) which has been discussed shortly at the beginning of Sect. 3.1 (see (3.1)). The main claim of this description (Rosensweig et al., 1969) has been, that it allows to scale fluids with different make-up to a common viscosity behavior.

To check this with the fluids used in the experiments discussed above, the measured changes of fluids' viscosity in a magnetic field have been analyzed by this concept for the fluids with different content of large particles (see Sect. 4.3.2) and for APG513A. Fig. 4.35 shows the viscosity changes as a function of the stress ratio for APG513A. In this case the viscosity changes have been plotted separately for different shear rates. Obviously the stress ratio does not completely describe the influence of shear rate on the fluids viscous behavior. It is observed that an increase of shear rate at constant stress ratio lead to stronger magnetoviscous effects. In contrast, for high shear rates the curves coincide within the margin of error of the measured data.

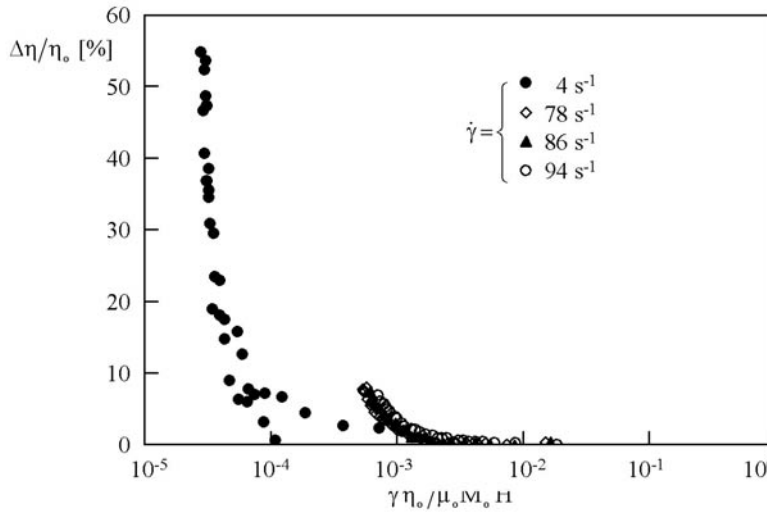

Fig. 4.35. The viscosity changes in APG513A as a function of the stress ratio given in (3.1).

An observation which is not intuitively clear in the first stage. To understand this, one has to call back what (3.1) stands for. The stress ratio is the relation of viscous and magnetic torques acting on a magnetic particle in the fluid. For high shear rates this stress ratio can be applied in the way it is since – as discussed before – for high shear rates all chains are broken and thus single particles can be assumed to be the magnetic units interacting with the magnetic field. The situation changes, as soon as chains are formed. In this situation the magnetic torque remains unchanged $N_{mag} = \mu_o M_o HV$ where V denotes the volume of the unit interacting with the field, i.e. the total chain. In contrast the viscous torque can not longer be written as $N_{vis} = 3\eta_o \dot{\gamma} V'$.

If we look to the force acting on a chain due to viscous friction as given in (4.22) and calculate from this the viscous torque acting on a chain containing n particles, we obtain

$$N_{vis} = 3\eta_o \dot{\gamma} \frac{n_{(\dot{\gamma})}^2}{8} V' \quad . \tag{4.28}$$

The important difference is the square of the chain length entering the viscous torque. This factor depends on shear rate and can thus not be taken as a constant in the stress ratio. That means that a decrease of shear rate, resulting in an increase of chain length, will over proportionally increase this torque and will thus increase the stress ratio calculated by (3.1). Therefore a comparison of magnetoviscous effects for identical values of the stress ratio defined in (3.1) is only valid as long as no chains appear. Appearance of chains would thus require a more complex expression for the stress ratio, which can not reasonably be based on the straight chain model given in Sect. 4.3.1 since in reality the chains will not be straight and their mutual orientation to the flow is not known too.

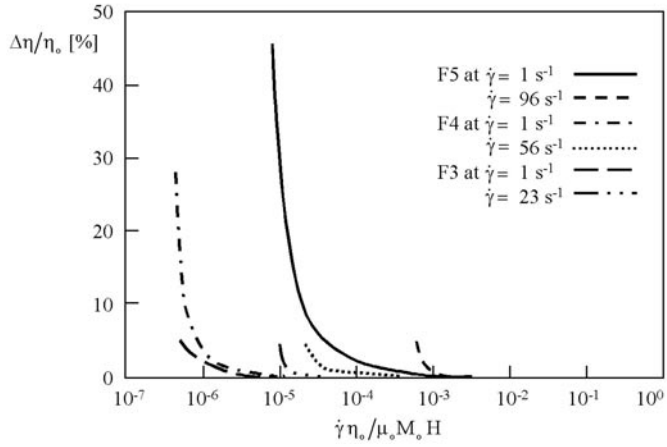

Fig. 4.36. The viscosity changes for fluids F1-F5 as a function of the stress ratio for $\dot{\gamma} = 1\,s^{-1}$ and for high shear rates indicated in the figure.

Therefore, in the light of the above given discussion, the observation made in Fig. 4.35 fits well with our earlier observation, that the fluid can be described by relatively simple models at high shear rate, where its microstructural make-up reduces to a single particle situation, while low shear rates allow changes of the microstructure in the field and thus make the description of the fluid more complex.

This point is strengthened if one compares the fluid APG513A with the liquids F1 to F5 containing different amount of large particles. As pointed out in Sect. 4.3.2 these fluids have similar overall magnetic concentration and differ just in the size distribution of particles. So the stress parameter concept expects, that, at least for the same shear rate, the dependence of viscosity on the stress parameter should be identical. Fig. 4.36 shows the data for these fluids for a common low, as well as for a high shear rate. In this case, for low shear rate as well as for high values of $\dot{\gamma}$, the fluids differ significantly in their dependence of viscosity on the stress ratio.

So, obviously, the stress ratio concept does still base on a couple of assumptions concerning the microstructure, making it difficult to use it in general for fluids which have different microscopic properties or which exhibit strong microstructural changes in a magnetic field.

Another possibility to give a general description of the fluids viscous behavior is the determination and classification of the relevant dimensionless flow function $f(\sigma/\sigma_*)$

$$f(\sigma/\sigma_*) = \frac{\eta_*}{\sigma_*}\,\dot{\gamma} \quad , \tag{4.29}$$

where σ_* and η_* denote positive constant reference values of stress and viscosity (Böhme, 1981). From the measured dependence of viscosity on shear rate $\eta(\dot{\gamma})$ one can plot the relation between stress and shear rate using the well known relation $\sigma = \eta\dot{\gamma}$. The mentioned plot of σ versus $\dot{\gamma}$ provides directly the information about $f(\sigma/\sigma_*)$, where the reference values η_* and σ_* can be defined freely in principle. For APG513A this relation is shown in Fig. 4.37 for zero field and for an applied field strength of 34 kA/m. Here the maximum stress – reached for the highest shear – is used as reference stress σ_*.

Two major features are obvious; the stress changes linearly with the shear rate for the zero field situation and a field-dependent shift of the stress appears. For vanishing field the linear relation goes through zero, that means the flow function is simply given by $f(\sigma/\sigma_*) = \sigma/\sigma_*$ – the flow function for a Newtonian fluid as it had to be expected for the zero field situation. An increase of the applied field strength gives rise to an offset of the stress – a so called yield stress is induced in the fluid. Furthermore the dependence of stress on shear rate above the yield stress is slightly nonlinear. Due to the fact, that the minimum shear rate in Fig. 4.36 is about 10 s^{-1}, one could suspect, that the fluid could also show a behavior without yield stress, like it is described by the Eyring model, given by $s = 1/c_1 a\sinh(\dot{\gamma}/c_2)$ where c_1 and c_2 are free fitting parameters. Nonetheless we'll stay here with the approach employing a yield stress since this is a behavior

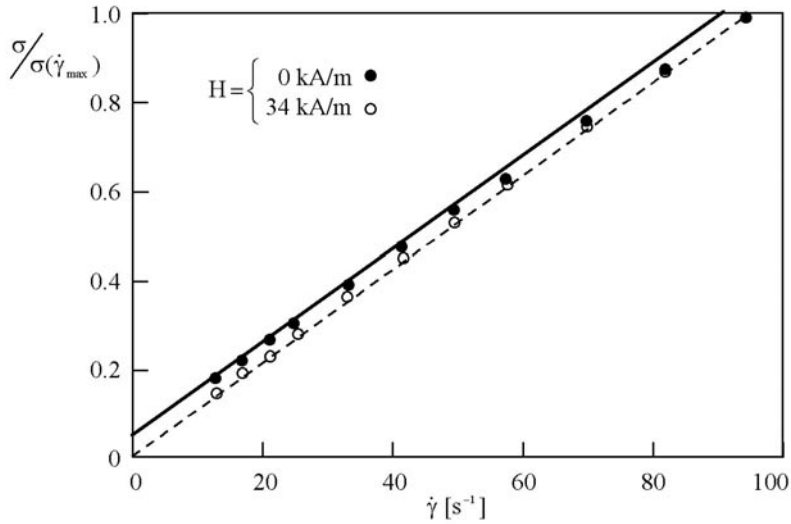

Fig. 4.37. The dependence of stress on shear rate for APG513A for vanishing field and for H=34 kA/m.

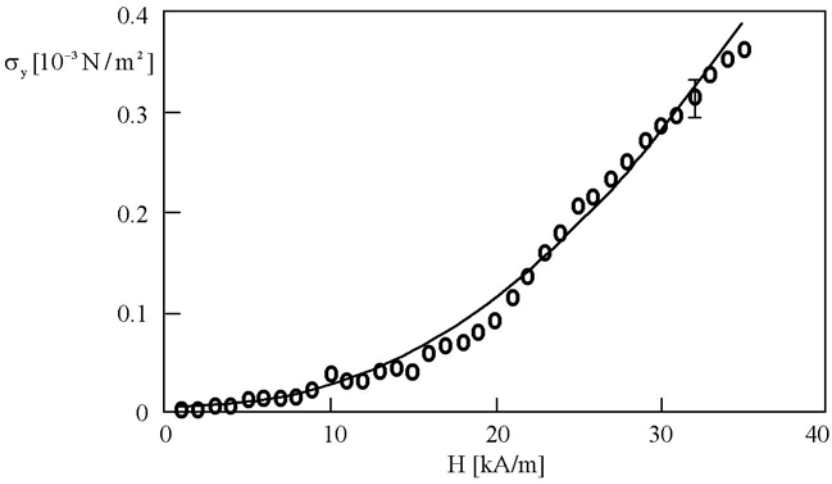

Fig. 4.38. The yield stress of APG513A as a function of the strength of the applied magnetic field. The full line represents a quadratic fit to the measured data.

known from magnetorheological fluids and thus it seems to be reasonable to follow this path here too. Such kind of behavior – the appearance of a yield stress σ_y and a shear rate dependent behavior of stress above the yield stress value can be written as

$$\sigma = \sigma_y + \eta_{(\dot{\gamma})}\,\dot{\gamma} \quad , \tag{4.30}$$

representing the typical behavior of a Bingham fluid. As mentioned, this kind of rheological behavior is in principle known for suspensions of magnetic particles, as will be discussed in Sect. 5.2 with respect to magnetorheological fluids. In our particular case the yield stress, being typical for a Bingham fluid, is extremely small – for the maximum field strength applied, it reaches a value about $3.6 \cdot 10^{-4}$ N/m^2.

Table 4.5. The yield stress for APG513A and for the fluids F2 to F5 for three different field strength'

Fluid	$\sigma_{y\,(H=10kA/m)}$ $[10^{-4}N/m^2]$	$\sigma_{y\,(H=20kA/m)}$ $[10^{-4}N/m^2]$	$\sigma_{y\,(H=33kA/m)}$ $[10^{-4}N/m^2]$
APG513A	0.23	1.05	3.6
F5	1	1.07	11.8
F4	0.5	2.08	6.2
F3	0.46	1.15	3.8
F2	0.12	0.25	1.9

Nonetheless, it is measurable and Fig. 4.38 shows the dependence of σ_y on the strength of the magnetic field. Within the measuring accuracy σ_y increases proportional to H^2 – again a behavior found for many field strength dependent phenomena since the effects depend usually on the product MH being proportional to H^2 for small values of H. The same behavior, i.e. a Bingham like type of the flow function, is found for the fluids with different content of large particles too. Thus the description of the fluids behavior by a Bingham model represents the general form of description we'd been searching for. The variations resulting from the different microscopic make-up result now in a change of the absolute value of the yield stress, which is given in Table 4.5 for the different fluids for various magnetic field strength. The overall dependence of the yield stress on magnetic field strength follows again a unique quadratic law as seen in Fig. 4.39.

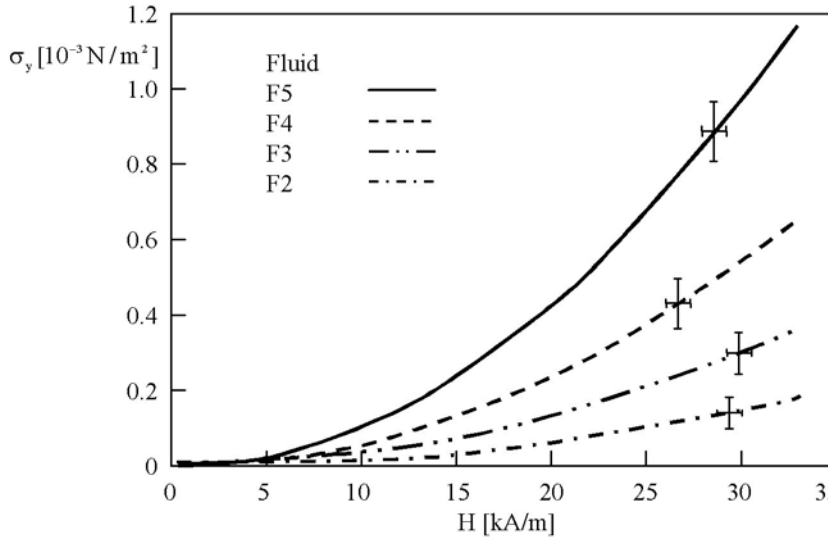

Fig. 4.39. The yield stress of fluids F1-F5 as a function of the strength of the applied magnetic field. A clear dependence of the yield stress on the amount of large particles is observed.

4.4 Viscoelastic effects in ferrofluids

The formation of structures of magnetic particles due to interparticle interaction rises the question whether further non newtonian effects – besides the shear thinning discussed in Sect. 4.3 – or even viscoelastic effects may appear. Viscoelasticity due to deformation or interaction of chains of magnetic particles is in principle known from magnetorheological fluids (see Chap. 5) and thus it is to be expected in ferrofluids exhibiting strong interparticle interaction. Since the length and rigidity of the chains depends on the strength of the applied magnetic field, a field-dependent and field controllable viscoelasticity should appear in magnetic particle suspensions. The advantage of its investigation in ferrofluids would be given by the – compared with magnetorheological suspensions – well defined and easy to be described magnetic properties of the fluids. These results in an enhanced possibility to describe and understand the relevant microscopic processes. In addition, the long term stability of ferrofluids provides an excellent basis for detailed quantitative studies.

4.4.1 Normal stress differences in magnetic fluids

One of the first predictions of viscoelasticity in ferrofluids has been the calculation of normal stress differences in the presence of particle chains (Zubarev, 1992). That means that the main axis components of the stress tensor σ_{ii} are different and thus differences of the normal stresses can be defined in the way (Walters, 1975)

$$N_1 = \sigma_{11} - \sigma_{22} \quad N_2 = \sigma_{22} - \sigma_{33} \quad . \tag{4.31}$$

The normal stress differences vanish for a fluid at rest and they stay constant under flow reverse. Therefore one can extract a factor $\dot{\gamma}^2$ from the normal stress differences in (4.31) leading to

$$N_1(\dot{\gamma}) = \nu_1(\dot{\gamma}) \cdot \dot{\gamma}^2 \quad N_2(\dot{\gamma}) = \nu_2(\dot{\gamma}) \cdot \dot{\gamma}^2 \quad , \tag{4.32}$$

where ν_i denote the so called normal stress coefficients. These coefficients depend usually on shear rate in a way that they have a finite low shear limit ν_{io}

$$\nu_{io} = \lim_{\dot{\gamma} \to 0} \nu_i(\dot{\gamma}) \tag{4.33}$$

and they reduce with increasing shear rate (Böhme, 1981).

To measure these differences, various rheological methods like a direct force measurement in a plate-plate rheometer (Binding and Walters, 1976) or the observation of die swelling (Tanner, 1988) have been reported for the investigation of polymer solutions or other liquids exhibiting strong viscoelasticity. In ferrofluids the normal stress differences will depend strongly on shear rate since the chains leading to the effects will diminish in size with increasing shear as it has been shown in Sect. 4.3. Thus all methods using flow with high shear rate are not appropriate at all to perform investigations with ferrofluids. Furthermore, since the effects scale quadratic with shear rate as seen from (4.31), low shear rates e.g. in a cone plate rheometer, will reduce the forces due to the normal stress differences in a way, that a detection is not possible with the technique available (Schott, 1993).

A way out from this problem of detection of normal stress differences in ferrofluids is given by one of the most famous effects driven by their appearance – the so called Weissenberg effect. This phenomenon named after the Austrian physicist Carl Weissenberg (*1893, †1976) is characterized by the rise of a free surface of a liquid at a rotating shaft. In a newtonian fluid the free surface would lower at the shaft since the fluid is subjected to a centrifugal force directed radially outward. In contrast, the presence of normal stress differences will give rise to a force directed radial inward, i.e. towards the rotating rod. This force acts against the centrifugal force leading to a rise of the free surface at the rod.

This can be understood looking to the equilibrium of forces acting on a fluid element. Fig. 4.40 shows the situation discussed with the relevant parameters.

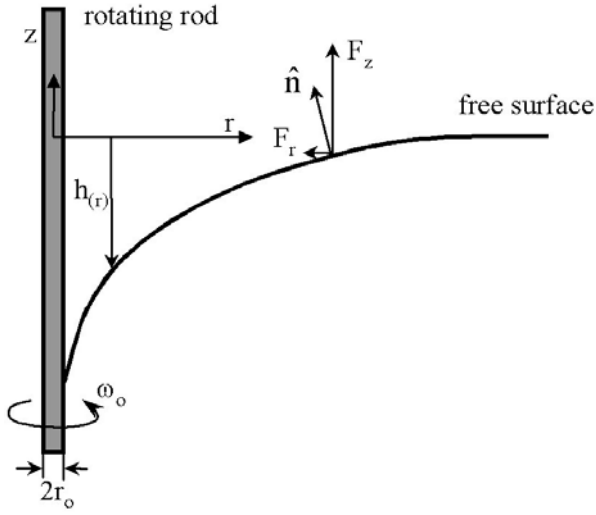

Fig. 4.40. Principle set up for the investigation of the Weissenberg-effect with all relevant parameters.

In a newtonian liquid, i.e. in the absence of normal stress differences, the pressure gradient in the liquid needs to compensate the centrifugal as well as the gravitational volume force since the fluid volume element moves neither in radial nor in z-direction

$$\nabla p = \rho r \omega_v^2 \hat{e}_r - \rho g \hat{e}_z \quad , \tag{4.34}$$

where ω_v denotes the angular acceleration of the volume element at radial position r and $\hat{e}_r$ and $\hat{e}_z$ are unit vectors in r- and z-direction respectively.

Obviously this pressure varies in radial direction and thus a flat surface can not be stable in the presence of a rotating rod since the pressure on a stable free surface has to be constant. Therefore the free surface has to be curved as shown in Fig. 4.40 and since the pressure has to be constant at the surface, its gradient needs to be parallel to the surface normal $\hat{n}$ with

$$\hat{n} \sim \hat{e}_z - \frac{dh}{dr} \hat{e}_r \quad . \tag{4.35}$$

With (4.34) this leads immediately to an equation, determining the shape of the free surface

$$\frac{dh}{dr} = \frac{r \omega_v^2}{g} \quad . \tag{4.36}$$

The angular acceleration of the volume element ω_v can be expressed by the rotation rate of the rod ω_o , using the radius of the rod r_o in the form

$$\omega_v = \omega_0 \frac{r_0^2}{r^2} \tag{4.37}$$

if it is assumed that the outer boundary of the fluid pool is at infinity. Therefore we obtain

$$\frac{dh}{dr} = \frac{\omega_0^2}{g}\,\frac{r_0^4}{r^3} \quad \text{and thus} \quad h_{(r)} = -\frac{1}{2}\,\frac{\omega_o^2}{g}\,\frac{r_o^4}{r^2} \tag{4.38}$$

describing the shape of the free surface of a newtonian liquid at the rotating rod, being bend downward at the rod as expected. In a non-newtonian liquid with normal stress differences an additional radial volume force due to the normal stress differences has to be considered

$$\frac{1}{r}\left[-(N_1+N_2)+\frac{d}{dr}(r\,N_2)\right]\hat{e}_r \quad . \tag{4.39}$$

Using this in (4.34) and replacing the N_i by (4.32) one obtains for small shear rates $\dot{\gamma}$ a new determining equation for the free surface in the form

$$\frac{dh}{dr} = \frac{\omega_0^2}{g}\left[\frac{r_o^4}{r^3} - \frac{4}{\rho}(\nu_{10}+4\nu_{20})\,\frac{r_o^4}{r^5}\right] \quad , \tag{4.40}$$

where

$$\dot{\gamma} = r\,\frac{d\omega}{dr} = -2\omega_0\,\frac{r_0^2}{r^2} \tag{4.41}$$

has been used. Integrating (4.40) leads to a description of the free surface shape in the presence of finite values for the normal stress coefficients

$$h_{(r)} = \frac{\omega_o^{\,2} r_o^{\,2}}{g}\left[-\frac{1}{2}+\frac{\nu_{10}+4\nu_{20}}{\rho r^2}\right]\left(\frac{r_0}{r}\right)^2 \quad . \tag{4.42}$$

Directly at the rotating rod ($r = r_o$) the free surface height thus reads (Böhme, 1981)

$$h_{(r_o)} = \frac{\omega_o^{\,2} r_o^{\,2}}{g}\left[-\frac{1}{2}+\frac{\nu_{10}+4\nu_{20}}{\rho r_o^{\,2}}\right] \quad . \tag{4.43}$$

In magnetic fluids, field-dependent appearance of the Weissenberg effect is expected. If magnetic particle chains are formed these give rise to normal stress differences (Zubarev, 1992). As it has been discussed above, the size of the chains depends on magnetic field strength as well as on shear rate applied to the fluid. Thus – at fixed shear rate – an increase of magnetic field strength will give rise to an increase of chain length and therefore to a rise in the normal stress differences. That means, for H=0 the fluid will behave newtonian , showing no normal stress differences and therefore the free surface will be bend downward at the rotating axis (see Fig. 4.41). Increasing the magnetic field, chains are formed, normal stress differences occur and start to act in concurrence with the centrifugal forces leading to a less strong downward bending of the fluid surface.

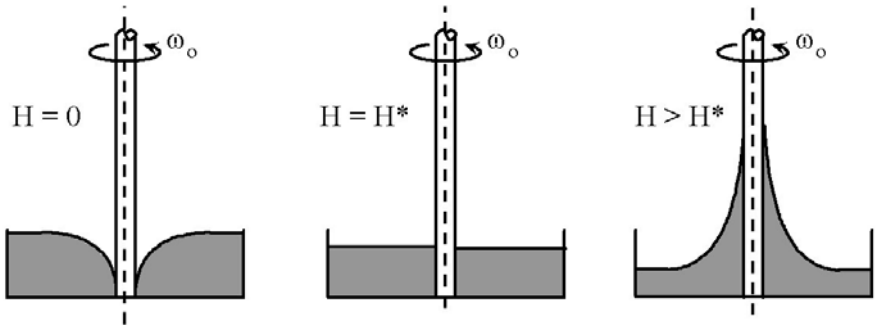

Fig. 4.41. On the determination of the stable surface of a fluid in the presence of a rotating rod. Detailed explanation is given in the text.

At a distinct field strength H* normal stress and centrifugal effects compensate and a flat surface of the liquid is observed. For magnetic field strength above H* the fluid will finally rise at the rotating axis.

If the magnetic field is been held constant at a certain value, and shear rate is varied, a shear induced breakage of the chains will occur, leading to a reduction of the normal stress differences and thus to a lowering of the free surface at the rotating axis. From an experimental point of view the situation where a flat surface is formed is of distinct importance. A flat surface means – as seen from (4.43), that normal stress effects and centrifugal forces equalize and thus – for given diameter of the rotating axis – the combination (ν_{10}+4ν_{20}) of the normal stress coefficients can be determined for the field H* to be

$$\nu_{10} + 4\nu_{20}\big|_{H^*} = \frac{1}{2}\rho r_o^2 \quad . \tag{4.44}$$

In addition, measuring the height of the fluid surface for different magnetic field strength below and above H*, the field strength for the combination (ν_{10}+4ν_{20}) as given in (4.44) can be obtained with a smaller experimental error than a single height of the fluid surface at the rotating axis could be determined.

Incidentally – as we have seen in the discussion of the magnetoviscous effect – the formation of chains in commercial ferrofluids is not strong at all and the chains themselves are so weakly coupled, that significant effects can only be expected at low shear rate. For the experimental situation in an experiment on Weissenberg effect this means, that the rotation frequency of the rod has to be low.

As seen from (4.43) this leads to a small value of the coefficient determining the absolute value of the height changes at the rotating rod. This should shortly be illustrated with an example. Assuming a typical size of the experimental set up with a rod diameter of 5 mm and a diameter of the fluid pool of about 50 mm, the frequency of the rod should be as low as $\omega_o = 5\ s^{-1}$ to obtain a mean shear rate about 1 s^{-1} in the fluid. With these values the decline of the fluid surface at the rod for the pure newtonian situation – i.e. for H=0 - would be in the order of 10^{-2} mm.

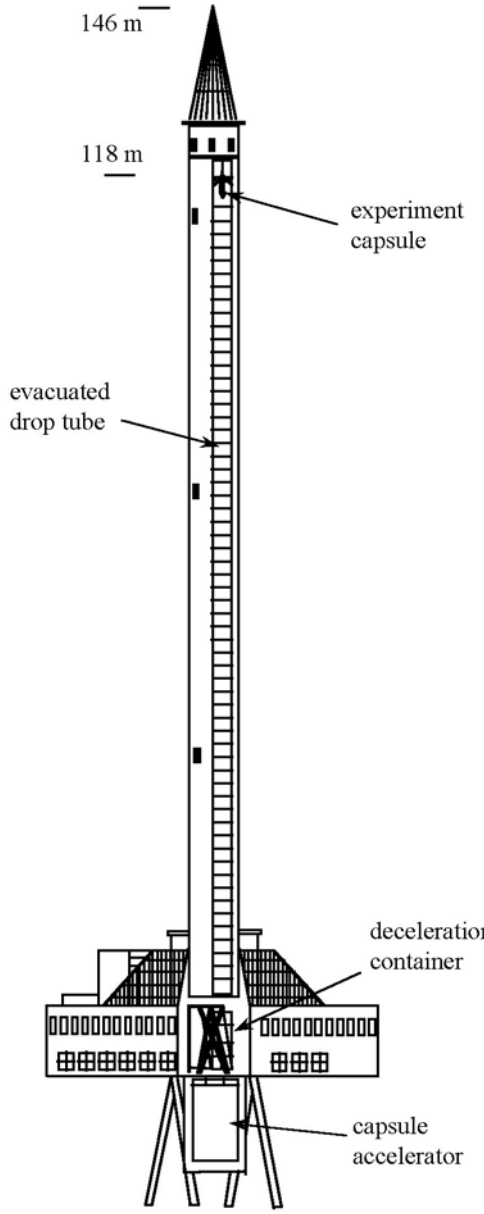

Fig. 4.42. The concept of drop tower "Bremen". A capsule containing the experiment is dropped in a 120 m high vacuum tube. During the 4.75 seconds of free fall the experiment experiences a residual acceleration as low as 10^{-6} g_o (g_o=9.81m/s^2 denoting the normal gravitational acceleration). At the bottom of the tube the capsule is decelerated in a container filled with small polystyrene spheres.

A value clearly beyond the resolution of normal optical observation as well as e.g. of impedance based measurement. Therefore, under normal experimental conditions, the possibility to measure the field-dependent change of height of the fluid surface at the rotating rod in a commercial ferrofluid is negligibly small. Nevertheless, (4.43) provides a way to use the Weissenberg effect as a proof for the existence of normal stress differences even in fluids with weak viscoelastic properties. As seen from (4.43) the height of the fluid surface scales inverse proportional to the gravitational acceleration acting on the fluid.

Thus an experiment under conditions of strongly reduced gravitational acceleration could serve as an amplification for the height changes making them measurable. For the example discussed above a reduction of gravitational acceleration to 10^{-3} g_o (g_o=9.81 m/s^2 being the normal gravitational acceleration in a laboratory experiment) would amplify the height changes for the pure newtonian situation to about 10 mm using the parameters discussed before. An effect which is clearly measurable. Changes of this value due to field-induced normal stress effects would thus also become detectable.

Several means for the performance of experiments under reduced gravitational acceleration are nowadays available. Besides the well known rocket, space shuttle or space station facilities which require an immense technical and financial effort for the performance of an experiment, two kind of ground based experimentation facilities are used.

On the one hand drop systems like the drop towers at NASA's facilities in Lewis, the drop tower "Bremen" of ZARM in Bremen (see Fig. 4.42) or the Japanese drop shaft in Hokkaido provide conditions of highly reduced gravitational acceleration of up to 10^{-6} g_o. For such drop systems the experimental time is usually in the order of 5 s. As discussed in the example above, the frequency of the rotating rod has to be less than 1 Hz to obtain reasonable shear rates. Therefore drop tower experiments bear the danger that the flow profiles are not completely established during the experiment and thus the data would not lead to well defined information about normal stress differences in ferrofluids.

An alternative for ground based, low cost microgravity experiments is the use of so called parabolic flights. In these flights the experiments are mounted in a normal air plane which is flying along a parabolic trajectory. During the pull up and pull out phases (see Fig. 4.43) the z-component of gravitational acceleration is about 1.8 g_o. After the pull up the plane is injected into a parabolic trajectory, the power of the engines is reduced to a compensation of air drag only and the acceleration acting on the experiments is reduced to about 10^{-3} g_o to 10^{-2} g_o for a period of about 20 s.

This time span is sufficient to perform experiments on the Weissenberg effect in ferrofluids even at low shear rate. The residual acceleration of this facility is obviously much worse than in drop towers, but its mean level is still sufficient to make the changes of the fluid surface height at the rod observable, as it has been discussed in the before mentioned example. Thus, in principle, a microgravity experiment should provide a possibility to detect normal stress differences in magnetic fluids by an observation of the Weissenberg effect.

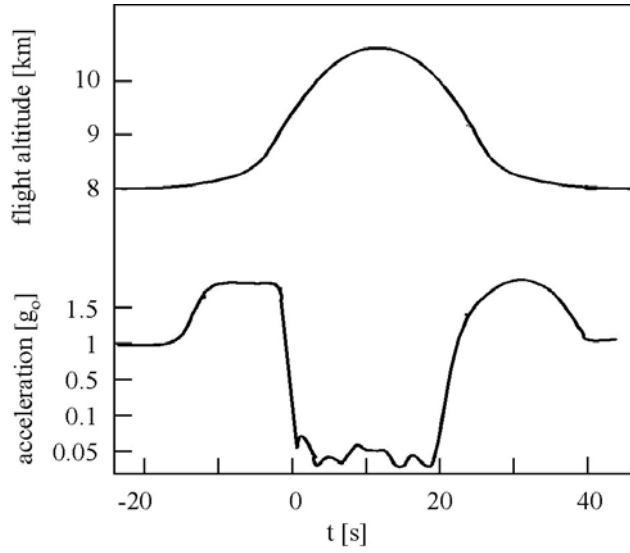

Fig. 4.43. Microgravity conditions can be obtained in aircrafts following a parabolic trajectory. During the 20 seconds of the free fall phase a residual acceleration of about 10^{-2}-10^{-3} g_o is obtained. The pull up – and pull out – phases result in an acceleration of about 1.6-1.8 g_o.

But it has to be considered, that (4.42) does not account for any surface tension effects, which may become significant under reduced gravity conditions. In this context Delgado et al. (Delgado et al., 1988) have shown that in strong viscoelastic systems the fluid surface is forced to form a spherical drop at the rotating axis, strongly reducing the amplification provided by the 1/g factor in (4.42). Another series of experiments with non magnetic fluids with variable strength of normal stress differences (Odenbach, 1995b) showed, that the formation of spherical drops only appears for fluids with relatively strong viscoelastic properties, while a

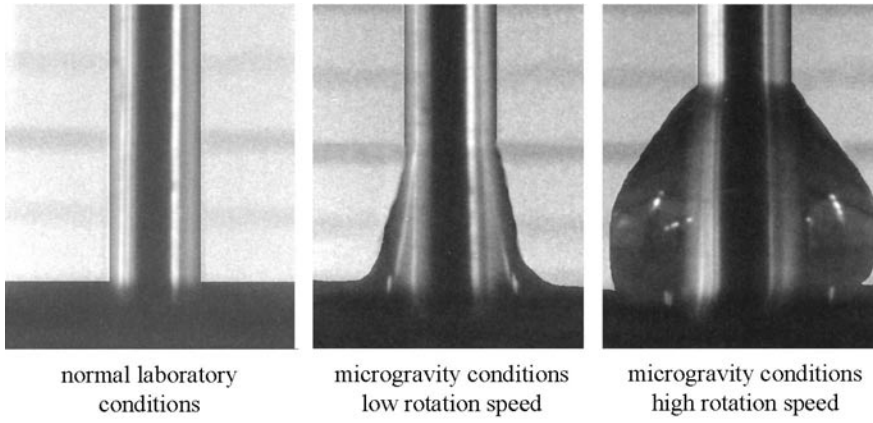

Fig. 4.44. The Weissenberg-effect in a polymer solution containing 3% Oppanol in heptane for various experiment conditions.

reduction of normal stress differences leads to a reduction of the influence of the surface tension since the climb of the fluid surface becomes smaller. The smaller climb results in a reduced deformation of the free surface and thus the tendency of spherical deformations is reduced. In fluids with very weak normal stress effects – showing no Weissenberg effect under 1g conditions – the normal hyperbolic shape of the surface at the rotating rod has been found (see Fig. 4.44), while a strong deformation of the surface leads again to the already mentioned drop like distortion of the surface.

In the situation where the hyperbolic shape is preserved also the full amplification of the variation of the height of the surface could be shown under parabolic flight conditions (Odenbach, 1995b). Thus the method is suitable to investigate ferrofluids where the normal stress effects are too small to be observed in laboratory experiments.

Therefore an experiment has been performed dedicated to observe the field-dependent change of the height of a free magnetic fluid surface at a rotating rod (Odenbach et al., 1999b). The ferrofluid used was APG513A, the same fluid as in many experiments discussed before, and thus a liquid showing effects based on chain formation of the magnetic particles – a basic assumption for the prediction that normal stress differences may appear in ferrofluids. The fluid was contained in a cylindrical vessel with a diameter of 70 mm. The vessel is equipped with a plexiglas wall to enable optical observation of the fluid surface (see Fig. 4.45). Since experimentation under reduced gravity conditions requires special safety standards, the vessel has to be 3 bar pressure tight. Therefore the rotating axis in the center of the fluid cell had a magnetic coupling to the driving motor. The strength and orientation of the magnets have been chosen in a way, that no influence of stray fields from the coupling system to the fluid appears.

To avoid wetting of the observation window with the ferrofluid due to enhanced surface tension effects under microgravity conditions, the fluid pool is equipped with a sharp edge wetting barrier (Dreyer et al., 1993; Dreyer et al., 1994). The whole system is placed in the center of an arrangement of four magnetic field coils lying on a spherical shell – a similar arrangement like it has been used in (Ambacher et al., 1992) (see Sect. 3.1). The coils produce a highly homogenous magnetic field of up to 40 kA/m parallel to the free surface of the fluid. An alignment of the field perpendicular to the free surface is impossible since it would drive the normal field instability (Rosensweig, 1982) and thus would give rise to a spike pattern disabling any kind of observation of the Weissenberg effect.

The rotation rate of the rod can be varied continuously from $\omega = 1\ s^{-1}$ to $\omega = 20\ s^{-1}$ with a stability of $0.05\ s^{-1}$. This corresponds to mean shear rates from about $0.2\ s^{-1}$ to $4.5\ s^{-1}$ for a rod with 8 mm diameter. The whole setup has been mounted in a rack as it is shown in Fig. 4.46. The rack contains all necessary power supplies and the video observation allowing a visual monitoring of the free surface of the ferrofluid.

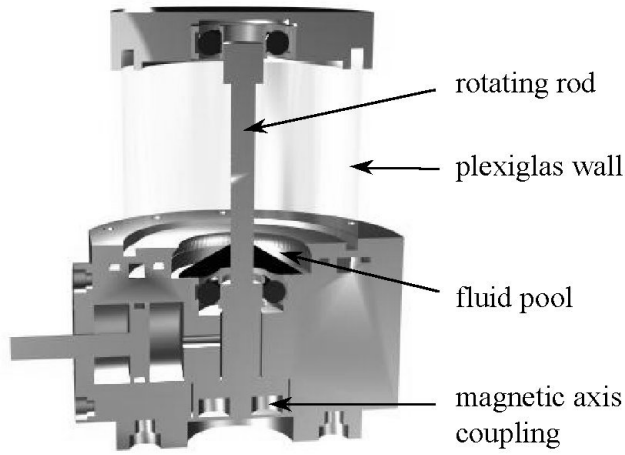

Fig. 4.45. Fluid cell for the investigation of the Weissenberg-effect in magnetic fluids in parabolic flight experiments.

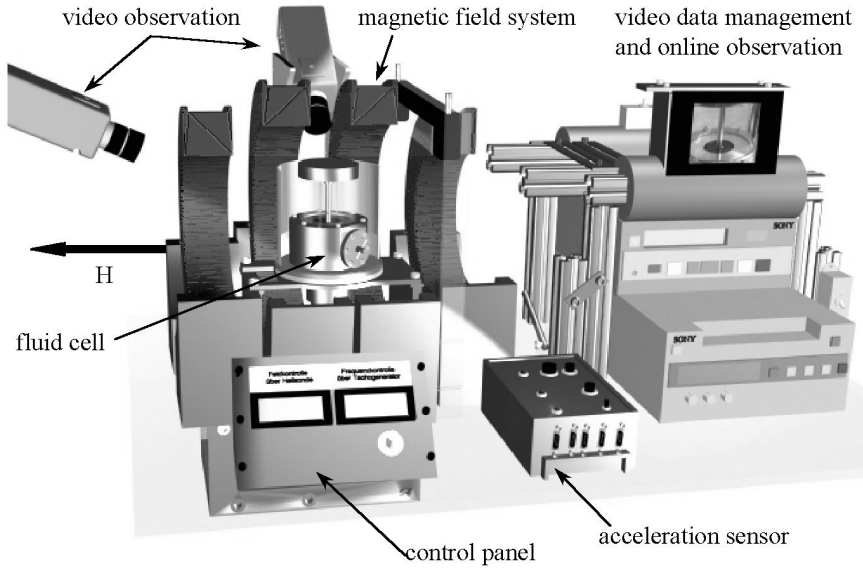

Fig. 4.46. Sketch of the main part of the flight rack for the investigation of the Weissenberg-effect in magnetic fluids in parabolic flight experiments.

To ensure that the susceptibility disturbance due to the rod does not influence the free surface behavior, a test series of experiments with different applied magnetic fields and the rod at rest has been performed under microgravity conditions. Even for the strongest field available no deformation of the fluid surface has been found with the rod at rest, guaranteeing that no disturbances of the measurement appear.

As discussed above, numerous experimental parameters can influence the behavior of the fluid surface. Namely changes of the rod diameter, the rotation rate, the field strength and last but not least the fluid composition can lead to completely different areas of information on the viscoelastic behavior of ferrofluids. To use the limited number of experiment runs as efficient as possible, three different types of experiments have been carried out.

In the first series the shear rate and the rod diameter have been kept constant at $\dot{\gamma} = 0.57\ s^{-1}$ and $2r_o = 5$ mm while the magnetic field strength has been varied from 0 A/m to 40 kA/m using the ferrofluid APG513A. Fig. 4.47 shows the variation of the height of the fluid surface at the rotating rod.

For zero field, the surface bends downward as it is expected for a newtonian liquid. With increasing strength of the applied field the surface rises, indicating the appearance of normal stress differences. For a field strength of about 30 kA/m the surface becomes flat, allowing to calculate the combination $(\nu_{10}+4\nu_{20})$ of the normal stress coefficients. And finally, a slight positive surface deformation appears. This result illustrates the expected appearance of normal stress differences due to field-dependent build up of particle chains.

As second kind of experiments the magnetic field strength has been fixed at H=26 kA/m for APG513A using a rod with 5 mm diameter, while the shear rate has been varied from 0.25 s^{-1} to 2.75 s^{-1} . As seen from Fig. 4.48, the height of the fluid surface diminishes with increasing shear rate indicating the shear dependent breakage of the chains which reduces the normal stress differences in the liquid.

Fig. 4.49 shows the field dependence of the surface elevation for three different shear rates, all three measured with a rod diameter of $2r_o = 5$ mm. This figure shows the increase of H* for the same combination $(\nu_{10}+4\nu_{20})$ with increasing shear rate. The results are compiled in Table 4.6. These experiments illustrate the shear dependence of the appearance of normal stress differences in ferrofluids.

Finally several experiments have been performed to get an insight into the dependence of the effect on the fluids' composition. Therefore two major parameters of the fluid have been varied – the overall magnetic particle concentration for fluids from similar production processes and the content of large particles in the fluid - a parameter, which has been shown in Sect. 4.3.2, to be of significant importance for chain formation in the fluid. In Fig. 4.50 the fluids APG513A with 7.2 vol.% of magnetite and EMG 900 with 15 vol.% of magnetite particles, both from the production of Ferrofluidics, are compared for $\dot{\gamma} = 0.57\ s^{-1}$. Obviously the higher particle concentration leads to a steeper increase of the surface height with field strength indicating a stronger formation of chains. The critical field strength for the same value of the combination of normal stress coefficients is reached at a value, approximately 3 times less than for APG513A.

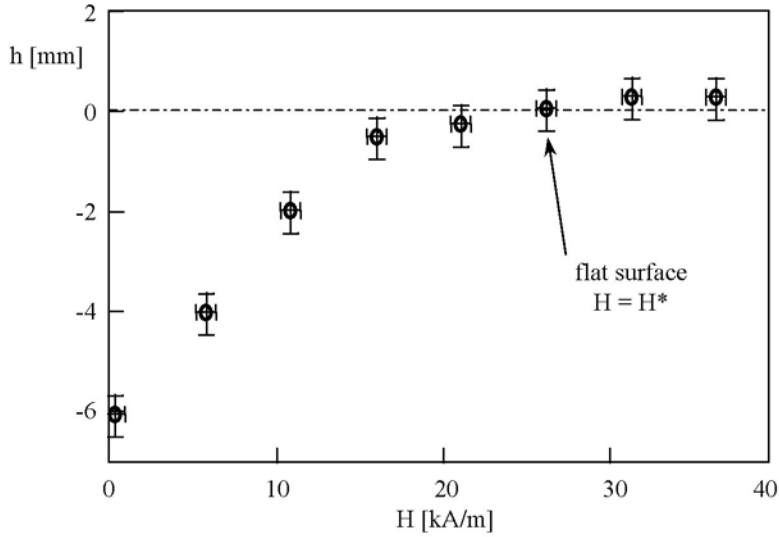

Fig. 4.47. The variation of the height of the fluid surface at the rotating rod as a function of magnetic field strength observed in APG513A for $\dot{\gamma} = 0.57 s^{-1}$ and $2r_o = 5$ mm at a residual acceleration level of $5 \cdot 10^{-3} g_o$.

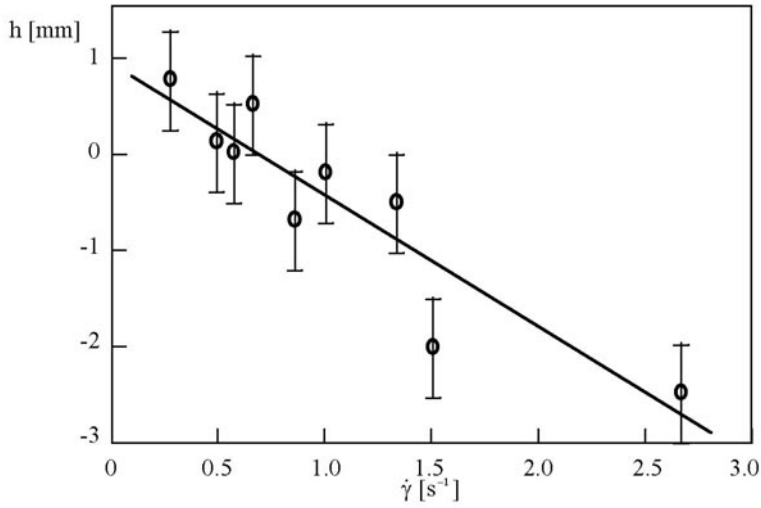

Fig. 4.48. The height of the fluid surface of APG513A at the rotating rod for an applied magnetic field of 26 kA/m as a function of shear rate ($2r_o = 6$ mm).

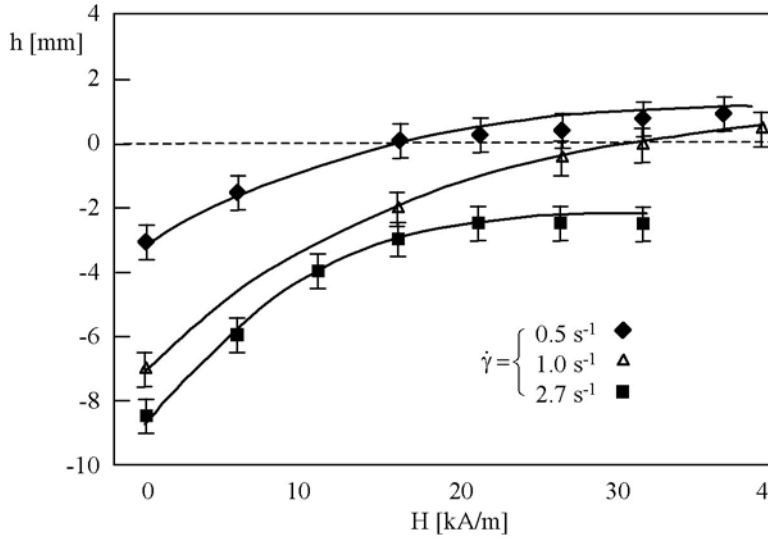

Fig. 4.49. The surface elevation for APG513A for three different shear rates as a function of magnetic field strength illustrating the critical magnetic field strength H^* necessary to obtain a flat surface. The solid lines are guides to the eyes.

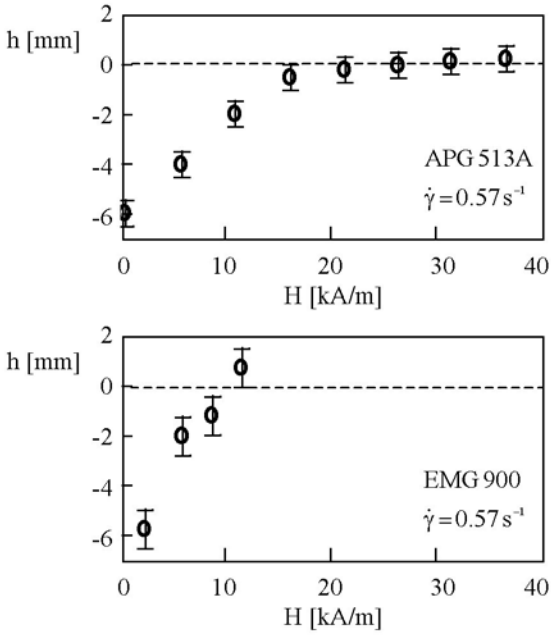

Fig. 4.50. The height of the surface at the rod for two different liquids and $\dot{\gamma}$ =0.57s^{-1} as a function of magnetic field strength.

Table 4.6. Values of $(\nu_{10}+4\nu_{20})$ for different fluids and shear rates

Fluid	$\dot{\gamma}$ [s^{-1}]	H* [kA/m]	$(\nu_{10}+4\nu_{20})$ [kg/m]
APG513A	0.5	24	$1 \cdot 10^{-2}$
	0.57	30	$4 \cdot 10^{-2}$
	1.0	35	$1 \cdot 10^{-2}$
EMG 900	0.57	11	$4 \cdot 10^{-2}$

Experiments with stronger fields for EMG900 leading to a clearer appearance of a positive surface elevation are incidentally impossible since the fluid at the rod is destabilized by the magnetic field perpendicular to the elevated free surface.

The dependence of the normal stress effects upon the microscopic make-up of the fluids is seen in Fig. 4.51. It compares the fluids F2 and F4 with significantly different content of large particles (see Sect. 4.3.2) and APG513A, all containing about 7.2 vol.% of magnetic material with mean particle diameter of 10 mm. The upper part of the figure shows the behavior of the free surface for $\dot{\gamma}$ =0.57 s^{-1} and a rod diameter of 5 mm.

Obviously APG513A shows the strongest effect while F4 and F2 have weaker normal stress effects. The decrease of the effects from APG513A over F4 to F2 corresponds well with the amount of large particles which is illustrated by the magnetoviscous behavior in these three liquids, shown in the lower part of the figure. As higher the content of large particles is, as stronger is the tendency for the formation of chains and as higher are therefore the magnetoviscous effect as well as the normal stress differences.

This result has additional importance, since it rules out the assumption, that the change of the shape of the fluid surface is a result of a magnetic field-dependent stabilization of the free fluid surface in a field parallel to the surface (Zelazo and Melcher, 1969) and not a consequence of the appearance of normal stress differences. The stabilization effect depends just on the strength of the applied field and the concentration of magnetic material in the fluid but not on the particle size. Thus it would have to be identical for all three fluids. The difference in the behavior therefore shows clearly that the rise of the height of the fluid surface is forced by normal stress differences in the ferrofluid under influence of an applied magnetic field.

Thus to summarize these results, experiments on the Weissenberg effect have shown, that the field-dependent formation of chains of the large particles leads to the appearance of viscoelastic effects in ferrofluids.

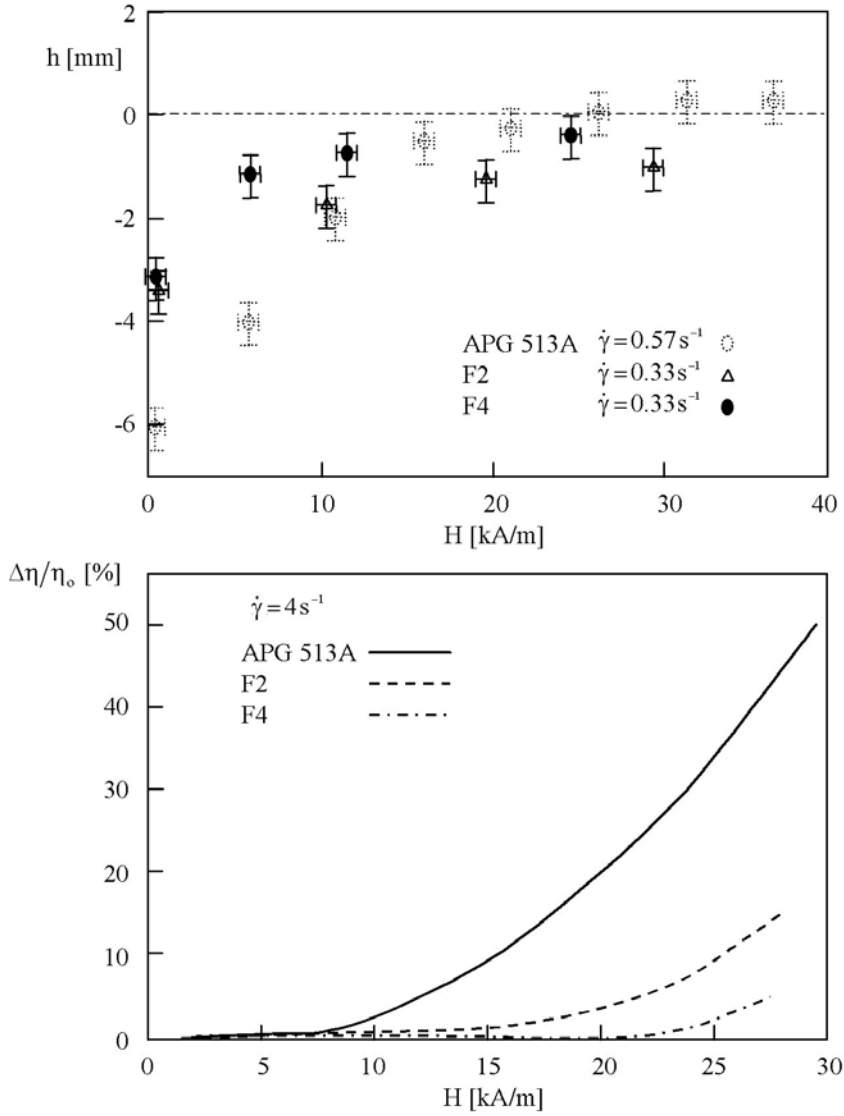

Fig. 4.51. The influence of the microscopic make-up of the fluids on the normal stress effects can be seen from the comparison of the dependence of the fluid surface height on field strength for fluids F2, F4 and APG513A containing 7.2vol.% of magnetite but different content of large particles (upper part). The lower part of the figure shows for comparison the magnetoviscous effect for the three fluids.

5. Magnetorheological Fluids

It has been discussed in detail, that the viscosity of suspensions of magnetic nanoparticles can be significantly influenced by moderate magnetic fields. Nevertheless the results presented in Chap. 4 have shown that strong changes are only achievable if shear rate is low, and furthermore it has been seen that effects like yield stress or normal stress differences are small compared to other viscoelastic fluids even at low shear rate. Independent from this backdraw, the possibility of magnetic field control of the fluids' viscous properties opens the door to the development and design of devices using this property as part of an electronic control circuit. Since the changes are – as mentioned – small in nowadays available ferrofluids, one has to shed a light to the question whether it is possible to find a way to enhance the magnetoviscous effects to an order of magnitude suitable for applications.

This question leads immediately to a discussion of so called magnetorheological fluids and this section is thus devoted to the possibilities in the use of magnetorheological fluids as well as to their backdraws, reducing their practical use. In this context it will furthermore be discussed, which changes of the make-up of ferrofluids could lead to a suspension combining the advantages of ferrofluids and magnetorheological fluids.

Nevertheless this section has not the aim to give a complete insight into the physics and applications of magnetorheological fluids since these are not directly within the scope of this work. They will only be described in an extent leading to information necessary for the discussion of ferrofluids.

5.1 Definition and basic properties of magnetorheological fluids

The term "magnetorheological fluids" commonly stands for suspensions containing micron sized particles made of magnetic material. The size difference of about three orders of magnitude between particles with diameters of about 10 nm used in ferrofluids and particles with a size of several microns determines all differences concerning the properties and behavior of the liquids. Magnetorheological fluids contain usually iron particles with a size from 2 to 20 μm in carrier liquids being suitable for use in technical devices. That means, that the carrier liquids have to be oils with low evaporation rates even at temperatures of about 100 °C as they are common for the use in technical devices and machines. The volume concentration of the particles is usually high, i.e. between 10 vol.% and 40 vol.%, to keep the

S. Odenbach (Ed.): LNP m71, pp. 123–129, 2002.

magnetoviscous effects as high as possible. To stabilize the dispersion, usually a small amount of dispersant is added to the carrier liquid, but no complex surfactant techniques are applied to avoid agglomeration of the particles. This basic make-up information provides us immediately with a couple of general properties of magnetorheological fluids. First of all it is clear that particles with a size of several micron are – in contrast to the nanosized particles in a ferrofluid – not longer magnetic single domain particles. Therefore the magnetic moment of the particles is not simply determined by their volume V and the spontaneous magnetization of the magnetic material as given for the particles in a ferrofluid in (2.3) but it needs to be calculated as a function of the strength of the applied magnetic field H. It is thus given by

$$m = \chi_p H V \tag{5.1}$$

where χ_p denotes the susceptibility of the magnetic material the particles are made of. This difference leads to the fact that the initial susceptibility of the fluid is not orders of magnitude larger than that of a ferrofluid as that might be expected from a comparison of particle sizes. Nevertheless the high values of χ_p for the usually used magnetic materials, e.g. $\chi_p \sim 10^1$ (Weast, 1969) for iron, result in (Kneller, 1962) high values of susceptibility at low fields, being in the order of 1 as it can be seen e.g. from experimental data in (Jolly et al., 1999). For the magnetorheological properties the variation of the particles' magnetic moment with field strength becomes important if one focuses on the coupling constant between the particles. This is now to be written in the form

$$\lambda = \frac{\mu_o \chi_P^2 H^2 V}{12 k_B T} \tag{5.2}$$

Calculating its value for a typical field strength of H=10 kA/m and the susceptibility of iron one obtains for particles with 10 μm diameter that λ is in the order 10^8. The high value of λ makes obvious that a strong tendency towards formation of chains and agglomerates is typical for a magnetorheological fluid in the presence of a magnetic field. Furthermore (5.2) shows that the interparticle interaction will mostly vanish for H=0 since the relatively large magnetic particles have nearly no permanent magnetic moment in the absence of a field. In vanishing field only remanence effects will lead to a resulting magnetic moment and these effects can be made small compared to those in the field. This means, that the presence of a magnetic field will dramatically change the microstructure of a magnetorheological fluid leading to strong changes in the magnetoviscous behavior of the fluid. The question of agglomerate formation in suspensions of large magnetic particles has attracted a lot of interest during the past years as well from the experimental as from theoretical point of view. Numerous experiments (Liu et al., 1995; Liu et al., 1996; Hagenbüchle et al., 1996; Bossis et al., 1992) have been carried out with strongly diluted magnetorheological fluids using optical methods for the determination of their microstructural properties. Nevertheless these experiments do not give full information about the microstructural changes in the fluid since the dilution leads to a change of interaction, changing the general phys-

ics of the fluid's behavior. As an example we will here only mention the observation of lateral attraction (Fermigier and Gast, 1992) of particle chains which was found to increase with increasing concentration of the suspension. Jolly et al. (Jolly et al., 1999) were able to show that the time scale of structure formation in the liquid is in the order of several hundred milliseconds. It was found to rise with increasing viscosity of the carrier liquid and with decreasing concentration of magnetic material in the liquid, leading to the statement, that the formation of structures in the fluid is a process dominated by magnetically forced diffusion.

It is already clear at this point, that the large size of particles suspended in a magnetorheological fluid provides the advantage of strong interparticle interaction and related strong changes of viscosity in the field. Nevertheless it is clear too that a suspension of particles of that size can not be stable against sedimentation in the gravitational field since – as we have discussed in Sect. 2.1 – thermal energy of the particles can only fight their energy in the gravitational field up to sizes of about 10 nm. As the reader may remember, this has been one of the stability conditions finally leading to the claim that particles in a stable ferrofluid should be nanosized. For the micron sized particles in a magnetorheological fluid the Stokes law allows to calculate the order of magnitude of the sedimentation velocity by

$$v = \frac{2r^2 g \rho}{9\eta} \tag{5.3}$$

to be in the order of several millimeter per day.

Thus the fluid will show significant demixing due to sedimentation in time scales small compared to the time scales of stability requirements for applications. The sedimentation problem in magnetorheological fluids is so important, that even experiments on rheology of such suspensions are already planned under microgravity conditions on the international space station. This may help to provide deeper insight into structure formation in the suspensions, but it will not overcome the serious problem, that technical devices like clamps (Carlson et al., 1994), clutches (Lampe, 1999) or brakes (Carlson et al., 1996) will fail after short time due to significant changes in the fluids properties forced by the demixing in the gravitational field.

An additional problem of magnetorheological fluids is the so called "in use thickening" an effect leading to a significant increase of the zero field viscosity of the fluids. This problem results from the appearance of nanosized oxide grains abrase from the surface of the magnetic particles by interparticle collisions. These oxide particles cause irreversible agglomeration leading to the mentioned viscosity increase (Carlson, 2001).

5.2 Viscous properties of magnetorheological fluids

As we have seen above, the coupling constant between the magnetic particles in a magnetorheological fluid vanishes for vanishing magnetic field strength. Therefore the fluid shows newtonian behavior in zero field conditions. The viscosity is

than determined by the viscosity of the carrier liquid and the volume fraction of suspended material, as it has been discussed in Sect. 2.3. If a magnetic field is applied interparticle interaction becomes significant and – as discussed above – so strong, that complex structures and large chains or rods of magnetic particles are formed. These will determine the viscous behavior of magnetorheological suspensions. Comparable to the properties of ferrofluids discussed above, magnetorheological fluids show a Bingham type behavior (see Fig. 5.1). The yield stress observed depends on the strength of the applied magnetic field and its absolute value is several orders of magnitude larger than that observed for commercial ferrofluids actually available. This enables the design of technical applications like e.g. dampers for seat damping in large trucks as they are described in (Carlson, 1994).

As seen from Fig. 5.2 such dampers can exert forces in the order of several kN. The controllability of the damping properties of the device enables an excellent damping of the vibrations of the whole system and even a reduction of resonance frequencies not well damped by conventional dampers with fixed damping properties (see Fig. 2.17).

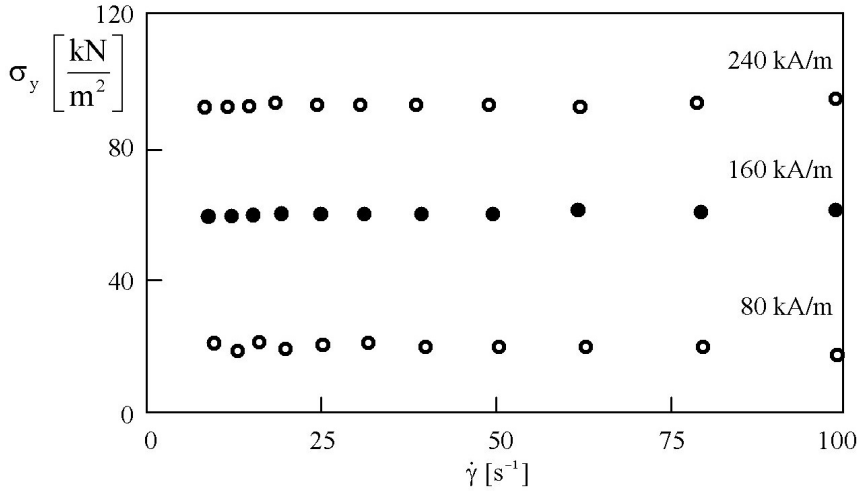

Fig. 5.1. The yield stress for a typical magnetorheological fluid for three different magnetic field strength (after Carlson, 1994).

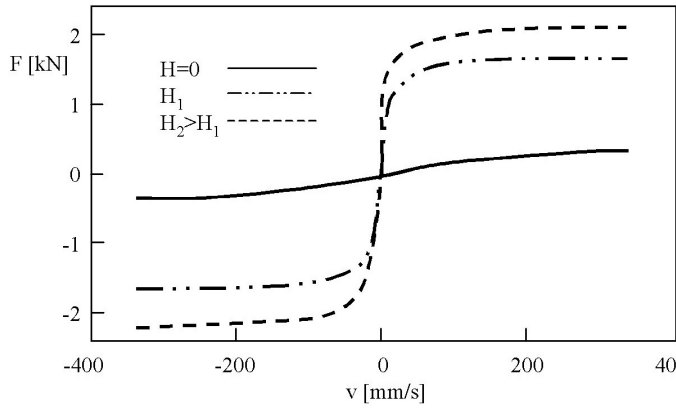

Fig. 5.2. The damping force of a commercial magnetorheological damper as a function of the velocity of the vibration for three different magnetic field strength (after Carlson, 1994).

5.3 Future development in magnetorheology

As seen above, magnetorheological fluids are in principle systems showing field-dependent viscosity changes which are sufficient to fulfill the needs of technical devices like dampers or clutches. Such devices have been shown to work well with magnetorheological fluids and to show excellent control behavior by magnetic field changes. Nonetheless the discussed sedimentation problem as well as the in use thickening makes it impossible to bring these applications to real use in machines, cars or other commercial systems. Even complex design structures remixing the fluid as long as the system is in operation do not overcome the problems completely and they provide no help if the device is at rest and furthermore they increase the device's costs in a way that commercial applications of magnetorheological fluids are presently in general not competitive with traditional engineering solutions.

Thus a practical use of the obvious advantages in controllability of magnetically influenced fluids requires the development of suspensions which combine the stability of ferrofluids with the strong magnetoviscous effect found in magnetorheological fluids. As has been discussed above, the principle magnetoviscous behavior of both kind of suspensions is comparable. Thus a ferrofluid with enhanced interparticle interaction but not too large particles should be a principle solution of the problem.

In general, two ways to reach this goal seem to be applicable. On the one hand the use of other magnetic material than magnetite could be a solution. As discussed in Sect. 4.3.2 Co-particles show much stronger interparticle interaction than magnetite particles of similar size due to their higher spontaneous magnetization. One can easily calculate from (4.18) that particles with a diameter about

20 nm would exhibit a coupling comparable to that found in magnetorheological fluids at technically suitable magnetic field strength. Since this coupling would be present even in the absence of magnetic fields, particles would have to be somewhat smaller to find an optimum combination of a high absolute value in e.g. yield stress in the fluid and a strong field-dependent change of the behavior of the liquid.

The second way to enhance a ferrofluids' magnetoviscous properties becomes obvious from the results discussed in Sect. 4.3.2 There it has been shown, that the magnetoviscous effects of commercial ferrofluids are dominated by a small amount of relatively large magnetite particles. Thus an increase of this particle fraction will also lead to an enhancement of the magnetoviscous properties of the fluid as shown in principle in Sect. 4.3.2. This concept has been driven to a maximum extent in the development of so called nano-MR fluids (Kormann et al., 1996a; Kormann et al., 1996b). These fluids are composed similar to ferrofluids, i.e. they contain nanosized magnetite particles covered with a disperging layer preventing irreversible agglomeration due to v.d.-Waals interaction. But in contrast to common ferrofluids these nano-MR fluids contain particles with a diameter of about 30 nm. As shown in (Kormann et al., 1996a) such suspensions exhibit still a high sedimentation stability. But in the presence of magnetic fields they form chains with a length of several μm. These chains lead to the appearance of a field-dependent yield stress in the suspension. As seen in Fig. 5.3 the yield stress rises quadratically with magnetic field strength as it has been observed for ferrofluids too (see Sect. 4.3.5). The fluid used for this measurement contained about 12 vol.% of 30 nm magnetite particles. Thus the total volume concentration is comparable to a ferrofluid but the particles' size is remarkably larger.

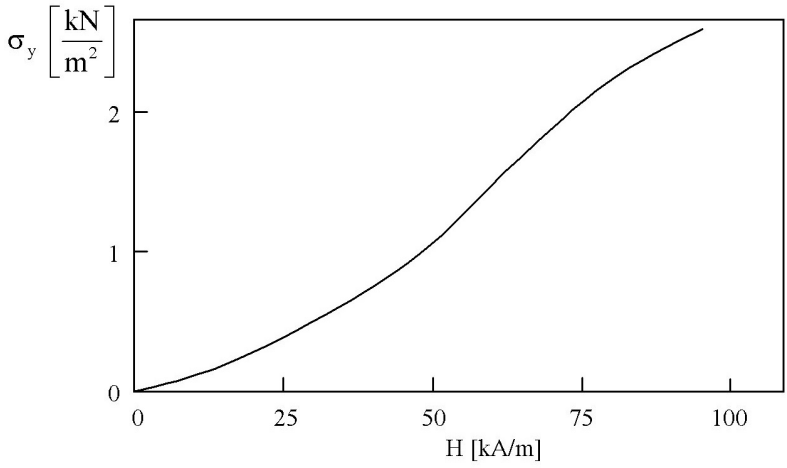

Fig. 5.3. The yield stress of nano-MR-fluid depends quadratically on the strength of the applied magnetic field (after Kormann, 1996b)

Due to the high amount of large particles the yield stress is about 6 orders of magnitude larger than that measured for a normal commercial ferrofluid (Fig. 4.37). Furthermore it is important to see, that the yield stress vanishes for zero field. In contrast to the cobalt fluids discussed above, the coupling between the particles in the absence of a magnetic field is weak enough to avoid significant structure formation. A fact which leads to pronounced changes in the viscous behavior due to the application of magnetic fields. Furthermore experiments (Kormann et al., 1996a; Kormann et al., 1996b) have shown that the interparticle interaction between the 30 nm particles is strong enough to enable strong magnetoviscous effects even at high shear rates suitable for technical application.

The future development will now have to combine the results of ferrofluid and magnetorheological research. The observation, that the interaction of large magnetite particles with a size of several tenth of nanometers can be sufficient to drive a technically applicable magnetoviscous effect opens a direction for the future research. An optimization will now have to be performed taking into account the size and volume concentration of the large particles, as well as the influence of the small particles providing a magnetic background medium, enhancing the interparticle interaction.

6. Conclusion and outlook

It has been shown, that the viscosity of a suspension of magnetic particles can be strongly influenced by magnetic fields of moderate strength. Particular interest has been devoted to the investigation of commercial ferrofluids, being designed for actual technical applications like loudspeakers or sealings. In a series of experiments we've found that the qualitative behavior of the fluids can be described by Shliomis' theory of rotational viscosity based on the assumption, that the free rotation of the suspended magnetic particles in a shear flow is hindered by the action of magnetic fields. In particular the experiments have been used to verify the general behavior for weak magnetic field, leading to an increase of viscosity proportional to the square of the strength of the magnetic field, and the predictions concerning the dependence of the magnetic field-induced viscosity changes on the mutual direction of the magnetic field and the vorticity of the flow.

In a detailed evaluation the experiments have shown, that the mentioned theory is not suitable to explain quantitatively the observed effects. Furthermore extended experimental investigations have shown, that additional effects like a shear dependence of magnetoviscosity or the appearance of viscoelastic effects appear in ferrofluids under the influence of magnetic fields. A special set of experiments using magnetic fluids exposed to different purification processes has been performed to prove the influence of the magnetic particles' size. The purification process – an exposure of the fluid to a magnetic field gradient – provides a highly size selective modification of the fluids' size distribution. In our particular situation a set of fluids with significantly different content of large particles in a size range between 15 nm and 20 nm has been produced. Magnetoviscous investigations of these fluids showed clearly that the amount of large particles is the most important parameter determining the field-dependent changes of viscosity in ferrofluids.

The finding that a reduction of the large particle content reduces the magnetoviscous effect, and the result that an increase of shear rate leads also to a decrease of magnetoviscosity forced the development of a microscopic model of ferrofluids describing them as bidisperse systems. In this model the known polydispersity of the magnetic particles has been reduced to a description where two significantly different fractions of particles are taken into account. One fraction containing the majority of the magnetic material consists of particles with a diameter close to the mean diameter and is referred to as the fraction of "small particles". The second fraction – of "large" particles – consists of the small portion of particles in the size range above 15 nm mentioned above. These particles are large enough to exhibit an interparticle interaction strong enough to force chain formation of the particles. Taking the existence of such chains as a part of the

S. Odenbach (Ed.): LNP m71, pp. 131–133, 2002.

model one can relate the shear thinning to a rupture of the chains induced by the shear flow. Moreover a quantitative analysis of the model using methods of statistical physics led to a quantitative explanation of the observed effects.

In this context a model – which we developed earlier for the stability of magnetic particle chains in a shear flow for the first explanation of the observed shear thinning – has been used to deter to quantitative agreement of theory and experiment not only for vanishing shear rate but for weak shear too.

The existence and rupture of chains of magnetic particles has been furthermore proved by the observation of normal stress differences in ferrofluids and their dependence on magnetic field strength and shear rate. Such effects had been predicted earlier by A. Zubarev for suspensions containing magnetic particle chains.

Besides the microscopic explanation of the magnetoviscous effects a macroscopic description has been found assuming the ferrofluid to show Bingham-type behavior – a situation well known from micronsized magnetic particle suspensions called magnetorheological fluids. The observed yield stress was found to be several orders of magnitude smaller than in magnetorheological fluids but it has been shown, that it depends clearly on the amount of large particles – similar to the findings for the rheological parameters discussed before.

Taking the actual situation of understanding of magnetoviscosity in ferrofluids – i.e. the assumption that even a few large particles in the fluid can give rise to a chain formation leading to significant changes in the viscous and viscoelastic behavior of the fluids – as a basis for an outlook to further development directions in the field, one can outline numerous fields of basic as well as technical interest.

First of all – from an experimental point of view – various investigations of magnetoviscous properties in different kind of fluids can be performed. An important question is the extension of the investigations to a measurement of complex viscosity in ferrofluids to get a deeper insight into the viscoelastic properties of the suspensions. Therefore the oscillating mode of the rheometer has recently been made operational and new results can be expected in the nearest future. The experimental findings on frequency dependence of the real and imaginary part of the fluids' complex viscosity will provide an additional proof for the bidisperse model with formation of particle chains. In addition the experimental data will enable the determination of the relaxation behavior of the liquid, and from this it will lead to information about the chain sizes determining the magnetoviscous behavior.

Furthermore, it has already been mentioned that a systematic change of the composition of the fluid can provide valuable new insights. Therefore a controlled separation as mentioned in Sect. 4.3.3 has been developed and is actually in use to obtain more detailed information on the importance of the large particle fraction. Another way to get a closer look to this question is to temper a well defined small amount of micronsized particles in a normal ferrofluid. The micronsized particles should then dominate the chain formation processes and therefore the magnetoviscous behavior of the fluids. A variation of the size and concentration of these particles would furthermore allow to optimize the magnetoviscous effects and to make the resulting compound fluids suitable for an application in technical devices. A proper combination of large particles and ferrofluids would thus not only

give a better understanding of the properties of ferrofluids, but the resulting combination of the features of ferrofluids and magnetorheological fluids could enable a technical spin off of the described research activities.

Besides the experimental work theoretical approaches have to be undertaken as well. In this respect the first interest will be devoted to an improvement of the bidisperse model and the included description of the chains properties. In particular the assumption of rigid chains will have to be dropped to allow bending of the chains in a flow and chain-chain interaction will have to be taken into account as soon as the concentration of large particles is significantly increased. On the other hand new theoretical models have been proposed describing transport processes in ferrofluids without any microscopical assumption on the basis of a pure thermodynamic approach (Müller and Liu, 2001). These models predict new transport coefficients which may lead to new interesting phenomena. One of these – connected with the symmetric velocity gradient in a flow – has meanwhile experimentally been proved to exist (Odenbach and Müller, 2001). Further investigations of the consequences of these models and the microscopic explanation of the observed effects will give rise to various new research topics.

Despite all experimental evidence for the influence of formation and rupture of chains of magnetic particles in the fluid one important point for the verification of the related models is still pending. Till now a direct observation of the microstructure of ferrofluids under shear has not been performed. As mentioned earlier this is mainly due to the optical opaqueness of ferrofluids hindering the employment of powerful optical tools often used in colloidal physics. To overcome this problem we're actually designing a specialized rheometer allowing the investigation of the microstructure of ferrofluids under shear by means of small angle neutron scattering. The advantage of neutrons is based on the one hand on the high permitivity for neutrons through a ferrofluid and on the other hand on the possibility to use the magnetic scattering contribution to obtain direct information about the magnetic structures in the fluid. Thus appropriate combination of modeling and experiments might lead to an observation of microstructural changes in fluids under influence of shear and magnetic field and to a relation of these results to the rheological behavior.

The mentioned results on rheological behavior of ferrofluids and its microscopic reasons can furthermore form the basis for technological development. As mentioned in Sect. 2.4 ferrofluids are known to have a high technological potential and the employment of magnetoviscous effects in technical devices has also been shown to be an interesting topic. The major problem to be solved on the way to magnetoviscous applications is an increase of the magnetoviscous effects by simultaneous preservation of the long term stability of the suspension. The recent understanding of the effects give hints how the fluids may have to be modified to fulfill the technical requirements. The modification of the large particle fraction – as it has been proposed above in the form of adding of micronsized particles – is a possible way to enhance the magnetoviscous effects.

Thus one can finally state that a step towards the understanding of the properties of magnetic fluids has been made, clarifying the direction of future basic research and opening possibilities for new technical approaches.

Appendix A

Characteristics of Ferrofluid APG 513 A

ferrofluid		APG 513 A
producer		Ferrofluidics
carrier liquid		Di-ester
magnetic material		magnetite
mean particle size	$\bar{d}$	10 nm
thickness of surfactant (approx.)	s	2 nm
mean volume of magnetic particles	V	$5.24 \cdot 10^{-25}$ m^3
mean volume of particles incl. surfactant layer	$\tilde{V}$	$1.44 \cdot 10^{-24}$ m^3
volume concentration of magnetic material	ϕ	0.072
saturation magnetization	M_S	$32 \cdot 10^3$ A/m
initial susceptibility	χ_{in}	1.57
density	ρ	$1.28 \cdot 10^3$ kg/m^3
density of carrier liquid	ρ_c	$1 \cdot 10^3$ kg/m^3
dynamic viscosity	η	0.128 kg/ms
kinematic viscosity	ν	$1 \cdot 10^{-4}$ m^2/s

Main Characteristics of the Used Magnetic Material

spontaneous magnetization of magnetite	M_o	$4.5 \cdot 10^5$ A/m
density of magnetite		$5 \cdot 10^3$ kg/m^3
crystal anisotropy of magnetite	K	$1 \cdot 10^4$ J/m^3

S. Odenbach (Ed.): LNP m71, p. 135, 2001.

List of symbols

Symbol	Meaning	Unit	First appearance*
A	Hamaker constant	J	2.9
a	tube diameter	m	(3.3)
B	magnetic flux	T	3.18
c	specific heat capacity	J/kgK	4.16
D	diffusion coefficient	m^2/s	4.25
d	particle diameter	M	2.1
d'	diameter of particle with surfactant	m	3.27
$\bar{d}$	mean particle diameter	m	(2.22)
d_{crit}	transition diameter from Néel to Brownian relaxation	m	(2.19)
d_{max}	maximal particle diameter in stable suspension	m	(2.6)
d_{ml}	magnetic particle diameter of large particles	m	(4.28)
E_g	energy of particles in gravitational field	J	(2.6)
E_H	energy of particles in magnetic field	J	2.2
E_{steric}	energy of steric repulsion between particles	J	2.10
E_T	thermal energy of particles	J	(2.2)
$E_{v.d.W.}$	energy of v.d.-Waals interaction between particles	J	2.9
$\hat{e}_r$	unit vector in radial direction		4.34
$\hat{e}_z$	unit vector in z-direction		4.34
F_E	free energy of particle system	J	4.26
F_K	Kelvin force	N	2.1
F_m	magnetic interaction force in particle chains	N	4.19

* The numbers indicate the equation of first appearance. Numbers in brackets indicate the first appearance of symbols which appear in the text – in this case the nearest equation is mentioned.

S. Odenbach (Ed.): LNP m71, pp. 137–141, 2001.

F_{vis}	viscous force disrupting particle chains	N	4.20
F	flow function		4.1
f	rotation frequency in Taylor Couette experiment	s^{-1}	3.40
f*	transition frequency for Taylor Couette flow	Hz	3.41
f_{grav}	gravitational force density	N/m^3	(2.15)
f_{mag}	magnetic force density	N/m^3	2.14
f_o	Larmour frequency of magnetization vector	s^{-1}	2.18
g_0	gravitational acceleration	m/s^2	(4.45)
g_n	chain length distribution function		4.26
H	magnetic field strength	A/m	2.1
H*	critical field strength for equilibrium of normal stress and centrifugal force	A/m	(4.44)
H_i	inner field	A/m	3.18
H_o	amplitude of oscillating field	A/m	3.43
H_o	applied field	A/m	4.15
H_r	radial field	A/m	(3.42)
$\hat{H}$	unit vector in field direction		3.13
h	sample height	m	(2.6)
$h_{(r)}$	height of rise of fluid surface at rotating rod	m	4.42
I	moment of inertia of particles in unit volume	kg/m^2	3.10
K	crystal anisotropy	J/m^3	2.18
k_B	Boltzmann's constant	J/K	(2.2)
L	Langevin function		(2.12)
l	= 2d/d relative distance of particles		2.7
M	magnetization	A/m	2.1
$\overline{M}$	mean magnetization	A/m	2.24
$\tilde{M}$	Disturbation of magnetization	A/m	3.20
M_c	critical magnetization of normal field instability	A/m	4.12
M_E	Equilibrium magnetization	A/m	3.13
M_o	Spontaneous magnetization	A/m	2.3
M_S	Saturation magnetization	A/m	2.11
M_i	component of magnetization	A/m	3.44
m	magnetic moment of particles	Am^2	2.2
m_{chain}	magnetic moment particle chain	Am^2	4.26

N_{co}	torque transferred in Couette system	Nm	4.14
N_{cp}	torque transferred in cone plate system	Nm	4.14
N_{mag}	magnetic torque acting on particles	Nm	(4.28)
N_{vis}	Viscous torque	Nm	(4.28)
N_1, N_2	normal stress differences	N/m^2	4.30
n	number of particles in a particle chain		4.20
$\hat{n}$	surface normal		4.35
n_{max}	maximum number of particles in a chain under shear		(4.23)
P	pressure	N/m^2	
Δp	pressure difference	N/m^2	2.25
R	relative change of viscosity		3.34
$\widetilde{R}$	reduced relative change of viscosity		3.42
R^{max}	maximal relative change of viscosity		3.36
Re	Reynolds number		3.40
R_i	radius of inner cylinder in Taylor Couette arrangement	m	3.40
R_1, R_2	inner and outer radius of Couette part of rheometer	m	4.13
r	particle – particle distance	m	2.6
r_0	radius of rotating rod	m	4.4
S	density of internal angular momentum	kg/ms	3.10
SR	stress ratio		3.1
s	thickness of surfactant layer	m	(2.19)
T	absolute temperature	K	(2.2)
t	normalized thickness of surfactant layer $t = 2s/d$		2.10
V	particle volume	m^3	2.1
$\widetilde{V}$	particle volume with surfactant	m^3	2.17
V_1'	volume of large particles with surfactant	m^3	4.27
v	flow velocity	m/s	2.15
v_r, v_φ, v_ϑ	velocity components in spherical polar coordinates	m/s	4.5
w	gap width in Taylor Couette cylinders	m	3.40

Greek symbols

α	relation of magnetic and thermal energy		2.11
β	angle between field and vorticity		3.5
$\dot{\gamma}$	shear rate	s^{-1}	3.1
$\dot{\gamma}_{co}$	shear rate in Couette system	s^{-1}	4.13
$\dot{\gamma}_{cp}$	shear rate in cone plate system	s^{-1}	4.13
δ	surface distance of particles	m	(2.7)
δ_{ik}	Kronecker symbol		3.18
ε	magnetic parameter in theory of Hall and Busenberg		3.4
η	dynamic viscosity	kg / ms	2.17
η_c	dynamic viscosity of carrier fluid	kg / ms	2.20
η_o	dynamic viscosity without field	kg / ms	2.20
$\eta_{(H)}$	dynamic viscosity in magnetic field	kg / ms	3.4
η_r	rotational viscosity	kg/ms	3.26
η_*	reference viscosity	kg / ms	4.29
$\Delta\eta$	field-induced viscosity change	kg/ms	Fig. 3.11
θ	phase shift between M and H		3.46
μ_B	Bohr magneton	Am^2	(2.11)
μ_o	vacuum permeability	Vs/Am	2.1
$\nu_{(H)}$	kinematic viscosity in magnetic field	m^2/s	3.41
ν_i	normal stress coefficient	Ns^2/m^2	4.21
ν_{io}	zero shear limit of normal stress coefficient	Ns^2/m^2	4.33
ζ	surface density of surfactant	m^{-2}	2.10
ξ	ratio of magnetic and viscous torque on a particle		3.5
ρ	density of the fluid	kg/m^3	(2.15)
ρ'	density of the suspended solid fraction	kg/m^3	3.27
$\Delta\rho$	density difference between particles and carrier liquid	kg/m^3	(2.6)
σ	stress	N/m^2	(4.8)
σ_{ik}	component of stress tensor	N/m^2	3.18
σ_y	yield stress	N/m^2	4.30
σ_*	reference stress	N/m^2	4.29
τ_B	Brownian relaxation time	s	2.17
τ_N	Néel relaxation time	s	2.18
τ_{eff}	effective relaxation time	s	2.19
τ_s	rotational relaxation time of suspended particles	s	3.11

ϕ	volume fraction of magnetic material		(2.12)
ϕ'	concentration of particles with surfactant		3.4
ϕ_l'	volume fraction of large particles with surfactant		4.27
$\tilde{\phi}$	volume fraction of all suspended material		2.20
$\tilde{\phi}_c$	critical volume fraction at which suspension gets rigid		(2.23)
ϕ_{large}	volume fraction of large particles		Table 4.4
χ	susceptibility		3.44
χ_{in}	initial susceptibility		2.12
χ_p	susceptibility of particle material		5.1
ω	frequency of oscillating field	s^{-1}	3.10
ω_0	angular velocity of rotating rod	s^{-1}	4.37
ω_v	angular velocity of fluid volume element	s^{-1}	4.34
ω_p	angular velocity of particles in the flow	s^{-1}	3.32
λ	coupling parameter		4.17
λ_T	thermal conductivity	W/Km	Table 4.2
Ω	vorticity of the flow	s^{-1}	3.8

References

Alexiou, Ch., Arnold, W., Hulin, P., Klein, R., Schmidt, A., Bergemann, Ch. and Parak, F. G. (2001) Therapeutic efficacy of ferrofluid bound anticancer agent. *Magnetohydrodynamics*, **37**, 3

Ambacher, O., Odenbach, S. and Stierstadt, K. (1992) Rotational viscosity in ferrofluids. *Z. Phys. B-Condensed matter*, **86**, p. 29

Auzans, E., Zins, D., Blums, E. and Massart, R. (1999) Synthesis and properties of Mn-Zn ferrite ferrofluids. *J. Magn. and Magn. Mat.*, **34**, p. 1253

Bacri, J. C., Perzynski, R., Shliomis, M. I. and Burde, G. I. (1995) "Negative-Viscosity" Effect in a Magnetic Fluid. *Physical Review Letters*, **75**, 11 p. 2128

Batchelor, G. K. (1970) An introduction to fluid dynamics. Cambridge Univeristy Press, London

Berkovsky, B. M. and Polevikov, V. K. (1988) Numerical experiments in convection (in russian). Universitätsverlag, Minsk

Berkovsky, B. M., Medvedev, V. F. and Krakov, M. S. (1993) Magnetic Fluids, Engineering Applications. Oxford University Press, Oxford, New York, Tokyo

Berkovsky, B. M. and Bashtovoy, V. (1996) Magnetic fluids and applications handbook. begell house, inc., New York, Wallingford (UK)

Binding, D. M. and Walters, K. (1976) Elastico-viscous squeeze films, Part 3. The torsional-balance rheometer. *J. non-Newtonian Fluid Mech.*, **1**, p. 277

Blums, E., Mikhailov, Yu. A. and Ozols, R. (1986) Heat and Mass Transfer in MHD Flows. World Scientific Publishing Co. Pte. Ltd., Singapore

Blums, E. (1995) Some new problems of complex thermomagnetic and diffusion driven convection in magnetic fluids. *J. Magn. and Magn. Mat.*, **149**, p. 111

Blums, E., Cebers, A. and Maiorov, M. M. (1997) Magnetic Fluids. Walter de Gruyter, Berlin, New York

Blums, E., Odenbach, S., Mezulis, A. and Maiorov, M. (1999) Magnetic Soret effect in a hydrocarbon based colloid containing surfacted Mn-Zn ferrite particles. *J. Magn. and Magn. Mat.*, **201**, p. 268

Böhme, G. (1981) Strömungsmechanik nicht-newtonscher Fluide. B. G. Teubner Verlag, Stuttgart

S. Odenbach (Ed.): LNP m71, pp. 143–151, 2001.

Bossis, G., Lemaire, E., Persello, J. and Petit, L. (1992) . *Progr. Colloid. Polym. Sci.*, **89**, p. 135

Brenner, H. D. and Condiff, D. W. (1980) . *J. Coll. Interface Sci.*, **47**, p. 199

Brown, W. F. (1963) Thermal fluctuation of single domain particle. *Phys. Rev.*, **130**, 5 p. 1677

Carlson, J. D. (1994) The promise of contrallable fluids. *Actuator 94*, , p. 266

Carlson, J. D., Catanzarite, D. M. and Clair, K. A. St. (1996) Commercial mageto-rheological fluid devices. *International Journal of Modern Physics B*, **10**, 23 and 24 p. 2857

Carslon, J. D. (2001) What Makes A Good MR Fluid?. *ERMR 2001, 8th International Conference on ER and MR Fluids*, Nice, France

Chan, D. C. F., Kirpotin, D. B. and Bunn, P. A., Jr. (1993) Synthesis and evaluation of colloidal magnetic iron oxides for the site-specific radiofrequency-induced hyperthermia of cancer. *J. Magn. and Magn. Mat.*, **122**, p. 374

Chantrell, R. W., Popplewell, J. and Charles, S. W. (1978) Measurements of particle size distribution parameters in ferrofluids. *IEEE Transactions on Magnetics*, **14**, 5 p. 975

Chantrell, R. W., Bradbury, A., Popplewell, J. and Charles, S. W. (1982) Agglomeration formation in magnetic fluid. *J. Appl. Phys.*, **53**, 3 p. 2742

Charles, S. W. (1996) personal communication.

Chong, J. S., Christiansen, E. B. and Baer, A. D. (1971) Rheology of concentrated suspensions. *J. Appl. Polymer Sci.*, **15**, p. 2007

Chu, S. H. and Lee, S. J. (2000) An experimental study on the squeezing flow of electrorheological suspensions. *J. Rheol.*, **39**, 44

Chukrov, A. Y. (1986) Convective stability of dilute colloid in the presence of magnetic diffusion in an inhomogeneous field. *Magnetohydrodynamics*, **22**, 3 p. 254

Cowley, M. D. and Rosensweig, R. E. (1967) The interfacial stability of a ferromagnetic fluid. *J. Fluid Mech.*, **30**, 4 p. 671

Dailey, J. P., Phillips, J. P., Li, C. and Riffle, J. S. (1999) Synthesis of silicone magnetic fluid for use in eye surgery. *J. Magn. and Magn. Mat.*, **194**, p. 140

Davidson, P. A. and Thess, A. (2000) Lectures Notes on liquid metal magnetohydrodynamics. *in press: Springer Publ.*, ,

de Gennes, and Pincus, (1970) . *Phys. Kondens. Materials*, **11**, 189

Delgado, A. (1988) First Study of Non-Newtonian Flow Behaviour in Microgravity. *Microgravity Science and Technology*, **1**, 4

DiPrima, R. C. and Swinney, H. L. (1981) Instabilities and transition in flow between concentric rotating cylinders. Springer, Berlin

Dreyer, M., Delgado, A. and Rath, H.-J. (1993) Fluid Motion in Capillary Vanes Under Reduced Gravity. *Microgravity sci. Technol.*, **4**, p. 203

Dreyer, M., Delgado, A. and Rath, H.-J. (1994) Capillary Rise of Liquid between Parallel Plates under Microgravity. *Journal of Colloid and interface science*, **163**, p. 158

Einstein, A. (1906, 1911) On the movement of small particles suspended in a stationary liquid demanded by the molecular kinetic theory of heat. ,

Embs, J., Müller, H. W., Wagner, C., Knorr, K. and Lücke, M. (2000) Measuring the rotational viscosity of ferrofluids without shear flow. *Physical Review E*, **61**, 3 p. 2196

Fannin, P. C., Scaife, B. K. P. and Charles, S. W. (1993) Relaxation and resonance in ferrofluids. *J. Magn. and Magn. Mat.*, **122**, p. 159

Fannin, P. C. (1994) An experimental observation of the dynamic behaviour of ferrofluids. *J. Magn. and Magn. Mat.*, **136**, 1 and 2 p. 49

Fannin, P. C. and Coffey, W. T. (1996) Contribution of particle inertial effects to resonance in ferrofluids. *Physical Review E*, **52**, 6 p. 6129

Fanselau, G. (1929) Die Erzeugung weitgehend homogener Magnetfelder durch Kreisströme. *Z. Phys.*, **54**, p. 260

Felderhof, B. U. and Kroh, H. J. (1999) Hydrodynamics of magnetic and dielectric fluids in interaction with the electromagnetic field. *Journal of Chemical Physics*, **10**, 15 p. 7403

Feltin, N. and Pileni, M. P. (1997) New technique to make ferrite nanosized particles. *Journal de Physique IV*, **7**, C1 p. 609

Fermigier, M. and Gast, A. P. (1993) Structure evolution in a paramagnetic latex suspension. *J. Coll. And Int. Sci.*, **154**, 2 p. 522

Finlayson, B. A. (1970) Convective instability of ferromagnetic fluids. *Journal of Fluid Mechanics*, **40**, 4 p. 753

Gerber, R. (1984) Magnetic filtration of ultra-fine particles. *IEEE Trans. Mag.*, **20**, 5 p. 1159

Grants, A., Irbitis, A., Kronkalns, G. and Maiorov, M. M. (1990) Rheological Properties of Magnetite magnetic Fluid. *J. Magn. and Magn. Mat.*, **85**, p. 129

Hagenbüchle, M., Sheaffer, P., Zhu, Y. and Lui, J. (1996) Static and dynamical light scattering of dilute magnetorheological emulsions. *Int. J. Mod. Phys. B*, **10**, p. 3057

Hall, W. F. and Busenberg, S. N. (1969) Viscosity of magnetic suspension. *J. Chem. Phys.*, **51**, 1 p. 137

Hayes, C. F. (1975) Observation of Association in a ferromagnetic colloid. *J. Colloid Interface Sci.*, **52**, 2 p. 239

Hergt, R., Andrä, W., Ambly d', C. G., Hilger, I., Kaiser, W. A., Richter, U. and Schmidt, H. G. (1998) Physical Limits of Hyperthermia Using Magnetite Fine Particles. *IEEE Transactions on Magnetics*, **34**, 5 p. 3745

Hess, P. H. and Parker, P. H., Jr. (1966) Polymers for stabilization of colloidal cobalt particles. *J. Appl. Polymer Sci.*, **10**, p. 1915

Hiergeist, R., Andrä, W., Buske, N., Hergt, R., Hilger, I., Richter, U. and Kaiser, W. A. (1999) Application of magnetite ferrofluids for hyperthermia. *J. Magn. and Magn. Mat.*, **2001**, p. 420

Huke, B. and Lücke, M. (2000) Magnetization of ferrofluids with dipolar interactions - a Born-Mayer expansion. *Physical Review E*, **62**, 5 p. 6875

Inaba, N., Miyajima, H., Takahashi, H., Taketomi, S. and Chikazumi, S. (1989) Magneto-optical absorption in infrared region for magnetid fluid thin film. *IEEE Trans. Magn.*, **25**, p. 3866

Jolly, M. R., Bender, J. W. and Mathers, R. T. (1999) Indirect measurements of microstructure development in magnetorheological fluids. *International Journal of Modern Physics B*, **13**, 14, 15 and 16 p. 2036

Jordan, P. C. (1973) Association phenomena in a ferromagnetic colloid. *Molecular Phys.*, **25**, 4 p. 973

Jordan, A., Wust, P., Fahling, H., John, W., Hinz, A. and Felix, R. (1993) Inductive heating of ferrimagnetic particles and magnetic fluids: physical evaluation of their potential for hyperthermia. *International Journal of Hyperthermia*, **9**, 1 p. 51

Khalafalla, S. E. and Reimers, G. W. (1973) Seperating non-ferrous fluid metals in incinerator residue using magnetic fluids. *Seperation Sci.*, **8**, 2 p. 161

Kittel, Ch. (1996) Introduction to Solid State Physics. *Wiley*, **7th ed.**,

Kneller, E. (1962) Ferromagnetismus. Springer-Verlag, Berlin, Göttingen, Heidelberg

Kormann, Cl., Laun, H. M. and Klett, G. (1996a) Magnetorheological fluids with nano-sized particles for fast damping systems. *International Journal of Modern Physics B*, **10**, 23 and 24

Kormann, Cl., Laun, H. M. and Richter, H. J. (1996b) MR fluids with nano-sized magnetic particles. *International Journal of Modern Physics B*, **10**, 23 and 24 p. 3167

Lampe, Dietrich (1999) Anwendung von magnetorheologischen Fluiden in Kupplungen. *antriebtechnik*, **38**, 7

Landau, L. D. and Lifschitz, E. M. (1985) Lehrbuch der theoretischen Physik: Elektrodynamik der Kontinua; Band 8. Akademie Verlag Berlin, Berlin

Langevin, P. (1905) Ferromagnetism. *Ann. Chim. Phys.*, **5**, p. 70

Lefebure, S., Dubois, E., Cabuil, V., Neveu, S. and Massart, R. (1998) Monodisperse magnetic nanoparticles: Preperation and dispersion in water and oils. *Journal of Materials Research*, **13**, 10 p. 2975

Lemaire, E., Bossis, G. and Grasselli, Y. (1992) Field induced structure in magneto and electro-rheological fluids. *Journal de Physique 2*, **2**, 3 p. 359

Lembke, U., Hoell, A., Wiedenmann, A. et al., (1999) . *J. Appl. Polymer Sci.*, **85**, p. 2279

Liu, J., Lawrence, E. M., Wu, A., Ivey, M. L., Flores, G. A., Javier, K. and Bibette, J. (1995) Field-indiced structures in ferrofluid emulsions. *Phys. Rev. Lett.*, **74**, 14 p. 2828

Liu, M. (1995) Fluid Dynamics of colloidal magnetic and electric liquid. *Phys. Review Letters*, **74**, 22 p. 4535

Liu, J., Mou, T., Zhu, Y., Haddadian, E., Pousset, J. and Lim, S. R. (1996) Effects of cell confinement on the evolution of field-induced structures in a magnetorheological fluid. *J. Intell. Mater. Syst. And Struct.*, **7**, p. 583

Liu, J. (1998) Experimental Proposal for ISS: Magnetorheological Fluids. *NASA ISS Information Service*, ,

Lücke, M. (1992) personal communication.

Mahr, T. and Rehberg, I. (1998) Nonlinear dynamics of a single ferrofluid-peak in an oscillating magnetic field. *Physica D*, **111**, p. 335

Maiorov, M. M. (1980) Measurement of the Viscosity of a Ferromagnetic Liquid in a Magnetic Field. *MGHDAG*, **16**, 4 p. 339

Maiorov, M. M. (1981) Magnetization curve of magnetic fluid and distribution of magnetic moment of ferroparticles. *10th Riga Conf. Magn. Gidrodin*, , p. 192

Martsenyuk, M. A., Raikher, Yu. L. and Shliomis, M. I. (1974) On the kinetics of magnetization of suspensions of ferromagnetic particles. *Sov. Phys. JETP*, **38**, 2 p. 413

Massart, R. (1981) Preparation of aqueous magnetic liquids in alkaline and acidic media. *IEEE Trans. Magn.*, **17**, 2 p. 1247

McTague, J. P. (1969) Magnetoviscosity of magnetic colloids. *J. Chem. Phys.*, **51**, 1 p. 133

Mermin, N. D. and Lee, D. M. (1976) Superfluid helium-3. *Scientific American*, **235**, 6 p. 56

Müller, H. W. and Engel, A. (1999) Dissipation in ferrofluids: Mesoscopic versus hydrodynamic theory. *Physical Review E*, **60**, 6 p. 7001

Müller, H. W. and Liu, M. (2001) The structure of ferro-fluiddynamics. *Phys. Rev. E (December 2001)*

Nakatani, I., Hijikata, M. and Ozawa, K. (1993) Iron-nitride magnetic fluids prepared by vapor-liquid reaction and their magnetic properties. *J. Magn. and Magn. Mat.*, **122**, p. 10

Neal, J. A. (1977) Aryl sulfonate-aldehyde composition and process for its preparation. *US Pat. 4 018 691*, ,

Néel, L. (1949) Effects of thermal fluctuations on the magnetization of small particles. *C. R. Acad. Sci. Paris*, **228**, p. 664

Neuringer, J. L. and Rosensweig, R. E. (1964) Ferrohydrodynamics. *Phys. Fluids*, **7**, 12 p. 1927

Neveu-Prin, S., Cabuil, V., Massart, R., Escaffre, P. and Dussaud, J. (1993) Encapsulation of magnetic fluids. *J. Magn. and Magn. Mat.*, **122**, 01. Mrz p. 42

Niklas, M. (1987) Influence of magnetic fields on Taylor vortex formation in magnetic fluids. *Z. Phys. B-Condensed matter*, **68**, p. 493

O' Grady, K., Bradbury, A., Charles, S. W., Menear, S., Popplewell, J. and Chantrell, R. W. (1983) Curie-Weiss behavior in ferrofluids. *J. Magn. and Magn. Mat.*, **31-34**, p. 958

Odenbach, S. and Gilly, H. (1996) Taylor vortex flow of magnetic fluids under the influence of an azimuthal magnetic field. *J. Magn. and Magn. Mat.*, **152**, p. 123

Odenbach, S. and Störk, H. (1998) Shear dependence of field-induced contributions to the viscosity of magnetic fluids at low shear rates. *J. Magn. and Magn. Mat.*, **183**, p. 188

Odenbach, S. (1998) Ferrofluids - magnetisable liquids and their application in density separation. *Magnetic and Electrical Separation*, **9**, p. 1

Odenbach, S. and Raj, K. (2000) The influence of large particles and agglomerates on the magnetoviscous effect in ferrofluids. *Magnetohydrodynamics*, **36**, 4 p. 379

Odenbach, S. (2000) Transport phenomena in magnetic fluids in cylindrical geometry. In: Physics of rotating fluids. Springer, Berlin, Heidelberg

Odenbach, S. and Müller, H. W. (2001) Stationary off-equilibrium magnetization in ferrofluids under vortical and elongational flow. *to be published*, ,

Odenbach, S. (1994a) Convection driven by forced diffusion in magnetic fluids. *Phys. Fluids*, **6**, 7 p. 2535

Odenbach, S. (1994b) Forced diffusion in magnetic fluids under the influence of a strong magnetic field gradient. *Z. Phys. B*, **94**, p. 331

Odenbach, S. (1995a) Microgravity experiments on thermomagnetic convection in magnetic fluids. *J. Magn. and Magn. Mat.*, **149**, p. 155

Odenbach, S. (1995b) Experiments on Weissenberg-effect Under reduced Gravity Conditions. *Microgravity Science and Technology*, **8**, 4 p. 236

Odenbach, S., Rylewicz, T. and Heyen, M. (1999a) A rheometer dedicated for the investigation of viscoelastic effects in commercial magnetic fluids. *J. Magn. and Magn. Mat.*, **201**, p. 155

Odenbach, S., Rylewicz, T. and Rath, H. (1999b) Investigation of the Weissenberg effect in suspensions of magnetic nanoparticles. *Phys. Fluids*, **11**, 10 p. 2901

Osborne, J. A. (1945) . *Physical Review*, **67**, 37

Papell, S. S. (1964) Low viscosity magnetic fluid obtained by the colloidal suspension of magnetic particles. *US Pat. 3 215 572*, ,

Papisov, M. I., Bogdanov, A., Jr., Schaffer, B., Nossiff, N., Shen, T., Weissleder, R. and Bradey, T. J. (1993) Colloidal magnetic resonance contrast agents: effect of particle surface on biodistribution. *J. Magn. and Magn. Mat.*, **122**, p. 383

Pileni, M. P. (1993) Water in oil colloidal droplets used as microreactors. *Advances Coll. Interface Sci.*, **46**, p. 139

Pshenichnikov, A. F., Gilyov, V. G. and Lebedev, A. V. (1998) Rheology of highly concentrated magnetic fluids. *8th International conference on magnetic Fluids*, ,

Rehberg, I. (1981) Phasenübergänge und hydrodynamische Instabilitäten. *Physik in unserer Zeit*, **12**, 5 p. 131

Resler, E. L., Jr. and Rosensweig, R. E. (1964) Magnetocaloric power. *AIAA J.*, **2**, 8 p. 1418

Rosensweig, R. E. (1966) Fluidmagnetic buoyancy. *AIAA J.*, **4**, 10 p. 1751

Rosensweig, R. E., Kaiser, R. and Miskolczy, G. (1969) Viscosity of magnetic fluid in a magnetic field. *J. Colloid Interface Sci.*, **29**, 4 p. 680

Rosensweig, R. E. (1982) Pattern formation in magnetic fluids. In Evolution of Order and Chaos in Physics, Chemistry, and Biology. Ed. Springer-Verlag, Berlin

Rosensweig, R. E. (1985) Ferrohydrodynamics. Cambridge University Press, Cambridge, New York

Rosensweig, R. E. (2001) personal communication.

Ruuge, E. K. and Rusetski, A. N. (1993) Magnetic fluids as drug carriers: targeted transport of drugs by a magnetic field. *J. Magn. and Magn. Mat.*, **122**, p. 335

Salueña, C. and Rubí, J. M. (1995) Frequency-dependent viscosity of a ferrofluid. *J. Chem. Phys.*, **102**, 9 p. 3812

Satoh, A., Chantrell, R. W., Kamiyama, S. I. and Coverdale, G. N. (1996a) Two-Dimensional Monte Carlo Simulations to Capture Thick Chainlike Clusters of Ferromagnetic Particles in Colloidal Dispersions. *Journal of Colloid and interface science*, **178**, p. 620

Satoh, A., Chantrell, R. W., Kamiyama, S. I. and Coverdale, G. N. (1996b) Three Dimensional Monte Carlo Simulations of Thick Chainlike Clusters Composed of Ferromagnetic Fine Particles. *Journal of Colloid and interface science*, **181**, p. 422

Schott, M. (1993) personal communication.

Schwab, L. (1989) Konvektion in Ferrofluiden. Diss. Univ. Munich, Munich

Shliomis, M. I. (1972) Effective viscosity of magnetic suspensioms. *Soviet Phys. JETP*, **34**, 6 p. 1291

Shliomis, M. I. (1974) Magnetic fluids. *Soviet Phys. Uspekhi (Engl. Transl.)*, **17**, 2 p. 153

Shliomis, M. I. and Morozov, K. I. (1994) Negative viscosity of ferrofluid under alternating magnetic field. *Physical Fluids*, **6**, 8 p. 2855

Spur, G., Uhlmann, E. and Patzwald, R. (2001) Rheometer for investigating the magnetoviscous effect in magnetic fluids. *Magnetohydrodynamics*, **37**, 3

Takeda, Y., Samec, K. and Kobayashi, K. (1991) Experimental Measurements Of 2D Velocity Vector Field Using Ultrasonic Velocity Profile Monitor (UVP).Experimental and Numerical Flow Visualization, FED-VOL. 128, Book No. H00706-1991, American Society of Mechanical Engineers

Taketomi, S. (1983) Magnetic fluid anomalous pseudo-Cotton Mouton effects about 107 times larger than that of nitrobenzene. *Jap. J. Appl. Phys.*, **22**, 7 p. 1137

Tanner, R. I. (1988) Rheological Measurements. *Elsevier Applied Science*

Taylor, G. I. (1923) Stability of a viscous liquid contained between two rotating cylinders. *Phil. Trans. Roy. Soc.*, **A 223**, p. 289

Thomas, J. R. (1966) Preparation and magnetic properties of colloidal cobalt particles. *J. Appl. Phys.*, **37**, 7 p. 2914

Thurm, S. and Odenbach, S. (2001) Magnetic separation of ferrofluids. *Magnetohydrodynamics*, **37**, 3

Vertogen, G. and de Jeu, W. H. (1988) Thermotropic liquid crystals, fundamentals. Springer Verlag, Berlin, Heidelberg, New York

Vislovich, A. N., Novikov, V. A. and Sinitsyn, A. K. (1986) Influence of magnetic fields on Taylor vortex formation in magnetic fluids. *J. Appl. Mech. Tech. Phys.*, **27**, 1 p. 72

Völker, T., Blums, E. and Odenbach, S. (2001) Thermodiffusive processes in ferrofluids. *Magnetohydrodynamics*, **37**, 3 p. 324

Wagener, M., Günther, B. and Blums, E. (1999) Preparation of oxidation resistant cobalt oil colloids. *J. Magn. and Magn. Mat.*, **201**, p. 18

Wagner, Joachim, Härtl, Wolfram and Hempelmann, R. (2000) Characterization of monodisperse colloidal particles: comparison between SAXS and DLS. *Langmuir*, **16**, p. 4080

Walters, K. (1975) Rheometry. Research Studies Press, London

Weast, R. C. (1969) Handbook of chemistry and physics. A ready-reference book of chemical and physical data. The Chemical Rubber Co., Cleveland, Ohio

Wen, W., Zheng, D. W. and Tu, K. N. (1999) Chain / column evolution and corresponding electrorheological effect. *J. Appl. Phys.*, **85**, 530

Weser, T. and Stierstadt, K. (1985a) Discrete Particle size distribution in ferrofluids. *Zeitschr. Phys. B-Condensed Matter*, **59**, p. 253

Weser, T. and Stierstadt, K. (1985b) Magnetoviscosity of Concentrated Ferrofluids. *Zeitschr. Phys. B-Condensed Matter*, **59**, p. 257

Whorlow, R. W. (1992) Rheological Techniques. Ellis Horwood, Ltd., Chichester, England

Wiedenmann (2001), A. (2001) Small-angle neutron scattering investigations of Co-ferrofluids using polarized neutrons. *Magnetohydrodynamics*, **37**, 3 p. 329

Wilde, G., Gorler, G. P. and Wilinecker, R. (1996a) Specific heat capacity of undercooled magnetic melts. *Appl. Phys. Lett.*, **68**, 21 p. 2953

Wilde, G., Gorler, G. P. and Wilinecker, R. (1996b) The specific heat of highly undercooled (Co, Ni, Fe)-Pd melts. *J. Non-Cryst. Solids*, **205-207**, 1 p. 317

Zaitsev, V. M. and Shliomis, M. I. (1969) The hydrodynamics of ferromagnetic fluid. *Journal of Applied Mechanics and Technical Physics*, **10**, 5 p. 24

Zelazo, R. E. and Melcher, J. R. (1969) Dynamics and stability of ferrofluids: surface interactions. *J. Fluid Mech.*, **39**, 1 p. 1

Zeuner, A., Richter, R. and Rehberg, I. (1998) Experiments on negative and positive magnetoviscosity in an alternating magnetic field. *Physical Review E*, **58**, 5 p. 6287

Zubarev, A. Yu. (1992) Theory of magnetic fluids with chain aggregates. *Magnetohydrodynamics*, **28**, 1 p. 18

Zubarev, A. Yu. and Yushkov, A. V. (1998) Dynamic properties of moderately concentrated magnetic liquids. *Journal of Experimental and Theoretical Physics*, **87**, 3 p. 484

Zubarev, A. Yu. and Iskakova, L. Yu. (1995a) Effect of Chain-Like Aggregates on Physical Properties of Magnetorheological Suspensions. *International Journal of Fluid Mechanics Research*, **22**, 3 and 4 p. 1

Zubarev, A. Yu. and Iskakova, L. Yu. (1995b) Theory of physical properties of magnetic liquids with chain aggregates. *JETP*, **80**, 5 p. 857

Zubarev, A. Yu., Odenbach, S. and Fleischer, J. (2001a) To the theory of dynamical properties of polydisperse magnetic fluids. *submitted to Physical Review E*

Zubarev, A. Yu., Odenbach, S. and Fleischer, J. (2001b) To the theory of dynamical properties of polydisperse magnetic fluids. II. Effect of chain-like aggregates. *submitted to Physical Review E*